

- I. PRELIMINARY STUDIES OF THE CHAIN-TRANSFER
CONSTANT OF METHYLFERROCENE
- II. PROTONATION OF METALLOCENES
- III. AN ANALYSIS OF THE N.M.R. SPECTRA OF
SUBSTITUTED FERROCENES
- IV. EXPERIMENTAL AND THEORETICAL STUDIES
OF THE CHARGE DISTRIBUTION ON
THE FERROCENYL CARBINYL CARBONIUM ION

Thesis by

Milton Irwin Levenberg

In Partial Fulfillment of the Requirements

For the Degree of

Doctor of Philosophy

California Institute of Technology

Pasadena, California

1965

(Submitted March 25, 1965)

ACKNOWLEDGMENTS

It is with deep gratitude that I thank Professor John H. Richards, my research advisor, for his patience and guidance during my graduate career at Caltech.

I wish to thank my parents for their understanding, support, and confidence in me; and my brother for his pride in me, an esteem which I also hold for him.

I would like to thank the faculty of the Chemistry Department for their encouragement and efforts on my behalf, and particularly Dr. Jurg Waser for his inspiring direction of my teaching assistant duties and Dr. George S. Hammond for the personal interest he has taken in me and the fine example he has set.

Finally, I would like to express my appreciation to the Institute for teaching fellowships, to the National Science Foundation, the Dow Chemical Company, the Shell Companies Foundation, and the Woodrow Wilson Foundation for the financial support of my graduate studies.

ABSTRACT

PART I:

Styrene monomer containing various concentrations of methylferrocene was allowed to polymerize at 70°C. The average molecular weight of the resulting polystyrene was determined, and the chain transfer constant of methylferrocene then calculated. The constant was found to be 0.7×10^{-4} , indicating some contribution to the stability of the methyl free radical by the ferrocenyl group.

The reactivity of methylferrocene to free radical attack is discussed, and the copolymerization of methylferrocene with styrene is considered.

PART II:

The n.m.r. spectra of ferrocene, ruthenocene, and osmocene in boron trifluoride monohydrate have been studied. Accurate measurements of relative peak areas and positions are reported. The species responsible for the n.m.r. spectra are discussed.

PART III:

A detailed analysis of the n.m.r. spectra of a series of alkylacetylferrocenes in a variety of solvents has been carried out. This has allowed a determination of the coupling constants between the various protons in these substances. For protons attached to the same ring, the following values are generally observed:

$J_{23} \sim 2.5$ cps and $J_{24} \sim 1.3$ cps. The magnetic anisotropy of the carbonyl group in 2-acetyl-1,1'-trimethylene ferrocene is also discussed.

PART IV:

The existence of the stable ferrocenylcarbinyl carbonium ion has been demonstrated by freezing point depression measurements in concentrated sulfuric acid. The n. m. r. spectrum of the carbonium ion has been observed and the chemical shifts of its protons relative to those of methylferrocene have been measured. The factors influencing the proton chemical shifts are discussed.

Techniques of molecular orbital calculations applicable to ferrocenyl systems are discussed and the results of a series of molecular orbital calculations on the ferrocenylcarbinyl carbonium ion are presented. The chemical shifts of the protons on the carbonium ion are predicted from the molecular orbital calculations, and the predictions are compared with the experimentally measured chemical shifts. The agreement is not as good as could be desired.

CONTENTS

Part		Page
I.	PRELIMINARY STUDIES OF THE CHAIN-TRANSFER CONSTANT OF METHYLFERROCENE	1
	A. Theory	2
	B. Discussion	11
	C. Experimental	26
	1. Styrene Monomer	26
	2. Polymerization	26
	3. Viscosimetry	27
	D. Appendix	31
	1. Chain Transfer Constant for Methylferrocene	31
	2. Ratio of Ferrocene to Styrene	32
	E. References	34
II.	PROTONATION OF METALLOCENES	36
	A. Introduction	37
	B. Results	38
	C. Discussion	41
	D. Experimental	53
	E. References	56
III.	AN ANALYSIS OF THE N.M.R. SPECTRA OF SUBSTITUTED FERROCENES	58
	A. Introduction	59
	B. Results	62
	C. Discussion	70
	D. Experimental	77
	1. N.M.R. Spectra	77
	2. Chemicals	77

CONTENTS (continued)

v

Part		Page
III.	(continued)	
E.	Appendix	79
	1. Derivation of the N.M.R. Parameters of an ABX System from the Experimental Spectrum	79
	2. N.M.R. Spectra of the Compounds Under Study	82
F.	References	95
IV.	EXPERIMENTAL AND THEORETICAL STUDIES OF THE CHARGE DISTRIBUTION ON THE FERROCENYL CARBINYL CARBONIUM ION	97
A.	Introduction	98
B.	Results	101
	1. Stability of Carbonium Ion	101
	2. N.M.R. Spectra	104
C.	Discussion	112
	1. Chemical Shifts	112
	a. Ring Current Effect	112
	b. Carbinyl Bond Anisotropy	114
	c. Change in Bond Hybridization	116
	d. Pi-Electron Charge Density on Carbon	116
	e. Inductive Effect	118
	f. Selective Solvation	119
	g. Ring Shift	120
	h. Anisotropy of Iron	121
	i. Summary	127
	2. Molecular Orbital Calculations	128
	3. The Charge on Iron	140
	4. Conclusions	142
D.	Experimental	144
	1. Compounds	144
	2. Freezing Point Depression	146
	3. N.M.R. Spectra	149
E.	References	151

CONTENTS (continued)

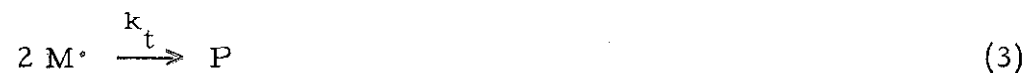
Part	Page
IV. (continued)	
F. Appendix	156
Fortran IV List of Computer Program MILMO4	
V. PROPOSITIONS	161

PART I

PRELIMINARY STUDIES OF THE
CHAIN-TRANSFER CONSTANT OF METHYLFERROCENE

THEORY

The simple free radical polymerization of a monomer proceeds by the following route:



"I" represents an initiator which generates a free radical pair in solution by an n^{th} order reaction. "M" is a monomer molecule, and "M·" is a growing polymer chain. In equation 3, "P" may represent a simple polymer formed by the coupling of two growing polymer chains, or it may represent an assortment of products from disproportionation reactions. For the purpose of calculating the kinetics of the reaction, the identity of "P" is not important; however, there is evidence that radical coupling is the predominant termination mechanism in styrene polymerizations (1-3).

The rates for the polymerization equations are given by the expressions:

$$R_d = \frac{-d[I]}{dt} = n k_d [I]^n \quad (4)$$

$$R_p = \frac{-d[M]}{dt} = k_i [I \cdot][M] + k_p [M \cdot][M] \quad (5)$$

$$R_p = 2 k_t [M\cdot]^2 \quad (6)$$

$$\frac{d[M\cdot]}{dt} = k_i [I\cdot][M] - 2 k_t [M\cdot]^2 \quad (7)$$

In the formation of a high polymer, reaction 2' must occur many times faster than reaction 2 to account for the large number of monomer units in the chain. Therefore, $k_i [I\cdot][M] \ll k_p [M\cdot][M]$, and $k_i [I\cdot][M]$ may be neglected in equation 5. The rate of polymerization may thus be written:

$$R_p = k_p [M\cdot][M] \quad (5')$$

At low degrees of polymerization, the rate of polymerization remains constant with time, implying that the concentration of $M\cdot$ reaches a steady state. This substantiates the "steady-state assumption" that the rate of change of concentration of an intermediate of very low concentration is small compared to its rates of formation and disappearance (4). Equation 7 may then be equated to zero, or:

$$k_i [I\cdot][M] = 2 k_t [M\cdot]^2$$

Similarly, the concentration of $I\cdot$ would reach a steady state and:

$$2 k_d [I]^n = k_i [I\cdot][M]$$

The most general form for the rate of polymerization would be:

$$R_p = k_p [M] \sqrt{\frac{k_i}{k_t} \frac{[I \cdot][M]}{2}} \quad (8)$$

$$R_p = k_p [M] \sqrt{\frac{k_d}{k_t} f [I]^n} \quad (8')$$

where "f" is the fraction of initiator fragments which successfully initiate a polymerization chain (5, 6).

The assumption has been made that the rates of all of the above reactions are independent of the molecular weight of the growing polymer chains, and that the reactivities do not change as the polymer grows in length.

For a typical peroxide initiated polymerization, $n=1$ and reaction 8' reduces to the expected relationship. In thermally initiated styrene polymerizations, the initiator, I, is itself styrene monomer and $I \cdot$ can be replaced in the equations by $M \cdot$, a growing styrene chain. The rate of polymerization may then be expressed by:

$$R_p = k_p \left(f \frac{k_d}{k_t} \right)^{\frac{1}{2}} [M]^{\left(\frac{n}{2} + 1 \right)} = k' [M]^{\left(\frac{n}{2} + 1 \right)} \quad (9)$$

There are conflicting reports on the order of the thermal initiation of styrene monomer and hence the mechanism of radical production. In 1943, Mayo (7) reported the thermal initiation of styrene monomer to be second order in styrene. Ten years later, however, he closely studied the thermally initiated polymerization of

styrene in bromobenzene and found the reaction to most closely follow 5/2 order kinetics (8). If we continue to assume a second order radical coupling for the chain termination step, an overall 5/2 order for the reaction implies a third order initiation step. On the other hand, a second order overall reaction would be observed if the initiation reaction was second order with monomer.

On this basis, Mayo (8) suggests a termolecular initiation process which he finds energetically feasible. Walling, however, is reluctant to completely abandon a second order initiation process, and suggests a possible reaction which would produce the required two monoradicals (9). For our purposes, we obtain the same results whichever initiation process is assumed.

The degree of polymerization, \bar{P} , is determined by the relative rates of polymerization and termination of the growing polymer chain (7):

$$\frac{\bar{P}}{2} = \frac{R_p}{R_t + R_{tr M}} = \frac{k_p [M\cdot][M]}{2 k_t [M\cdot]^2 + k_{tr M} [M\cdot][M]} \quad (10)$$

$$\frac{\bar{P}}{2} = \frac{k_p^2 [M]^2}{2 k_t R_p + k_{tr M} k_p [M]^2}$$

where $R_{tr M}$ and $k_{tr M}$ are the rate and rate constant for the "chain transfer" of the radical chain with monomer in solution. The phenomenon of chain transfer will be discussed shortly.

If disproportionation were the predominant means of termination rather than radical coupling, equation 10 would represent \bar{P} rather than $\frac{1}{2} \bar{P}$.

If the monomer in a polymerizing system is diluted with a solvent, the degree of polymerization of the resulting polymer is often lowered (1). The decrease of the average molecular weight is a function of the solvent. This phenomenon has been explained in terms of a "chain transfer" mechanism (11). The growing polymer radical attacks a solvent molecule, extracting an atom (usually hydrogen or halogen). This results in the termination of the polymer chain and the formation of a new species of free radical in solution. Under the proper conditions, this radical can then attack a monomer molecule, starting a new polymer chain growing. The net result is that the total rate of polymerization is not changed; however, the length of an average polymer chain is decreased. The overall reaction may be represented as follows:



The rate of chain transfer is:

$$R_{tr} = k_{tr} [M\cdot][S]$$

The expression for the degree of polymerization (equation 10) must now also include the termination of the radical chain by a chain transfer mechanism:

$$\bar{P} = \frac{R_p}{\frac{1}{2}R_t + R_{tr M} + R_{tr}} = \frac{k_p [M\cdot][M]}{k_t [M\cdot]^2 + k_{tr M} [M\cdot][M] + k_{tr} [M\cdot][S]} \quad (13)$$

$$\frac{1}{\bar{P}} = \frac{1}{\bar{P}_0} + C \frac{[S]}{[M]} + C_M \quad (14)$$

where $\bar{P}_0 = \frac{k_p [M]}{k_t [M\cdot]}$, $C = \frac{k_{tr}}{k_p}$, and $C_M = \frac{k_{tr M}}{k_p}$.

\bar{P}_0 is identical to \bar{P} in equation 10--the degree of polymerization without chain transfer.

The symbol "C" represents the "transfer constant" of the solvent. Equation 14 has been observed to hold for polystyrene systems with less than 10 per cent polymerization (8, 12). Table I lists some typical transfer constants for polymerizing styrene systems at 60°C and 100°C.

" C_M " is the self-transfer constant of the monomer, which has been found to be 0.60×10^{-4} for styrene at 60°C (6). The self-transfer

TABLE I
Chain Transfer Constants for Typical Solvents
in Styrene Systems (13)

Solvent	$C_{60} \times 10^4$	$C_{100} \times 10^4$
cyclohexane	0.024	0.16
benzene	0.018	0.184
toluene	0.125	0.65
ethylbenzene	0.67	1.62
cumene	0.82	2.0
<u>t</u> -butylbenzene	0.06	0.55
chlorobenzene		0.5
<u>n</u> -butyl chloride	0.04	
methylene chloride	0.15	
chloroform	0.5	
carbon tetrachloride	90	180
carbon tetrabromide	13600	
<u>n</u> -butyl mercaptan	220000	

constant, being an additive constant, will appear as a part of the experimentally measured degree of polymerization \bar{P}_o , and will not affect the results.

The transfer constant for a solvent may be found by determining the degree of polymerization for a system with a known solvent to monomer ratio. In a polystyrene system, with a monomer unit molecular weight of 104, the average molecular weight \bar{M} is given by:

$$\bar{M} = 104 \bar{P} \quad (15)$$

The molecular weight of a polymer may be determined by end group analysis, osmotic pressure, light scattering, sedimentation and diffusion rates, and intrinsic viscosity (14). All but the last method yield absolute values of molecular weights, but are often difficult to measure experimentally. Viscosity measurements, on the other hand, are easily performed, but must be calibrated against one or another of the other techniques.

The specific viscosity η_{sp} of a solution is found from the flow time of the solvent, t_o , and the flow time of the solution, t , in a viscometer, and is given by the following relationship:

$$\eta_{sp} = \frac{t - t_o}{t_o} \quad (16)$$

The intrinsic viscosity $[\eta]$ of a material is defined as (15):

$$[\eta] = \lim_{c \rightarrow 0} \frac{\eta_{sp}}{c} \quad (17)$$

where c is the concentration of the material in a solution.

An empirical relationship has been found between the intrinsic viscosity of a substance and its molecular weight (16). For polystyrene, this relationship is (6)

$$\bar{M} = 178,000 [\eta]^{1.37} \quad (18)$$

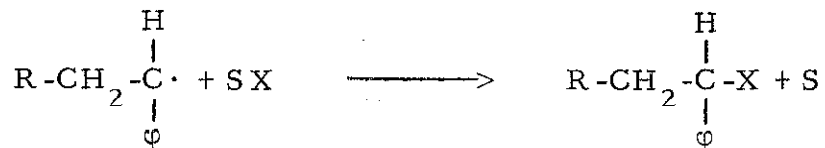
The average molecular weight of a polystyrene sample may thus be found by measuring its flow time at various concentrations in benzene.

DISCUSSION

A chain transfer constant is in reality a measure of the relative susceptibility to two substrates to attack by a free radical. If both the free radical and one of the substrates remain unchanged while a variety of compounds are considered as the second substrate, one obtains the relative reactivities of these compounds towards the free radical.

Much attention has been given to the free radical system of the polymerization of styrene. In a chain transfer experiment, the styrene monomer would represent the first substrate, while the growing styrene chain would represent the attacking free radical. In each experiment, the second substrate is competing with the styrene monomer for the attacking radical. A comparison of the ability of these substrates to compete with styrene provides an indirect measure of their ability to compete with each other.

The first step of the chain transfer reaction is the abstraction of an atom by the growing styrene chain:



The rate of this reaction is affected by a variety of factors, specifically steric effects, polar effects, the energy of bond formation, the ease of abstraction, and the stability of the remaining radical.

A list of typical chain transfer constants is presented in Table I. The chain transfer constant of methylferrocene has been found to be 0.7×10^{-4} , or about the same as ethylbenzene. The factors which contribute to this value will now be considered.

In a few of the systems presented in Table I, steric effects may be important. The proton under attack in cumene and chloroform may be sufficiently sterically blocked that a large attacking radical may experience difficulty approaching closely enough to form a bond. A second steric effect may be present in a system such as cumene, where large groups in ortho ring positions would prevent the radical intermediate from achieving planarity. This would result in loss of resonance stability of the free radical intermediate. Neither of these steric effects would be anticipated in methylferrocene or any other system where the attack is directed to a methyl group.

Electron donor radicals, such as the styrene radical, have shown a tendency to attack electron acceptors preferentially to other electron donors (17). In another part of this thesis it has been shown that the ferrocenylmethyl carbonium ion is stable, while no one has reported observing the corresponding carbanion. The observation has been made that ferrocene-carboxylic acid is less acidic than benzoic acid (the pK_a in 50% ethanol is 6.11, compared to 5.68 for benzoic acid) (18, 19). Infrared and reactivity data (20) also support the hypothesis that the ferrocenyl group is capable of releasing electrons

into a system. Methylferrocene would thus be considered an electron donor and, for this reason not as reactive as it might appear if tested with an acceptor radical such as the growing polyacrylonitrile radical.

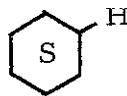
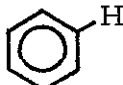
In a comparison of the chain transfer abilities of methylferrocene and alkylbenzenes, and, for that matter, most of the other compounds, one finds that the reaction is one of hydrogen abstraction. All hydrogen abstractions form the same benzyl-hydrogen bond, so the energy of bond formation is the same from one system to another.

The ease of abstraction of an atom by the attacking radical is a function of the existing bond strength and the polarizability of the abstracted atom. Once again, in most of the comparison systems the atom is hydrogen, and will have a constant degree of polarizability. Table II presents a list of some typical bond strengths.

An immediate dependence is noticed for the chain transfer constant on the bond dissociation energy of the bond which is ruptured in the chain transfer reaction. The easier the bond is to rupture, the more important the chain transfer reaction becomes. The greater reactivity of the halocarbons than that predicted from bond energy considerations alone can be accredited to a favorable polar effect. The trihalomethyl groups are electron acceptors, while the styryl radical is an electron donor. The reactivity of the halocarbons may also be enhanced by a steric effect. One would expect considerable steric "Back Strain" in the halocarbon, which would be relieved in the planar trihalomethyl radical product.

TABLE II

Typical Bond Dissociation Energies

Compound	Bond dissociation energy kcal/mole	Chain transfer constant $\times 10^4$
	95 ^a	0.02
	102 ^b	0.02
$\varphi\text{-CH}_2\text{-H}$	77.5 ^b	0.12
$\varphi\overset{\text{H}}{\underset{ }{\text{C}}}\text{HCH}_3$	75 ^c	0.7
$\varphi\overset{\text{H}}{\underset{ }{\text{C}}}(\text{CH}_3)_2$	74 ^c	0.8
$\text{CCl}_3\text{-H}$	90 ^b	0.5
$\text{CCl}_3\text{-Cl}$	68 ^b	90
$\text{CBr}_3\text{-Br}$	49 ^b	13,600

a. A. Streitwieser, Jr., "Molecular Orbital Theory," Wiley & Sons, N. Y. (1961), p. 397.

b. Reference 4, p. 50.

c. C. H. Leigh, M. Szwarc, J. Chem. Phys., 20, 844-7 (1952).

There is very little difference in most of the factors affecting the chain transfer constants of methylferrocene and toluene. The only factors which differ significantly from toluene to methylferrocene are the polar effects and the strengths of the R-H bonds under attack. The polar effect would lower the chain transfer constant of methylferrocene relative to toluene for equal R-H bond strengths. On this basis one may estimate the bond dissociation energy of the methyl proton in methylferrocene by comparison with known values for alkylbenzenes. The bond dissociation energy of methylferrocene is probably between 70 and 80 kcal/mole. This would imply a considerable degree of stabilization of the resulting radical by the ferrocenyl group.

Further evidence for the stability of the ferrocenylmethyl radical is given by the observed depression in the rate of polymerization of styrene by its presence. Methylferrocene is thus functioning as an inhibitor or retarder in the polymerization. Inhibitors and retarders which are not originally free radicals are known to form radicals by a chain transfer mechanism. The new radical thus formed is too unreactive to attack a monomer molecule, so the chain is effectively terminated.

One would like to know if every radical chain that was transferred to a methylferrocene molecule was eventually transferred back to the styrene system. This question may be answered, and at the same time an independent check of the chain transfer constant may be

obtained by measuring the concentration of ferrocene incorporated into the polymer. To this end several experiments were undertaken.

Samples of polystyrene were dissolved in benzene and poured onto a flat sheet of aluminum foil. The benzene was allowed to evaporate, producing thin, transparent films of polystyrene. Infrared spectra were taken of samples prepared in this way, both with and without methylferrocene present. Excellent spectra of polystyrene were obtained, but the concentration of methylferrocene was not great enough to be detected by this method.

Samples were dissolved in carbon tetrachloride, and their ultraviolet spectra were taken. The spectra are presented in Figure I, and the absorptivity of each sample at 3100 Å and 3900 Å is presented in Table III. On the basis of the known absorptions of pure solutions of polystyrene and of methylferrocene, the ratio of styrene units to ferrocene units was calculated in the chain-transferred copolymer. The calculation was repeated at both 3100 Å and 3900 Å, using the known weight of polystyrene in solution to correct for the styrene absorption. The entry in Table IV labeled "Two point colorimetry" represents the calculation where both absorptivities were used simultaneously to calculate the polystyrene concentration as well as the methylferrocene concentration. The calculations appear in the Appendix.

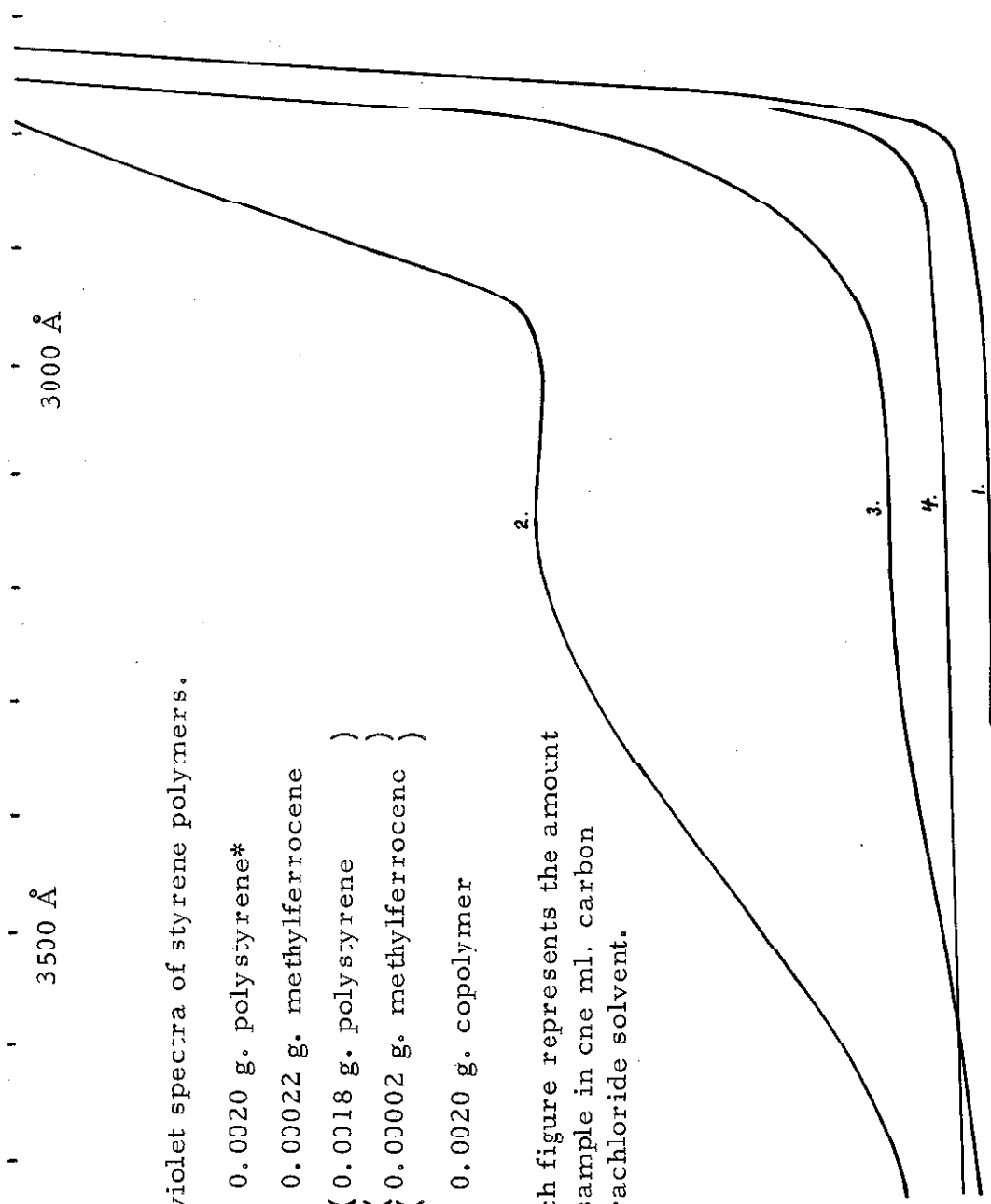


FIG. I Ultraviolet spectra of styrene polymers.

1. 0.0020 g. polystyrene*
2. 0.00022 g. methylferrocene
3. (0.0018 g. polystyrene)
 (0.00002 g. methylferrocene)
4. 0.0020 g. copolymer

* Each figure represents the amount of sample in one ml. carbon tetrachloride solvent.

TABLE III

Ultraviolet Absorptivity of Polystyrene Samples
in Carbon Tetrachloride

	3900 Å	3100 Å
polystyrene	5.4 per g/ml	8.73 per g/ml
methylferrocene	439 per g/ml	3910 per g/ml
copolymer	17.8 per g/ml	50 per g/ml
mixture*	0.09 per sample	0.755 per sample

* The mixture contains 1.8×10^{-4} g methylferrocene and
 2.0×10^{-3} g polystyrene per ml of carbon tetrachloride.

TABLE IV

Number of Styrene Units per Ferrocene Unit

Method	$\frac{[\text{styrene}]}{[\text{methylferrocene}]}$
chain transfer measurement	22.000
colorimetry at 3900 Å	67
colorimetry at 3100 Å	180
"two point" colorimetry	780

The very doubtful assumption has been made in these calculations that the methylferrocenyl group and the polystyrene chain in the copolymer each absorb in the UV independently of one another, and that each contributes to the absorbance just as it would as the pure component in solution. Inspection of the range of concentration ratios obtained in Table IV reveals that this assumption is not at all valid, though one would expect the two pi electron systems to be isolated from each other by a saturated three carbon chain.



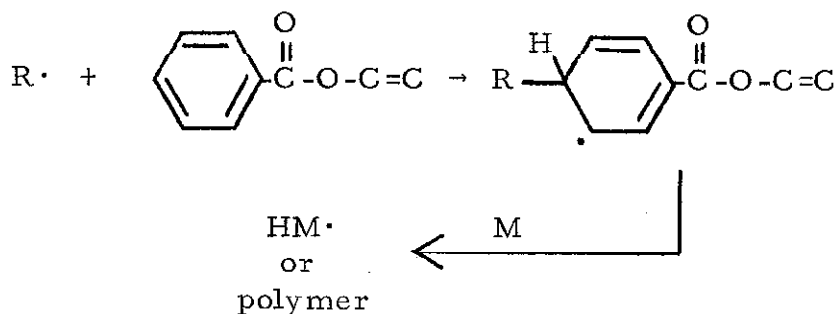
The anomalous UV absorption of the polymer may be due to the formation of a complex in solution between the pi systems of the ferrocenyl groups and the styryl groups. To test this hypothesis, the UV spectrum was observed for a mixture of polystyrene and methylferrocene in carbon tetrachloride. As can be seen from Figure I, the spectrum is just what one would predict for the sum of the two pure components, showing no unusual interactions.

It is of significance to note that all colorimetry measurements put the concentration of methylferrocene in the polymer two orders of magnitude higher than the concentration necessary to account for the observed chain transfer. Even though the colorimetric measurements have been found to be inaccurate, it is not likely that they are so far wrong as to account for an error of this size. The unexpectedly high UV absorption is not due to additional methylferrocene complexed with

the polymer. The polystyrene samples were dissolved in benzene and reprecipitated from methanol several times (see Experimental section) and the UV absorption spectrum of the polymer remained invariant the entire time. An additional sample of pure polystyrene in solution with methylferrocene was completely repurified by the same procedure.

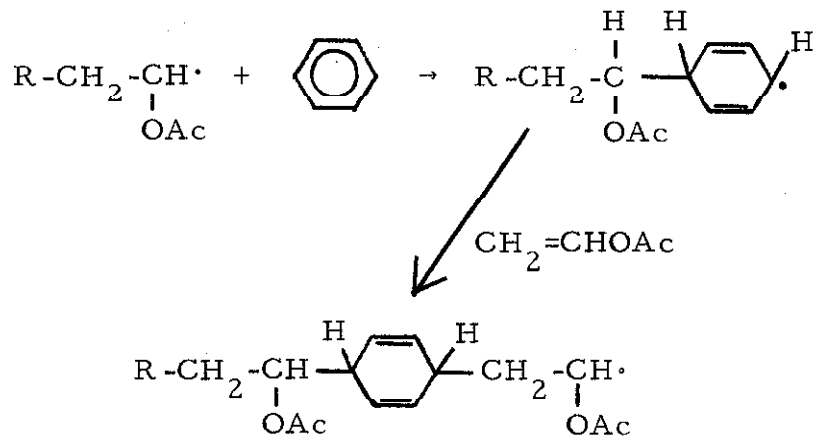
Dr. Hammond (22) has suggested the possible formation of a copolymer of styrene and methylferrocene to account for the anomalous UV absorption spectra. Analogous radical reactions have been suggested several times in the literature.

An attack on an aromatic ring has been suggested to account for the cross-linkages in vinyl benzoate and vinyl acetate copolymers (23).



Similarly, Stockmayer (24) has observed that benzene and other aromatics retard the polymerization of vinyl acetate to a much higher degree than can be accounted for by a chain transfer mechanism. He has suggested a copolymerization between vinyl acetate and benzene. By

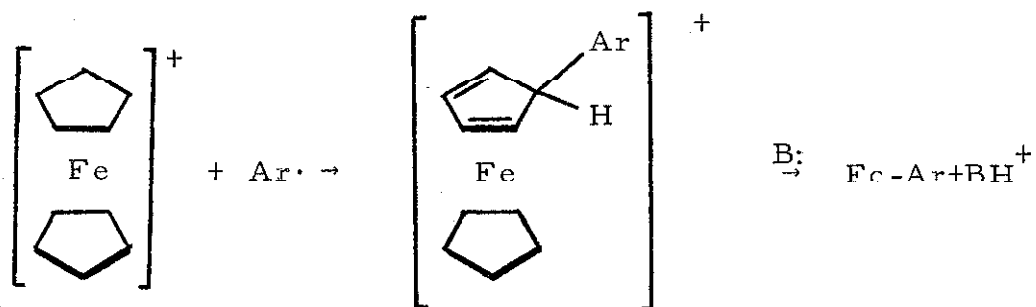
using C^{14} -labeled benzene in the polymerization, he has found the anticipated degree of inclusion of benzene in the polymer.



Stockmayer further predicts that the analogous reaction in a styrene system will have a reaction constant not less than 10^{-5} at 60°C .

Nitrobenzenes had, in fact, been found to retard the polymerization of styrene (25).

Little (26) has observed the coupling of the ferrocenium ion with an aromatic free radical and suggests the following reaction path:

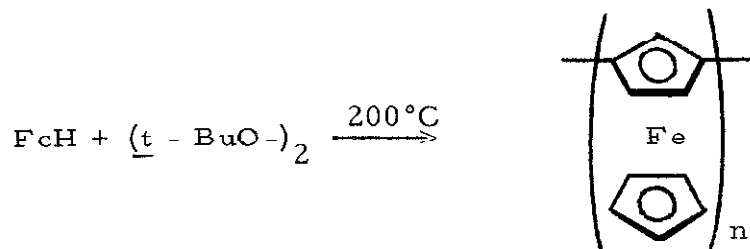


where $\text{Ar}\cdot$ is $\cdot\text{---}\text{C}_6\text{H}_4\text{---N=N---C}_6\text{H}_4\text{---X}$, etc.

Beckwith (27) has found that ferrocene is, in general, unreactive to free radical attack, while the ferrocenium ion is highly reactive. All

of the reactions which he has described, however, are of a chain transfer nature, and would not account for the copolymerization of ferrocene with styrene.

One report does exist in the literature (28) of the formation of a polymer from ferrocene heated with an equal amount of t-butyl peroxide. The polymer is reported to have a molecular weight of 2500, and to be produced in a 16 per cent yield. This polymer has been formed, however, in a solution containing an abnormally high radical concentration, and is probably not a representative ferrocene reaction.



The inclusion of ferrocene in the styrene polymer would result in the occasional appearance of ferrocenyl radicals on the growing polymer chains. If these groups immediately attack further styrene monomers, the net result would be an increase in the number of ferrocenyl units in the final polymer (such as has been observed), but no change in the chain transfer constant or rate of polymerization compared to a system without copolymerization. If the ferrocenyl radicals on the polymer do not react with styrene monomer immediately, some will eventually couple with other radicals, resulting in the premature

termination of two polymer chains. This behavior would result in an overall depression of the rate of polymerization, an effect which has also been observed. Further evidence should be sought to support each of these effects.

The chain transfer constant for unsubstituted ferrocene should be studied to find out if the styryl radical is capable of attacking the ring protons as well as the methyl group. If the growing styrene chain is capable of incorporating ferrocene into the polymer, then the possibility of the formation of a copolymer should be considered.

A polymerization in a suitably high concentration of ferrocene may yield a polymer containing sufficient ferrocene for an n.m.r. study. A resolved n.m.r. spectrum of the protons on the ferrocenyl rings would provide sufficient information to determine the number of ring substituents and hence the location of the ferrocene on the polymer (in the chain or as a terminal group).

The chain transfer constant of methylferrocene should be studied as a function of the monomer to transfer agent ratio to insure that the reaction is first order with transfer agent, and to obtain a more precise value for the transfer constant.

A preliminary experiment was performed to try to detect the electron paramagnetic resonance spectrum of the ferrocenylmethyl radical. Crystalline methylferrocene was irradiated with 45 Kv

tungsten X-rays, both at room temperature and liquid nitrogen temperature for 20 hours. Both samples were examined in an X-band e.p.r. spectrometer. One hundred kilocycle modulation was used, and the magnetic field was swept from 1000 to 4000 gauss. No signal was observed at either temperature. This observation does not exclude the existence of free radicals, as the spectral lines may be exchange broadened to the point where they could not be observed over the noise. Alternatively, the anisotropy of the crystal field may be so large that the lines may be broadened out by the random orientation of the radicals in the powder sample.

EXPERIMENTAL

Styrene monomer: Stabilized styrene monomer (200 ml) was washed four times with 5% NaOH solution. The monomer was then washed four times with distilled water, the final wash solution having a pH less than 8. The monomer was dried over anhydrous calcium chloride and distilled in a Vigreux column. The fraction boiling at 40.0-40.5°C and 15 mm Hg was collected and stored at about 5°C until used.

Polymerization: Weighed quantities of methylferrocene were dissolved in styrene monomer. The styrene solutions were transferred to glass ampules and frozen with liquid nitrogen. They were evacuated to less than 1 mm Hg on a vacuum line, and then isolated from the line. The styrene was allowed to melt and de-gas, and then was refrozen. This procedure was repeated twice more to remove as much gas as possible from the solutions. The ampules were then sealed and put in an oil bath at $70.05 \pm 0.02^\circ\text{C}$. At the appropriate time, each ampule was taken out of the bath and a known weight of its contents poured into 200 ml methanol. The resulting precipitate of polystyrene was allowed to digest for at least a day, and then was collected by vacuum filtration. The polystyrene was dissolved in 25 ml benzene and re-precipitated in 200 ml more methanol. The process was repeated once more, and the final polystyrene samples were carefully dried under vacuum and weighed.

Viscosimetry: Viscosity measurements were made with a #100 Ostwald Viscometer. A weighed quantity of the polystyrene was dissolved in 25.0 ml benzene. A 10.0 ml sample was put aside for dilution and 10 ml were transferred to the viscometer. Fall times were measured until a consistent set of data was obtained, and an average value was used in the calculations. The reserve sample was diluted with 10.0 ml benzene and a 10.0 ml sample was again put in reserve. Fall times were measured for the remaining sample and the cycle was repeated. Dilutions were continued in this way until the fall time of the solution approached that of pure benzene.

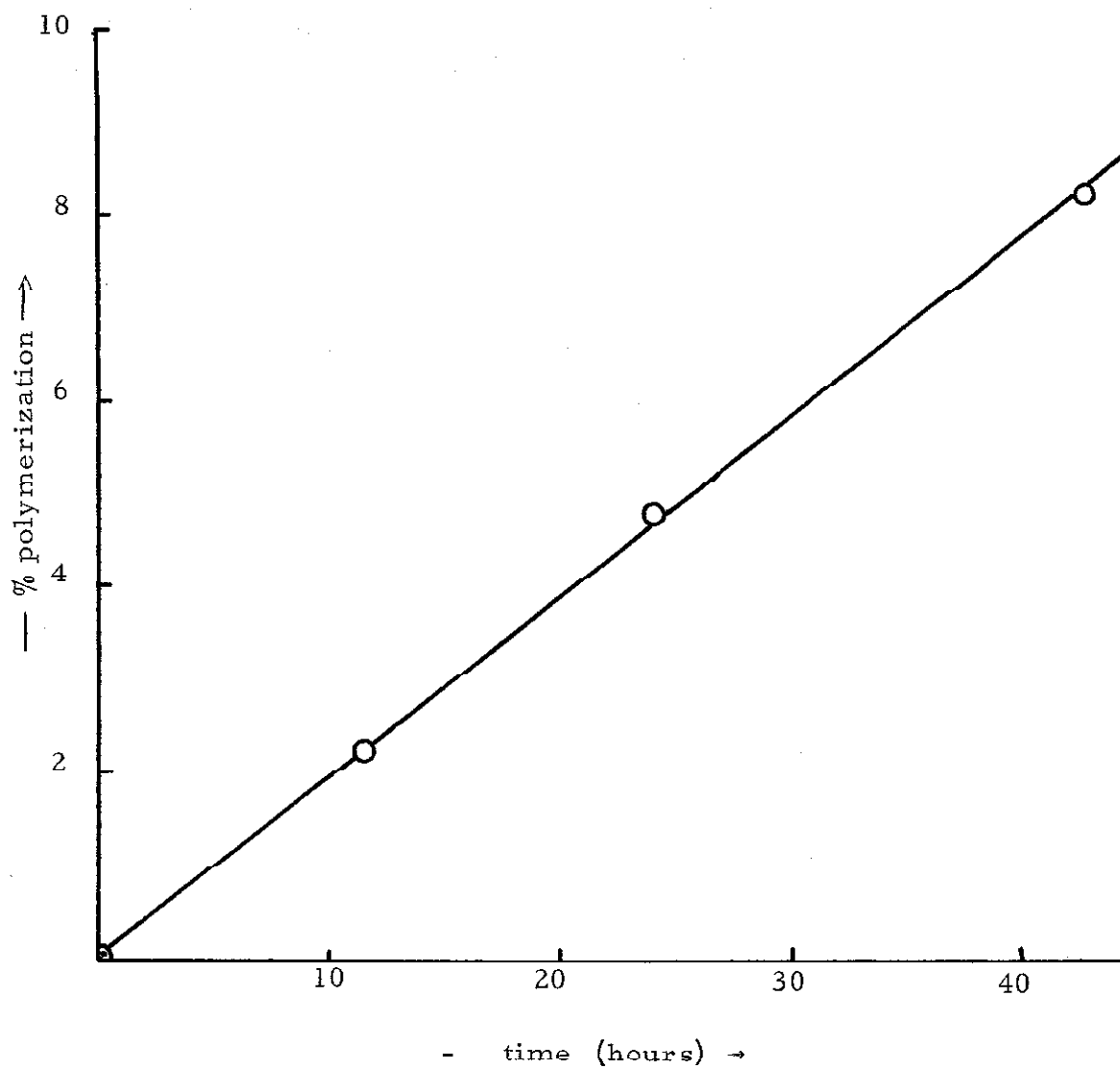


FIG. II. Rate of polymerization of styrene at 70.0°C.

FIG. III. $\frac{\eta_{sp}}{c}$ vs. concentration for solutions of polystyrene in benzene.

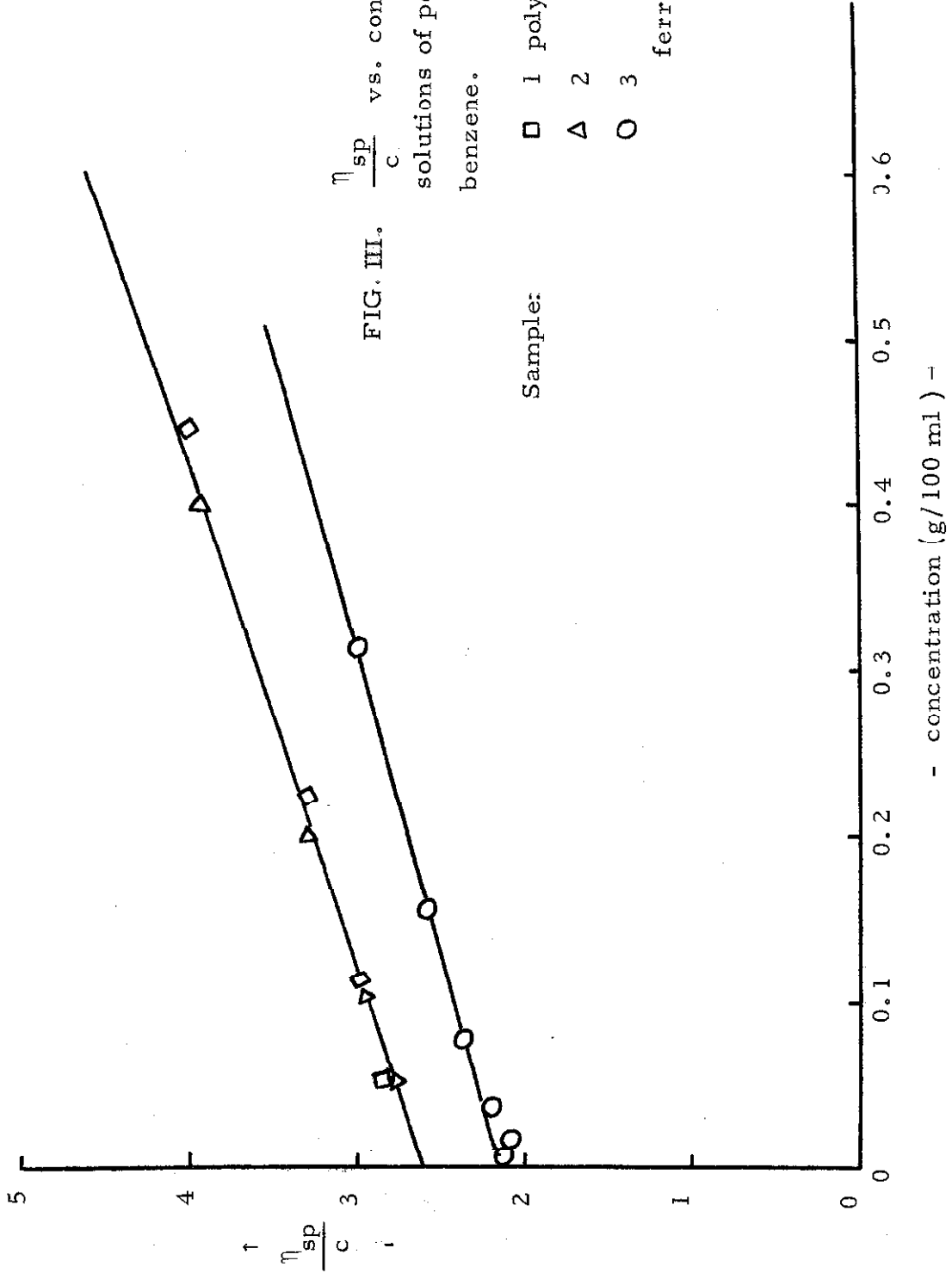


TABLE V

Degree of Polymerization of Styrene Samples

Sample	$\frac{[S]}{[M]} = \frac{[F_c - CH_3]}{[\phi - CH = CH_2]}$	% Polymerization	$[\eta]$	\bar{M}	\bar{P}
1	0	7.05	2.62	6.64×10^5	6,380
2	0	4.53	2.62		
3	0.611	1.52	2.18	5.16×10^5	4,960

APPENDIX A: Chain Transfer Constant for Methylferrocene

$$\text{Eq. 14: } \frac{1}{\bar{P}} = \frac{1}{\bar{P}_0} + C \frac{[S]}{[M]}$$

$$\bar{P}_0 = 6,380 \quad \frac{[S]}{[M]} = 0.61$$

$$\bar{P} = 4,960$$

$$\frac{1}{4.96} = \frac{1}{6.38} + 0.61 \times 10^3 \times C$$

$$C = 0.74 \times 10^{-4}$$

Ferrocene Incorporated in Polymer by Chain

Transfer Reaction

$$C \frac{[S]}{[M]} = \frac{R_{\text{transfer}}}{R_{\text{polymerization}}} = \left| \frac{[F_c]}{[sty]} \right|_{\text{final polymer}} = .45 \times 10^{-4}$$

$$\left| \frac{[sty]}{[F_c]} \right|_{\text{in polymer}} = 2.2 \times 10^4$$

APPENDIX B: Ratio of Ferrocene to Styrene by Ultraviolet
Absorption Spectroscopy

wavelength of measurement		3900 Å	3100 Å
copolymer absorption	=	17.8 per g/ml	50 per g/ml
pure polystyrene absorption	=	5.4 "	8.7 "
Δ	=	12.4	41.3
methylferrocene absorption	=	439 "	3910 "
methylferrocene per gram polystyrene		.0283 g	.0105 g
mole ratio is 0.52 x weight ratio			
$\frac{[\text{Fc-Me}]}{[\text{poly}]}$	=	.0147	.0055
or			
1 ferrocene per (styrene units)		68	180

Calculation of Concentrations in a Sample of Known
Composition by Ultraviolet Spectroscopy

Sample: 0.00018 g Fc-Me = x
 0.0020 g polystyrene = y

"A" is the absorption per gram per milliliter of solution

Absorption of $A_{3900 \text{ \AA}} = 0.09$ $A_{3100 \text{ \AA}} = 0.755$
known solution:

$$A_{3900 \text{ \AA}} = 439 x + 5.4 y = 0.09$$

$$A_{3100 \text{ \AA}} = 3910 x + 8.73 y = 0.755$$

or: x = 0.00019 g Fc-Me

 y = 0.0012 g polystyrene

Calculation of Concentrations in the Copolymer from the
Ultraviolet Absorptions at Two Points

$$A_{3900} = 0.28 \qquad A_{3100} = 0.79$$

Calculated
concentrations:

$$x = 1.05 \times 10^{-4} \text{ g Fc-Me}$$

$$y = 4.3 \times 10^{-2} \text{ g styrene}$$

wt ratio $\frac{x}{y} = 2.44 \times 10^{-3}$

or: 1 Fc-CH₃ per 780 styrene monomers

REFERENCES

1. W. E. Mochel and J. H. Peterson, *J. Am. Chem. Soc.*, 71, 1426 (1949).
2. W. V. Smith, *J. Am. Chem. Soc.*, 71, 4077 (1949).
3. J. C. Bevington, H. W. Melville, and R. P. Taylor, *J. Poly. Sci.*, 12, 449 (1954).
4. C. Walling, "Free Radicals in Solution," J. Wiley & Sons, New York, 1957, p. 66.
5. L. M. Arnett, *J. Am. Chem. Soc.*, 74, 2027 (1952).
6. F. R. Mayo, R. A. Gregg, and M. S. Matheson, *J. Am. Chem. Soc.*, 73, 1691 (1951).
7. F. R. Mayo, *J. Am. Chem. Soc.*, 65, 2324 (1943).
8. F. R. Mayo, *J. Am. Chem. Soc.*, 76, 6133 (1954).
9. Ref. 4, p. 183.
10. H. Staudinger and L. Schwalbach, *Ann.*, 488, 8 (1931).
11. P. J. Flory, *J. Am. Chem. Soc.*, 59, 241 (1937).
12. R. A. Gregg, F. R. Mayo, *Disc. Faraday Soc.*, 2, 328 (1947).
13. Ref. 4, pp. 152-3.
14. P. J. Flory, "Principles of Polymer Chemistry," Cornell University Press, Ithaca, N. Y. (1953), Chapter VII.
15. E. O. Kraemer, *Ind. Eng. Chem.*, 30, 1200 (1938).
16. H. Staudinger and W. Heuer, *Ber.*, 63, 222 (1930).
17. Ref. 4, p. 158.
18. D. W. Hall, Ph. D. Thesis, California Institute of Technology (1963), p. 72.

19. E. M. Arnett and R. D. Bushick, *J. Org. Chem.*, 27, 111-5 (1962).
20. E. A. Hill, III, Ph. D. Thesis, California Institute of Technology (1961), pp. 1-13.
21. Ref. 4, p. 165.
22. Private communication with Dr. G. S. Hammond.
23. G. E. Ham and E. L. Ringwald, *J. Polymer Sci.*, 8, 91 (1952).
24. W. H. Stockmayer and L. H. Peebles, Jr., *J. Am. Chem. Soc.*, 75, 2278 (1953).
25. C. C. Price and D. A. Durham, *J. Am. Chem. Soc.*, 65, 757 (1943).
26. W. F. Little and A. K. Clark, *J. Org. Chem.*, 25, 1979 (1960).
27. A. L. J. Beckwith and R. J. Leydon, *Tetr. Letters*, No. 6, 385 (1963).
28. V. V. Korshak, S. L. Sosin, and V. P. Alekseeva, *Doklady Akad. Nauk SSSR*, 132, 360 (1960), Chemistry Section. Also English translation, pp. 517-520.

PART II

PROTONATION OF METALLOCENES

INTRODUCTION

The solvolytic behavior of diastereomeric ferrocenylcarbonyl acetates has been examined(1,2) and interpreted as indicating a direct bonding of the metal atom to the cationic carbon of α -metallocenyl-carbonium ions. This direct participation of the metal electrons in chemical bonds other than those to the cyclopentadienyl rings should also be present in other suitably chosen systems.

Green (3) has studied biscyclopentadienylrhenium hydride and its protonated cation and found the hydride protons bonded directly to the rhenium atom. This observation suggests that a similar bond may also be found in ferrocene in a strongly acid medium.

The present work was undertaken as a further probe of the ability of the central metal atom in a metallocene molecule to participate in chemical reactions of the metallocene.

RESULTS

The chemical shifts obtained in these studies are reported in Table I. This work was a cooperative effort with a similar study undertaken at Brandeis University by Rosenblum and co-workers (3), and their results are also presented in Table I.

The first apparent discrepancy in the two sets of results is that the proton resonances were found by Rosenblum to be at consistently higher magnetic fields than those indicated by the present study. This difference is probably the result of selective solvation effects on reference standards. Rosenblum used trimethylacetic acid as an internal reference, and assigned to it a tau value of 8.77. This is the value suggested by Tiers (4) for the neutral molecule in carbon tetrachloride solutions, and should not be applied to a system where the molecule may exist as $\text{Me}_3\text{CCO}_2\text{H}_2^+$. Tetramethylammonium bromide was used as a reference in our studies. This would exist as the tetramethylammonium ion both in the boron-trifluoride hydrate solutions and in ethanol and carbon tetrachloride, which were used as the solvents to determine the tau value of the Me_4N^+ . The tau value determined in these solvents agrees with the value observed by Tiers (4) in trifluoroacetic acid to within 0.03 ppm.

The second and more significant disparity between this work and the results observed by Rosenblum occurs in the spectrum of

TABLE I

Chemical Shifts of Protonated Metalloenes

metallocene ^a	This Work			Rosenblum(3)		
	τ^b	$\Delta\tau$ metal-ring	area ratio	τ	$\Delta\tau$ metal-ring	area ratio
ferrocene	4.67 ^c	6.94	9.9±0.5	4.99	7.08	11±2
	11.61			12.07		
ruthenocene	4.29	12.53	10.4	4.67	12.5	16±2
	16.82			17.2		
osmocene	4.31 ^c	6.20	10.4	4.83	-----	
	9.35 ^c					

a. All compounds studied as 5-20% solutions in $\text{BF}_3 \cdot \text{H}_2\text{O}$.

b. Chemical shifts measured against $\text{Me}_4\text{N}^+ \text{Br}^-$ as an internal reference.

$\text{Me}_4\text{N}^+ \text{Br}^-$ was assigned $\tau = 6.70$.

c. Doublet, $J = 1.4$ cps.

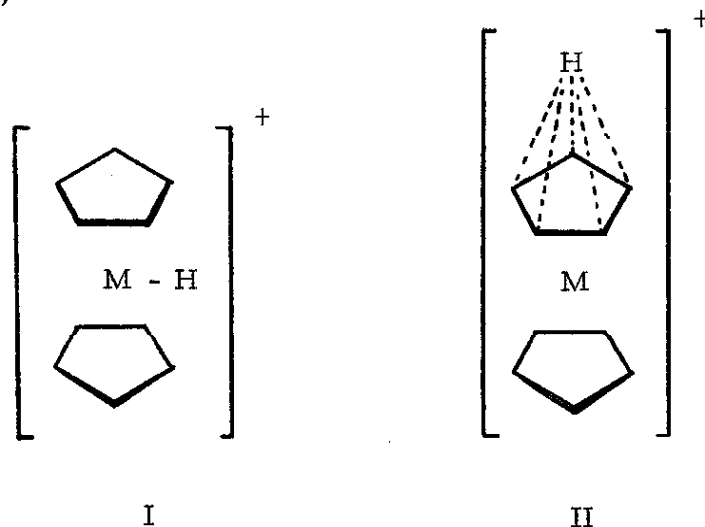
d. Triplet, $J = 7.0$ cps.

osmocene in boron trifluoride hydrate. Rosenblum reports only a solvent peak and a sharp singlet attributed to the cyclopentadienyl ring protons. We also observed a 1:2:1 triplet at $\tau = 9.35$, which is not observed if the osmocene is dissolved in trifluoroacetic acid instead of boron trifluoride monohydrate.

The triplet was found to coalesce to a single sharp peak when fluorine was decoupled from the proton resonances of the sample by irradiation at 56.4297 mc. The fluorine nuclear magnetic resonance spectrum was examined in detail, and a weak multiplet was observed 900 cps downfield from the main fluorine resonance. The multiplet has a 7 cps coupling constant, and the center five peaks of what is probably an eleven peak multiplet are clearly resolved above the noise (see Figure IV). These observations prove that the triplet was generated by the osmocene ring protons being split by two fluorine atoms on the molecule.

DISCUSSION

Structures I and II have been considered to account for the n. m. r. spectrum of the metallocenes in boron trifluoride hydrate solutions (3).



As the ring protons of ferrocene are split into a doublet (Fig. I), either structure could account for the spectrum. In I the doublet would be caused by the spin-spin interaction of the ring protons with the metal-bonded proton, while in II the doublet would be caused by a slight chemical shift of the protons on the top ring relative to the bottom ring protons. However, the doublet separation remains constant when the spectrum is observed at 40 mc or at 60 mc, so it cannot be caused by a chemical shift phenomenon, but must originate in a spin-spin coupling interaction. Structure II must therefore be eliminated.



A further piece of evidence in support of structure I is the observation that biscyclopentadienylrhodium hydride has an analogous structure (2). Table II presents the τ values Wilkinson found for biscyclopentadienylrhodium hydrides.

Wilkinson also substituted deuterium for the protons on the metal atom. He observed the anticipated loss of spin-spin coupling to the ring protons and loss of the $\tau = 23$ resonance, which was further proof for his interpretation of the spectra. When a similar experiment was attempted with ferrocene, the boron trifluoride deuterate solution caused rapid and complete equilibration of the ring protons with the solvent.

The n. m. r. spectra of the protonated metallocenes provide a means of estimating the rate of exchange of the metal-bonded proton with solvent. The spin-spin doublet of the ring proton peak of ferrocene in Figure I appears to be just starting to coalesce, so the lifetime of a proton on the iron may be estimated to be slightly more than $1/(2\pi \cdot 1.4) = 0.1$ sec. If the boron trifluoride solution is not completely saturated with boron trifluoride such that there is a trace of hydronium ion, the rate of exchange of the iron bonded proton increases sufficiently so that the doublet peak coalesces into a broad singlet. The ring protons on ruthenocene in boron trifluoride hydrate, on the other hand, appear as a sharp singlet (Fig. II), so the lifetime of a proton on the ruthenium atom is much less than 0.1 sec. Since there

TABLE II

Tau Values for Biscyclopentadienylrhenium Hydrides

	Ring Protons	Metal Protons
 Re - H in benzene	5.95 ^a	23.1
		
$\left[\begin{array}{c} \text{Cyclopentadienyl ring} \\ \text{H - Re - H} \\ \text{Cyclopentadienyl ring} \end{array} \right]^+$	in dilute HCl 4.0	23.2

a. Measured relative to an external water standard and converted to the Tiers scale.

is no indication of the metal proton peak starting to coalesce with the solvent peak, one also has a lower limit to the lifetime of this metal-bound proton. Its lifetime, τ , may then be estimated as:

$$\tau \gg 1/(2\pi \cdot 935) \text{ or } \tau \gg 10^{-4} \text{ sec}$$

The triplet which is observed in the spectrum of the boron trifluoride hydrate solution of osmocene is believed to be generated by a phenomenon not previously observed in these systems. Its exact nature will be discussed shortly. The osmocene must exist as some form of complex or charged species to account for its solubility in boron trifluoride hydrate and in trifluoroacetic acid; yet only the triplet is unaccounted for in the one case and nothing at all appears in the corresponding proton resonance region of the other. If the metallocene is still protonated, which seems likely in the trifluoroacetic acid solution, the proton probably exchanges so rapidly with the solvent that the two peaks have coalesced. This would imply a rate of exchange of the proton with solvent much greater than 10^4 per second. Table III presents the limits of rates of exchange of the metal-bound proton with solvent for each of the metallocenes.

TABLE III

Rate of Exchange of Metal-bound Proton with Solvent

ferrocene		ruthenocene		osmocene
R_{Fc}	< 10/sec <	R_{Ru}	$\ll 10^4/\text{sec} \ll$	R_{Os}

The 7 cps triplet appearing in the proton resonance spectrum of osmocene in boron trifluoride hydrate at $\tau = 9.85$ (Fig. III) has been shown to be caused by a fluorine spin-spin coupling, though the exact nature of the species responsible for the spectrum is still undefined. A clue to its identity may be present in Table IV, which lists the properties which set osmocene apart from the other metallocenes studied. All of the data in part "A" of the table indicate that osmocene is the weakest Lewis base. The data in part "B" of Table IV, to the contrary, suggest the opposite trend in the metallocenes. As osmium is the largest of the three metals, the effects observed in Table IVB may be accounted for by the greater accessibility of the non-bonding metal orbitals of the osmium atom to the reaction center. An explanation for the n.m.r. triplet can be considered which requires a central metal atom that is less basic than iron, but sterically more accessible.

The triplet in the proton resonance spectrum has about one tenth the area of the main ring peak, so the complex which generates it would account for about 10 per cent of the osmocene in solution. This osmocene complex is probably in a slow equilibrium with the rest of the osmocene. The remaining 90 per cent probably exists in a protonated form similar to the other metallocenes, but with the proton exchanging with solvent rapidly enough to prevent the appearance of another resonance peak.

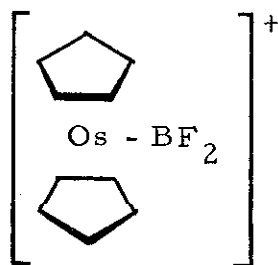
TABLE IV

Properties of Metallocenes

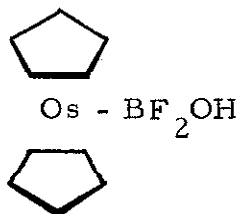
A.	ferrocene	ruthenocene	osmocene
Electronegativity of metal(5)	1.8	2.2	2.2
Oxidation potential $E_{\frac{1}{4}}$ vs. SCE (6)	+0.307v	+0.693v	+0.633v
Relative reactivity toward electrophilic attack (7)	$\bar{F}_c >$	$\bar{R}_u >$	\bar{O}_s
Strength of Lewis base (3) ^a	$\bar{F}_c >$	$\bar{R}_u >$	\bar{O}_s
Distance between cpd rings	3.25A(8)	3.68A(9)	3.71A(10)
B.			
S_{Ni} solvolysis rates (11)	$\bar{F}_c <$	$\bar{R}_u <$	\bar{O}_s
Strength of hydrogen bonds (12)	$\bar{F}_c <$	$\bar{R}_u <$	\bar{O}_s

- a. The relative rates of exchange of the proton on the metallocene metal presented in this paper indicate that the order of increasing basicity of the metallocenes is: $\bar{O}_s < \bar{R}_u < \bar{F}_c$.

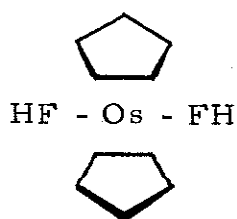
Structures III, IV, and V are suggested to account for the triplet.



III

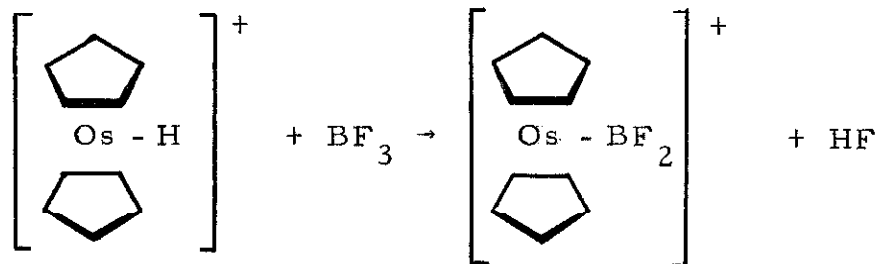


IV

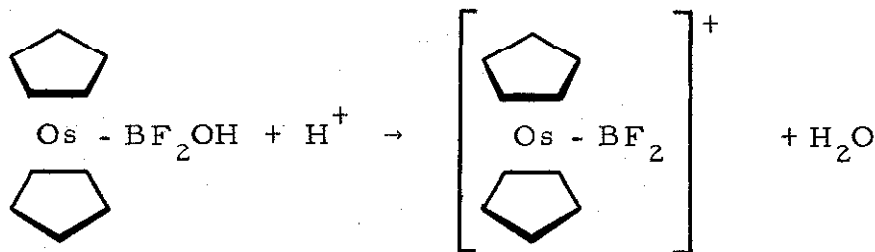


V

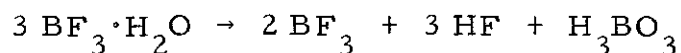
Complex III may be formed by the reaction of boron trifluoride with protonated osmocene:



or by protonation and dehydration of an intermediate similar to IV:



All of the rest of the required boron fluorides have been observed in boron trifluoride-hydrate solutions (13), including hydrogen fluoride (14) from the reaction:



Boron exists in nature as two stable isotopes: B^{10} with a nuclear spin of 3 and a 19% natural abundance, and B^{11} with a spin of 3/2 accounting for the remaining 81% of the boron. One would expect to find boron-fluorine spin-spin interaction in structures III and IV unless the nuclear electric quadrupole of the boron is causing the nuclei to relax too rapidly. If the boron is relaxing at an intermediate rate relative to the boron-fluorine coupling constant, the fluorine resonance would be broad. If, on the other hand, the relaxation frequency of the boron is considerably greater than the coupling constant, the fluorine resonance would be sharp and no evidence of coupling to the boron would be observed.

The fluorine magnetic resonance spectra of boron trifluoride complexes with amines and others have been studied (15). Only in a complex with triethylamine is the electric quadrupole relaxation slow enough to allow the observation of a boron-fluorine coupling ($J = 18$

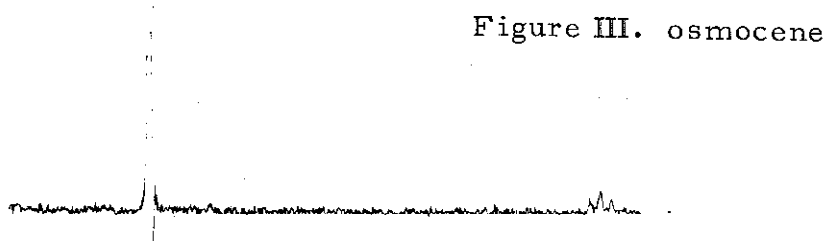
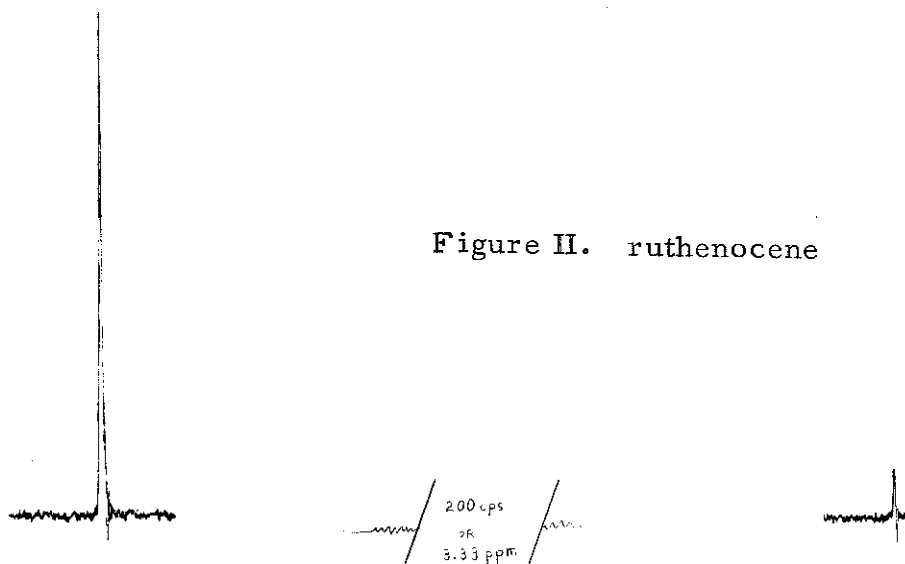
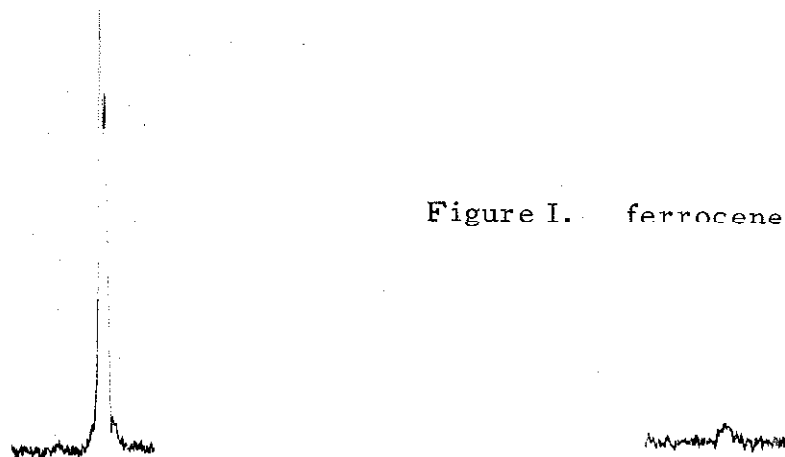
cps). The quadrupole relaxation in a boron trifluoride-pyridine complex is fast enough to remove any spin-spin splitting in its spectrum. Spin-spin interactions were not observed in the boron trifluoride complexes with anisole and tetrahydrofuran, but the analysis is complicated by a rapid exchange of ligands in the complex.

One may generalize that a less symmetric electric field around the boron will allow a greater interaction of the boron nuclear quadrupole with the field and a faster rate of relaxation. The line width of the fluorine resonance of boron trifluoride hydrate is ≤ 7 cps at half height, with no indication of splitting by the boron nucleus. The electric field around boron in the osmocene complex III or IV is certainly no more symmetric than around boron in the solvent, so the rate of relaxation of boron in III or IV may easily be sufficient to remove any boron-fluorine coupling.

The magnetic anisotropy of the ligand would be responsible for the large chemical shift of the ring protons in the proton resonance spectrum. In structure IV, the hydroxyl proton, and in structure V, the fluorine-bonded proton would be exchanging with solvent so rapidly that it would not be observed as a separate resonance line.

There is not enough information at this time to indicate which, if any, of the structures is correct. Structure III, however, is preferred, since its positive charge would account for the solubility of the complex in the very polar solvent.

The n. m. r. spectrum of osmocene in (a) fluoroboric acid, or (b) an etherate solution of boron trifluoride might provide additional information on the nature of the species due to the formation of a somewhat similar complex.



The proton magnetic resonance spectra of metallocenes in boron trifluoride hydrate.

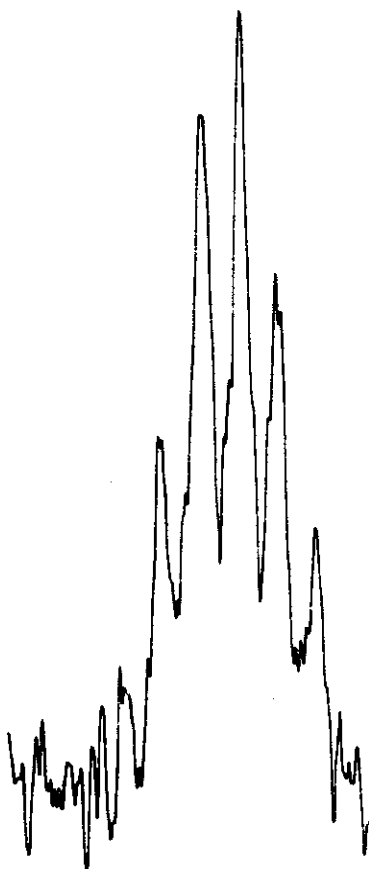


FIG. IV. The fluorine resonance spectrum of osmocene in boron trifluoride hydrate. This multiplet is 900 cps downfield from the main solvent resonance and the peaks are 7 cps apart.

EXPERIMENTAL

The ruthenocene was donated by Dr. Hans Essler, and the osmocene was prepared by Dr. E. A. Hill. All metallocenes were purified by recrystallization from n-hexane.

Commercially available boron trifluoride was purified by passing it through a solution of boric acid in concentrated sulfuric acid. The boron trifluoride was then passed into water at 0°C until the water would absorb no more gas. Additional boron trifluoride was slowly bubbled into the resulting solution for six more hours to insure saturation. Unless the saturation of the solution with boron trifluoride was insured in this way, the n.m.r. spectrum of the final metallocene solution did not exhibit the splitting of the ring proton resonance into the doublet with 1.4 cps splitting.

A length of standard 5 mm pyrex tubing was fused to an A-60 n.m.r. tube and a standard taper joint fused onto this. Samples could then be evacuated and sealed in the n.m.r. tube with no difficulty.

About 0.2 g of crystalline metallocene was introduced into the n.m.r. tube. One milliliter of freshly prepared boron trifluoride hydrate was carefully added to the sample, and the tube tapped just long enough to drive most of the bubbles to the surface. The partially

dissolved metallocene solution was immediately frozen with liquid nitrogen, and then evacuated to 20 microns. With the tube isolated from the vacuum system by means of a stop-cock, the sample was allowed to thaw, and the remaining crystalline metallocene was dissolved in the boron trifluoride hydrate solution. The sample was refrozen and re-evacuated. The tube was carefully sealed with a torch and the sample allowed to thaw.

Samples of ferrocene, ruthenocene, and osmocene were treated in this way, and the n.m.r. spectrum of each was observed on a Varian A-60 n.m.r. spectrometer.

The chemical shifts of the samples were measured relative to an external tetramethylsilane standard in carbon tetrachloride. A correction of 0.07 ppm downfield was introduced to account for the different bulk magnetic susceptibilities of boron trifluoride hydrate and carbon tetrachloride. The correction factor was obtained by comparing the chemical shifts of tetramethylammonium bromide in the two solvents using tetramethylsilane in carbon tetrachloride again as an external standard.

The double resonance experiment was performed with the aid of an "NMR Specialties, Inc." model SD-60 spin decoupler. The proton resonance spectrum was observed on the Varian HR-60 spectrometer while the sample was irradiated at 56.4297 mc to decouple

fluorine spin-spin splittings. When the irradiating energy was turned on, the triplet that normally appears at $\tau = 9.35$ in the spectrum of the boron trifluoride hydrate solution of osmocene coalesced into one sharp peak.

REFERENCES

1. J. H. Richards and E. A. Hill, *J. Am. Chem. Soc.*, 81, 3484 (1959); *J. Am. Chem. Soc.*, 83, 4216 (1961).
2. M. L. H. Green, L. Pratt, and G. Wilkinson, *J. Chem. Soc.*, 3916 (1958).
3. T. J. Curphey, J. O. Santer, M. Rosenblum, and J. H. Richards, *J. Am. Chem. Soc.*, 82, 5249 (1960).
4. G. v. D. Tiers, "Characteristic NMR Shielding Values for Hydrogen in Organic Structures," Minnesota Mining and Manufacturing Co., St. Paul, Minn., 1958.
5. L. Pauling, "The Nature of the Chemical Bond," Cornell University Press, N. Y. (1960), p. 93.
6. T. Kuwana, D. E. Bublitz, and G. Hoh, *J. Am. Chem. Soc.*, 82, 5811 (1960).
7. M. D. Rausch, E. O. Fischer, and H. Grubert, *J. Am. Chem. Soc.*, 82, 76 (1960).
8. E. A. Seibold and L. E. Sutton, *J. Chem. Phys.*, 23, No. 10, 1967 (1955).
9. G. L. Hardgrove and D. H. Templeton, *Acta Cryst.*, 12, 28-32 (1959).
10. F. Jellinek, *Z. Naturforsch.*, 14b, 737-8 (1959).
11. E. A. Hill and J. H. Richards, *J. Am. Chem. Soc.*, 83, 3840 (1961).
12. D. S. Trifan and R. Bacskai, *J. Am. Chem. Soc.*, 82, 5010-11 (1960).
13. C. A. Wamser, *J. Am. Chem. Soc.*, 73, 409 (1951).
14. A. V. Topchiev, S. V. Zavgorodnii, and Ya. M. Paushkin, "Boron Fluoride and Its Compounds as Catalysts in Organic Chemistry," Pergamon Press, N. Y., 1959, p. 21.

15. S. Brownstein, M. Eastham, and G. A. Latremouille, J. Phys. Chem., 67, 1028 (1963).

PART III

AN ANALYSIS OF THE N. M. R. SPECTRA OF
SUBSTITUTED FERROCENES

INTRODUCTION

Though significant work has appeared on the high resolution n. m. r. spectra of various metallocenes (1,2), no detailed analysis of these systems with three or four dissimilar proton interactions on the same ring has been reported. Detailed analyses have, however, been reported for many other aromatic systems. Representative results appear in Table I. In these analyses, the matrix elements have been calculated and the energy levels and intensities of transitions have been tabulated for the general cases of the AB (3), AB₂ (3), ABX (3,4), A₂B₂ (5), and AB₂X₂ (6) systems (7).

The purpose of the present work was to examine homoannularly disubstituted and monosubstituted ferrocene derivatives, treating them as representative ABX and ABCD systems, respectively. To this end, the n. m. r. spectra of a series of acetyl-alkylferrocenes have been studied in a variety of solvents and the chemical shifts and coupling constants are reported.

TABLE I

Typical N.m.r. Parameters for Five- and Six-Membered Rings

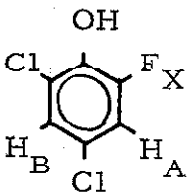
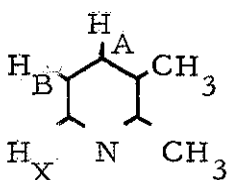
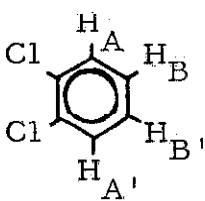
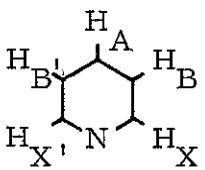
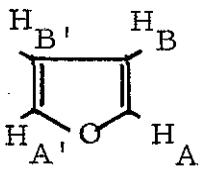
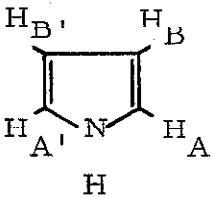
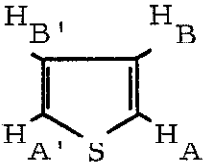
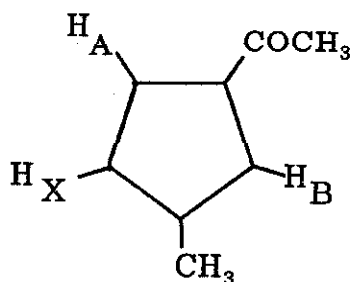
Compound	Ref.	Coupling Constants	Chemical Shifts
	4	$J_{AX} = 9.6$ $J_{BX} = -2.1$ $J_{AB} = 2.3$	
	3	$J_{AX} = 1.3$ $J_{BX} = 5.0$ $J_{AB} = 7.35$	$\nu_A - \nu_B = 11.7$ $\nu_{AB} - \nu_X = 43.4$
	5	$J_{AA} = 0$ $J_{BB} = 8.3$ $J_{AB'} = 1.7$ $J_{AB} = 8.3$	$\Delta \nu = 10.1$
	6	$J_{BB'} = 1.6$ $J_{XX'} = 0.4$ $J_{AB} = 7.5$ $J_{AX} = 1.9$	$J_{BX} = 5.5$ $J_{BX'} = 0.9$ $\nu_A - \nu_B = 15.0$ $\nu_A - \nu_X = 45.6$
	8	$J_{AB} = 1.3$ $J_{AB'} = 1.3$ $J_{BB'} = 3.5$	$\Delta \nu = 42$

TABLE I (continued)

Compound	Ref.	Coupling Constants	Chemical Shifts
 <p style="text-align: center;">H</p>	8	$J_{AB} = 2.1$ $J_{AB'} = 2.1$ $J_{BB'} = 2.8$	$\Delta\nu = 8$
	9	$J_{AB} = 5.0$ $J_{AB'} = 1.1$ $J_{AA'} = 2.7$ $J_{BB'} = 3.3$	$\Delta\nu = 5.0$

RESULTS

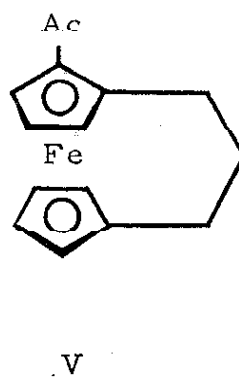
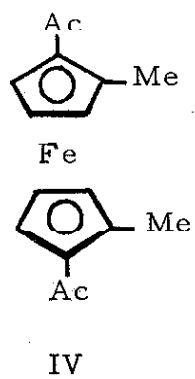
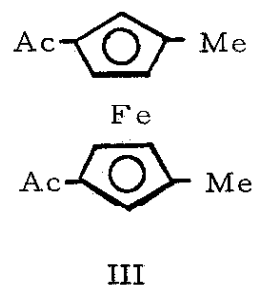
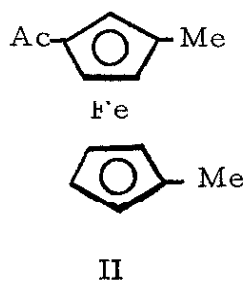
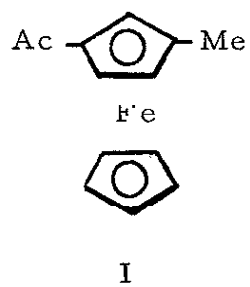
The n. m. r. spectrum of 1, 1'-diacetyl-3, 3'-dimethylferrocene (III) in benzene is presented in Figure 1. The cluster of peaks at lower magnetic field has twice the area of the higher field multiplet. The substance was therefore treated as an ABX system with the protons defined as in VI, an assignment which is also consistent with the expected effect of the acetyl substituent on the chemical shifts of the various protons.



VI

The carbonyl group in acetyl ferrocene is normally coplanar with the cyclopentadienyl ring (1, 10). Because of the magnetic anisotropy of the carbonyl groups (11), one will expect the protons adjacent (alpha) to the acetyl group to be more strongly deshielded than the beta proton. That the methyl group does not substantially perturb the ring proton resonance is indicated by the fact that the ring protons in methylferrocene all appear at 238 cps relative to TMS with no significant difference in chemical shift between the alpha and beta protons.

TABLE II
Compounds Studied



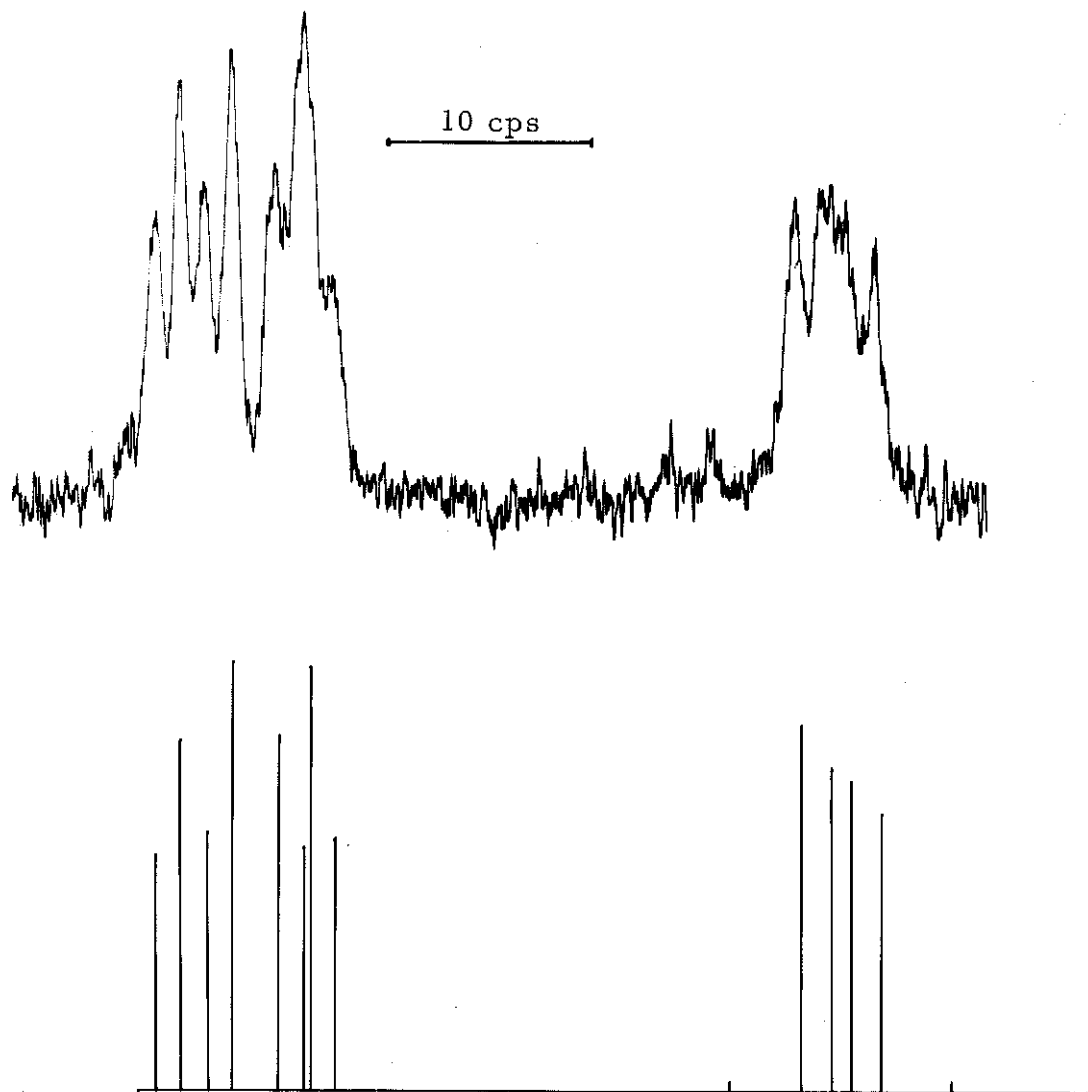


Figure 1: The n.m.r. spectrum of 1,1'-diacetyl-3,3'-dimethylferrocene in benzene.

This would lead one to expect the two alpha protons to appear at lower field than the single beta proton, which is borne out by the relative areas of the two absorptions. The analysis of this spectrum by the procedure of Pople et al. (12) leads to the following parameters:*

$$\begin{array}{ll} J_{AB} = 1.2 \text{ cps} & \nu_A - \nu_B = 5.4 \text{ cps} \\ J_{AX} = 2.5 \text{ cps} & \nu_{AB} - \nu_X = 29 \text{ cps} \\ J_{BX} = 1.5 \text{ cps} & \end{array}$$

Though the experimental spectrum does not contain enough information to determine the absolute sign of any coupling constant. J_{AX} and J_{BX} must have the same sign. This consideration applies to all the ABX systems reported in this paper and all coupling constants have been arbitrarily assigned positive values.

In a similar fashion, the parameters were obtained for the other systems and are reported in Table IV. The parameters so obtained were used to calculate theoretical spectra using the Wiberg computer program (13) on an IBM 7090. The spectrum calculated for III is shown in Figure 1. In all cases, the calculated and experimental spectra were in good agreement.

A different approach was used to analyze the spectrum of the mono-substituted ring of V. Reasonable values were assigned to the coupling constants between each set of protons in what is essentially an ABCD system. Likely sets of chemical shifts were chosen, and theoretical spectra were calculated using the Wiberg program. Several sets of parameters predicted spectra remarkably similar to the observed

* A description of this analysis is given in Appendix I.

one. This ambiguity is coincidental and due to the unusual circumstances that coupling constants $J_{23} \approx J_{34} \approx J_{45} \approx 2J_{21} \approx 2J_{25} \approx 2J_{35}$.

The problem was complicated by the fact that the multiplet from one of the protons is hidden under the AB multiplet of the other ring. The difficulty was resolved by observing the n.m.r. spectrum of V at 100 mc.* where the multiplets were shifted enough to allow a unique assignment of parameters. The correct combination was chosen on the basis of relative peak intensities. The approximate parameters were entered into a computer program of Swalen (14) which, by application of a reiterative technique, determined that set of parameters most closely fitting the experimental spectrum. The resulting parameters are included in Table IV, and the experimental and theoretical spectra of V are shown in Figure 2.

These calculations do not specify whether the acetyl group is over the 2' proton or the 5' proton. Consideration of the magnetic anisotropy of the carbonyl suggests that the acetyl is over the 2' proton, as indicated in Table IV. This point will be discussed in greater detail shortly.

* For this we thank the Varian Associates.

Figure 2: The n.m.r. spectrum of the unacetylated ring of 2-acetyl-1,1'-trimethyleneferrocene in benzene. The first multiplet of the experimental spectrum also includes the AB portion of the other ferrocene ring.

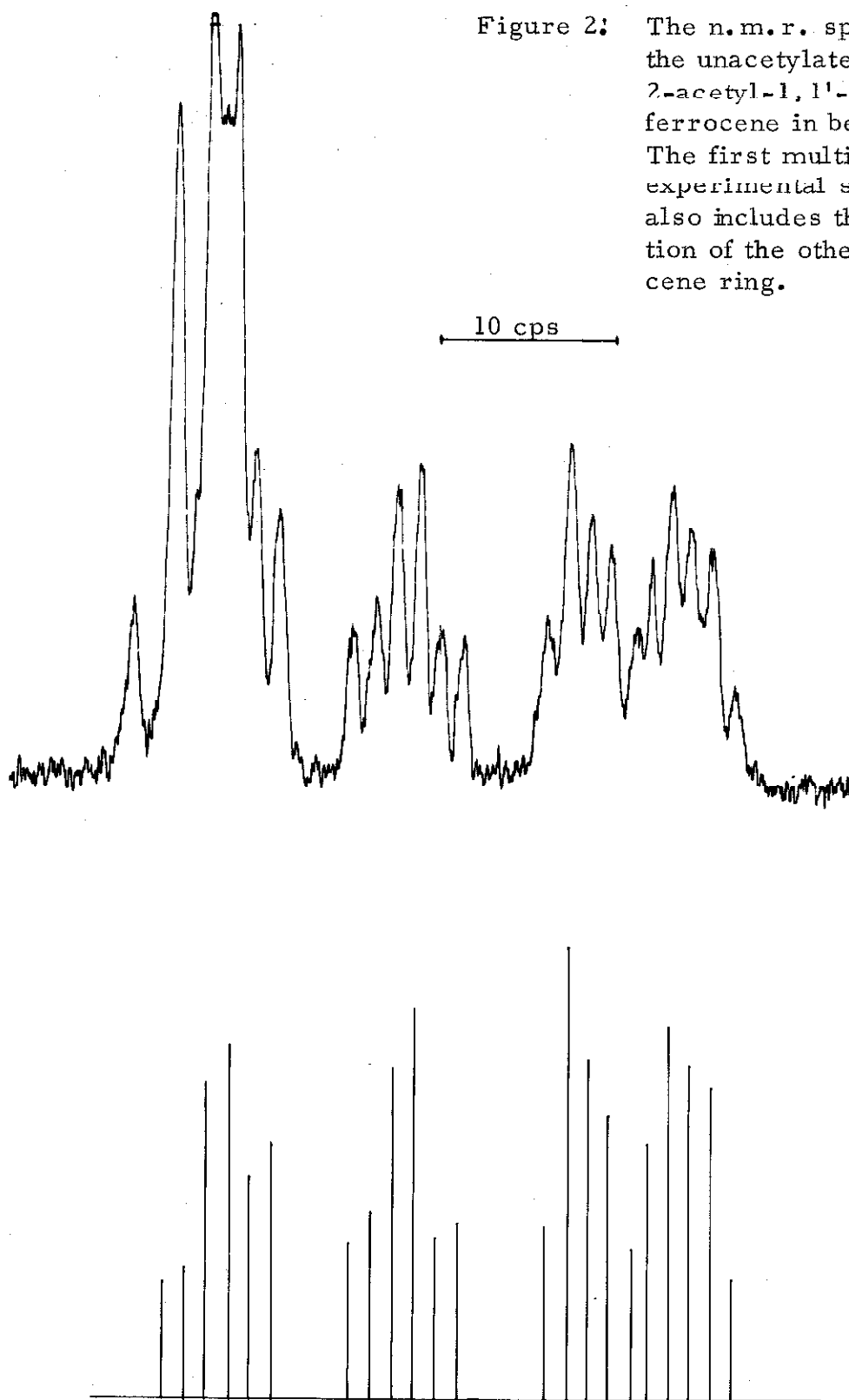


TABLE III

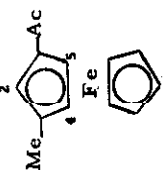
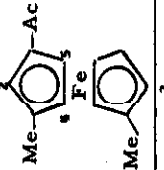
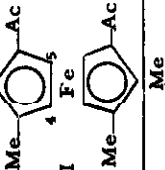
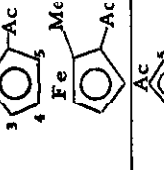
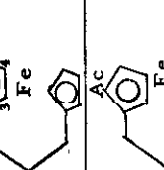
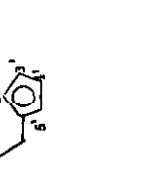
Chemical Shift of Ferrocene Relative to Tetramethylsilane^a

Solvent	CCl_4	CHCl_3	C_6H_6
Chemical Shift ^b	246	252	243

a. Measurements made with ~ 10 mg of ferrocene and 0.04 ml TMS together in 1 ml of solvent.

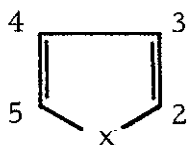
b. Reported in cycles per second downfield from TMS.

TABLE IV
 N. M. R. PARAMETERS

Compound	Solvent	ν_1	ν_2	ν_3	ν_4	ν_5	J_{23}	J_{24}	J_{25}	J_{34}	J_{35}	J_{45}
I 	CCl_4	0.0	-32.7	-	-13.5	-29.5	-	1.0	1.4	-	-	2.5
	$CHCl_3$	+1.6	-32.3	-	-16.6	-31.3	-	1.1	1.5	-	-	3.1
	ϕH	+10.2	-30.2	-	-2.4	-30.6	-	1.45	1.4	-	-	2.45
II 	CCl_4	+9.4	-24.4	-	-8.1	-24.6	-	1.5	1.1	-	-	2.5
	$CHCl_3$	+10.2	-24.7	-	-9.7	-25.5	-	1.03	1.5	-	-	2.77
	ϕH	+16.0	-23.6	-	+1.8	-27.4	-	1.5	1.4	-	-	2.5
III 	CCl_4	-	-22.4	-	-6.4	-24.5	-	1.6	1.3	-	-	2.3
	$CHCl_3$	-	-22.2	-	-8.2	-25.4	-	1.6	1.2	-	-	2.6
	ϕH	-	-14.8	-	+11.5	-20.2	-	1.5	1.2	-	-	2.5
IV 	CCl_4	-	-	-5.6	-6.6	-20.1	-	-	-	2.5	1.3	2.5
	$CHCl_3$	-	-	-6.5	-7.0	-20.8	-	-	-	2.5	1.6	2.6
	ϕH	-	-	+10.7	+11.2	-3.7	-	-	-	2.5	1.6	2.6
V 	CCl_4	-	-	-6.7	-6.1	-23.8	-	-	-	2.5	1.5	2.6
	ϕH	-	-	+1.8	-1.2	-15.4	-	-	-	2.5	1.3	2.7
V 	CCl_4	-	+26.25	-4.06	+8.91	+13.70	2.37	1.24	1.22	2.41	1.20	2.40
	ϕH	-	+27.63	+1.37	+11.62	+21.94	2.39	1.23	1.23	2.48	1.22	2.45

DISCUSSION

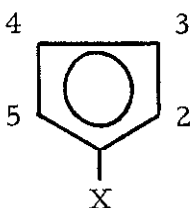
An interesting feature of these results is the close similarity between the coupling constants observed between the protons on the aromatic cyclopentadienyl ring of ferrocene and between the protons attached to various aromatic five-membered heterocycles, e. g., furan (8), pyrrole (8), and thiophene (9). In these cases, the following range of coupling constants has been reported:



X = O, S, NH

J_{23}	1.3-5.0 cps
J_{24}	0.9-1.5 cps
J_{25}	2.7 cps
J_{34}	2.8-3.5 cps

These are to be compared with the analogous coupling constants of ferrocene derivatives.



J_{23}	2.3-3.1 cps
J_{24}	1.0-1.6 cps
J_{25}	1.1-1.5 cps
J_{34}	2.5 cps

The coupling constants of protons attached to some six-membered benzenoids systems have also been measured (3, 4, 5, 6), and typical values for coupling between ortho, meta, and para protons are:

$$J_o = 5.0-8.6 \text{ cps}$$

$$J_m = 1.3-2.7 \text{ cps}$$

$$J_p = 0.0-0.9 \text{ cps}$$

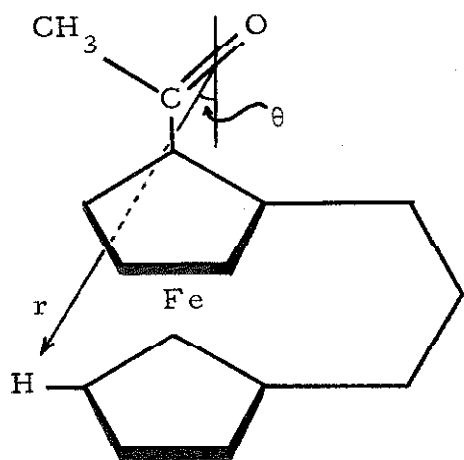
From these comparisons, it is clear that the coupling between protons adjacent to each other on a five-membered aromatic system are consistently and significantly lower than analogous couplings between protons bonded to benzenoid rings. A similar ring-size effect has been observed on cis-cycloolefins (15-17).

Another interesting result is the effect of solvent on the observed coupling constants. If there is an acetyl residue attached to the ring in question, the solvent can have a significant effect on the coupling constants as well as on the relative chemical shifts. In those rings which do not have acetyl substituents, however, this effect is sharply diminished. The explanation clearly lies in the non-uniform solvation caused by the acetyl group, which results in non-uniform magnetic shieldings at the various ring positions and variations in local electron distributions. Coupling constants in some other systems have previously been observed to depend on the electronegativity of adjacent groups (18).

A correlation was sought between the observed chemical shifts of the ring protons in 1-acetyl-2,1'-trimethyleneferrocene and the shifts anticipated on the basis of the magnetic anisotropy of the carbonyl

group. The distance and angle from the carbonyl group to each proton for all possible orientations of the acetyl group was calculated on the basis of an X-ray structure for α -ketotrimethylene ferrocene (19).

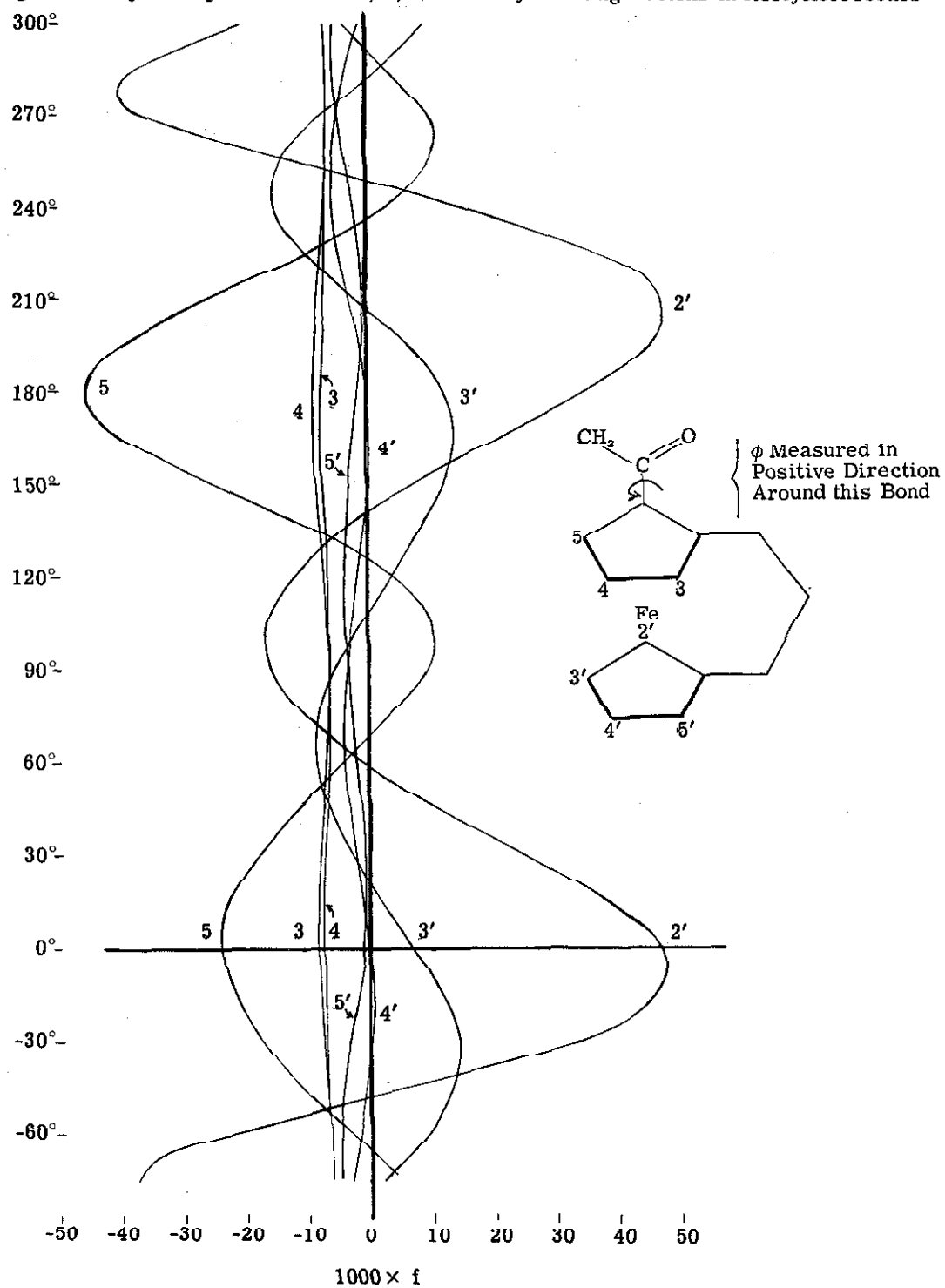
The magnetic anisotropy of the carbonyl group was approximated by a dipole-dipole interaction, f , of the form:



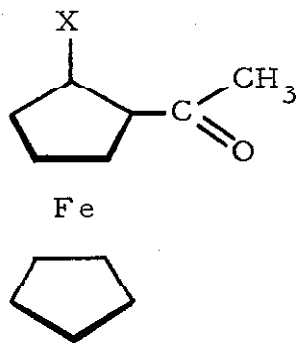
$$f = \frac{3 \cos^2 \theta - 1}{r^3}$$

between the center of the carbon oxygen bond and the proton in question (11, 20). For each proton, f will be a function of the angle between the plane of the acetyl group and the plane of the cyclopentadienyl ring. This function is shown in Figure 3.

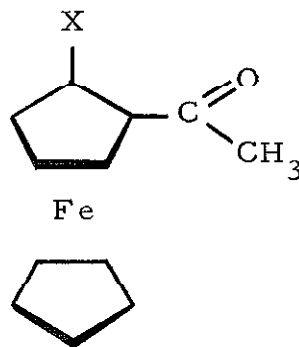
Spectroscopic evidence (2, 10) has shown the acetyl group in 1-acetyl-2-alkylferrocenes to be nearly planar with the cyclopentadienyl ring. Moreover, solvolysis experiments on methyl-2-(1, 1'-trimethyleneferrocenyl)-carbonyl acetates and related compounds (21) indicate a high degree of steric interference to an orientation where

Figure 3: Dipole-Dipole Interaction, f , of Carbonyl on Ring Protons in Acetylferrocenes

the acetyl methyl group is near the bridge, as in VIIa.



VIIa



VIIb

N. m. r. evidence indicates a rapid conversion between structures VIIa and VIIb for acetylferrocene ($X=H$); however, steric factors favor structure VIIb for compound V. This would correspond to an angle near 0° in Figure 3.

If one assumes that the carbonyl magnetic anisotropy of the acetyl group is the dominant factor selectively affecting the protons on the unacetylated ring of compound V, several conclusions may be drawn about the proton assignment and the orientation of the acetyl group. An examination of Figure 3 shows that between -40° and $+70^\circ$, the 2' proton will be more shielded than proton 3'. Moreover, between $+30^\circ$ and $+60^\circ$, the chemical shifts of all of the protons on the bottom ring

are in one of the sequences anticipated from the theoretical analysis of the spectrum. (At $\approx 50^\circ$ the agreement is quantitative.) Moreover, at any orientation of the acetyl group from -50° to $+50^\circ$, the calculated chemical shifts of the protons on the acetylated ring of V are in the sequence experimentally observed. (At $\approx 0^\circ$ the agreement is quantitative.)

Thus, a range of angles will give the correct relative order of the various protons, but no single angle of the carbonyl group predicts the quantitative aspects of the spectrum in detail. Surely, other factors, e.g., non-uniform resonance or inductive effects, will perturb significantly any model based solely on considerations of magnetic anisotropy. However, the fact that one can obtain such good qualitative agreement suggests strongly that the magnetic anisotropy of the carbonyl group plays a dominant role in determining the relative chemical shifts of the various hydrogens.

These results confirm and amplify Rinehart's qualitative argument (2). However, an additional important point is that the chemical shift assignments which the author found for compound V do not agree with the assignments suggested by Rinehart (2) for the the same compound (his compound II). My analysis of the spin-spin coupling constants demonstrates that the multiplet Rinehart lists at $\tau = 5.76$ is due to protons at ring positions 3, 4, and 3' rather than protons 4, 2', and 3', as he indicates.

The data presented in this paper on the theoretical contribution to chemical shifts due to the carbonyl magnetic anisotropy should be directly applicable to any ferrocene system having the same relative positions of the two cyclopentadienyl rings and the carbonyl group.

EXPERIMENTAL

N. m. r. Spectra. -- The spectra of 1-5% solutions in spectral grade benzene, chloroform, and carbon tetrachloride were observed on a Varian Associates A-60 n. m. r. spectrometer.

The spectra were calibrated against ferrocene as an internal standard, and the chemical shifts in Table IV are reported on this basis. The chemical shifts of ferrocene from tetramethylsilane in the various solvents used are reported in Table III to allow facile comparison of the chemical shifts observed here with those reported by other authors.

Chemicals. -- 1-Acetyl-3-methylferrocene(I), 3-acetyl-1,1'-dimethylferrocene(II), and 2-acetyl-1,1'-trimethyleneferrocene(V) were previously prepared by E. A. Hill (21).

1,1'-Diacetyl-3,3'-dimethylferrocene(III) and 1,1'-diacetyl-2,2'-dimethylferrocene(IV) were prepared by the acetylation of dimethylferrocene using standard Friedel-Crafts techniques (10,22-24) The products were separated by a series of chromatographs and identified by IR and n. m. r. spectra and by melting points.

Compound III exists in what is called the trans isomer by Rinehart (24), and IV is an almost equal mixture of cis and trans isomers. The IR spectra of the cis isomers of both III and IV have been reported (24) to be identical to the IR spectra of their trans

isomers, and one would expect very little difference in their n. m. r. spectra. I have observed a slight splitting of the methyl and of the acetyl proton peaks in the n. m. r. spectrum of IV in benzene. They are each split by about one cps into two peaks of about equal magnitude.

Compound IV was chromatographed on deactivated alumina, and the leading and trailing portions of the band were isolated. These showed a change of about 20 per cent in the relative intensities of the two acetyl peaks in the n. m. r. spectrum of one fraction as compared to the other, indicating a slight enrichment of one of the isomers over the other.

APPENDIX I

Derivation of the N. m. r. Parameters of an ABX System from
the Experimental Spectrum

Pope et al. (12) defines a set of parameters for a three spin ABX system by the following equations:

$$D_+ \cos 2\theta_+ = \frac{1}{2} (\nu_A - \nu_B) + \frac{1}{4} (J_{AX} - J_{BX}) \quad (1)$$

$$D_+ \sin 2\theta_+ = \frac{1}{2} J_{AB} \quad (2)$$

$$D_- \cos 2\theta_- = \frac{1}{2} (\nu_A - \nu_B) - \frac{1}{4} (J_{AX} - J_{BX}) \quad (3)$$

$$D_- \sin 2\theta_- = \frac{1}{2} J_{AB} \quad (4)$$

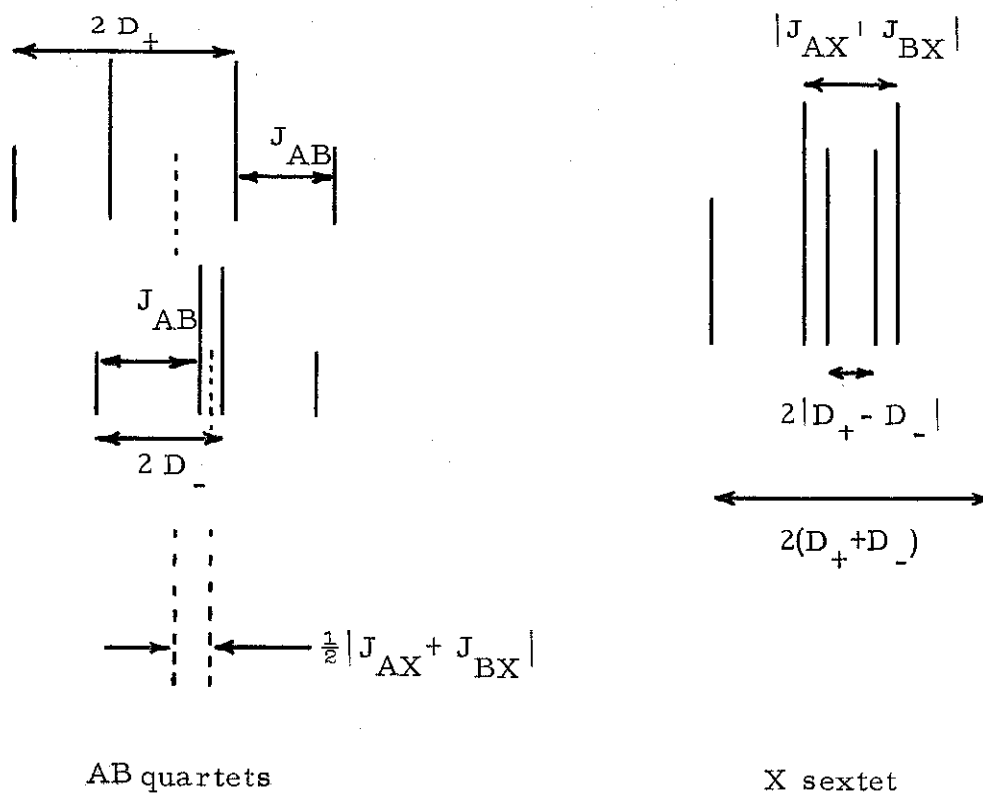
where J_{ij} represents the coupling constant between the i^{th} and the j^{th} nuclei, and ν_i is the resonance frequency of the i^{th} nucleus in the magnetic field. The equations may be rewritten:

$$\frac{1}{2} (\nu_A - \nu_B) + \frac{1}{4} (J_{AX} - J_{BX}) = \sqrt{D_+^2 - \left(\frac{J_{AB}}{2}\right)^2} \quad (5)$$

$$\frac{1}{2} (\nu_A - \nu_B) - \frac{1}{4} (J_{AX} - J_{BX}) = \sqrt{D_-^2 - \left(\frac{J_{AB}}{2}\right)^2} \quad (6)$$

The AB portion of the n. m. r. spectrum consists of two possibly overlapping quartets, and the X portion of the spectrum is in first order a sextet with a plane of reflection through the center.

The indicated relationships exist between the peaks:



The interval $|J_{AB}|$ appears four times in the AB portion of the spectrum, and D_+ and D_- each appear twice. From these and equations 5 and 6, both $(\nu_A - \nu_B)$ and $(J_{AX} - J_{BX})$ may be calculated. $|J_{AX} + J_{BX}|$ may be obtained from the spectrum and a set of values for J_{AX} and J_{BX} may be determined. As discussed in the text of the thesis, the sign of J_{AB} is unknown, and only the relative signs of J_{AX} and J_{BX} are specified by this analysis. Any combination of signs of the coupling constants meeting this requirement will determine a spectrum identical to the spectrum determined by any other combination of signs.

Since only the absolute value of $(J_{AX} + J_{BX})$ is experimentally measured by the spectrum, the correct relative assignment of the two coupling constants is also unspecified, and must be determined by other means. For example, a typical set of coupling constants may be either $J_{AX} = 2.5$ cps and $J_{BX} = 1.2$ cps, or $J_{AX} = -1.2$ cps and $J_{BX} = -2.5$ cps. In each case, the author has arbitrarily assigned the larger value to the coupling constant between adjacent protons. This assignment not only appeals to one's intuitive expectations, but also consistently results in similar constants for adjacent AX pairs of protons and adjacent AB pairs of protons. This correspondence would not occur if the other assignment were made.

APPENDIX II

Nuclear Magnetic Resonance Spectra of the Compounds under Study

Only the part of each spectrum is shown which has been analyzed.

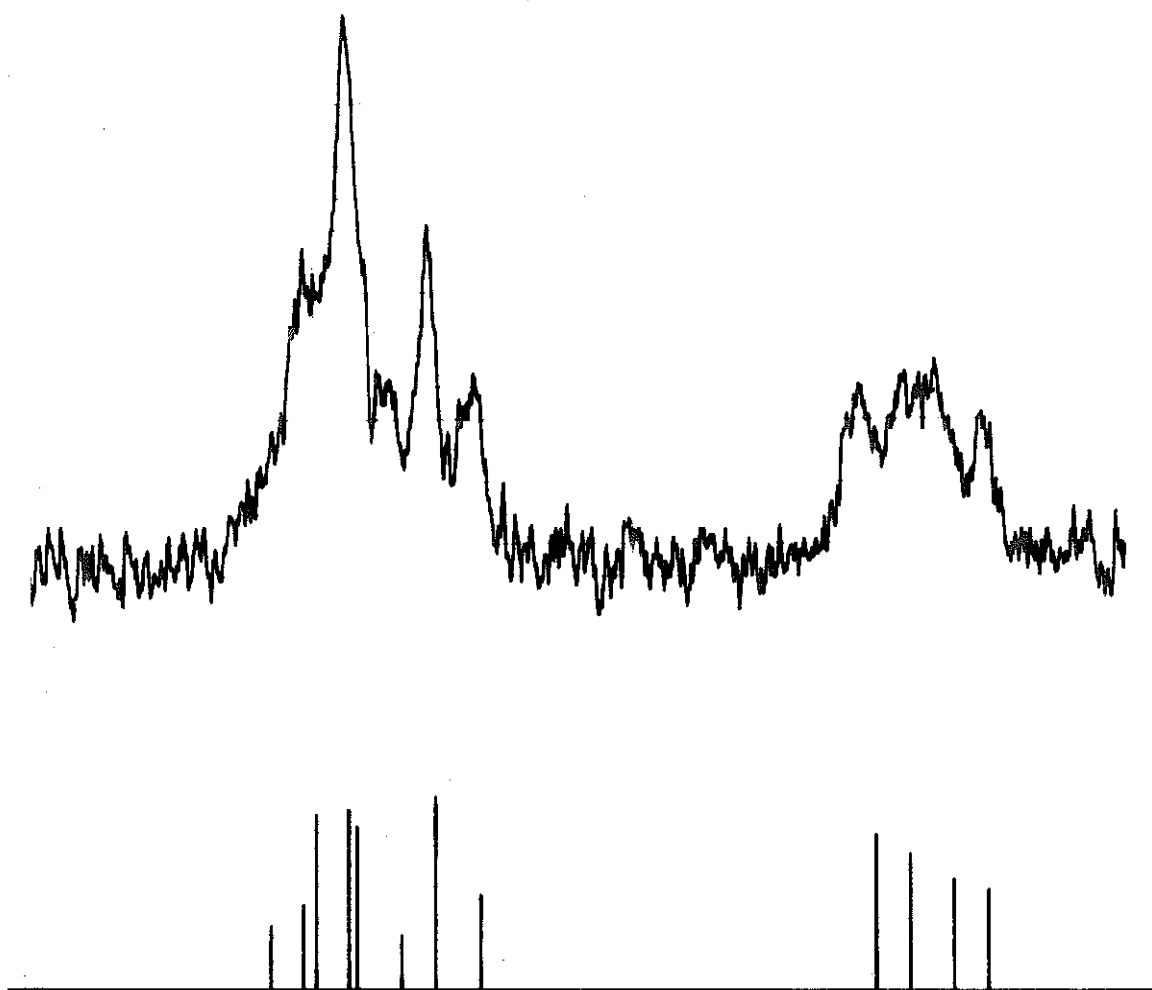


Figure 4: The n.m.r. spectrum of 1-acetyl-3-methylferrocene in carbon tetrachloride.

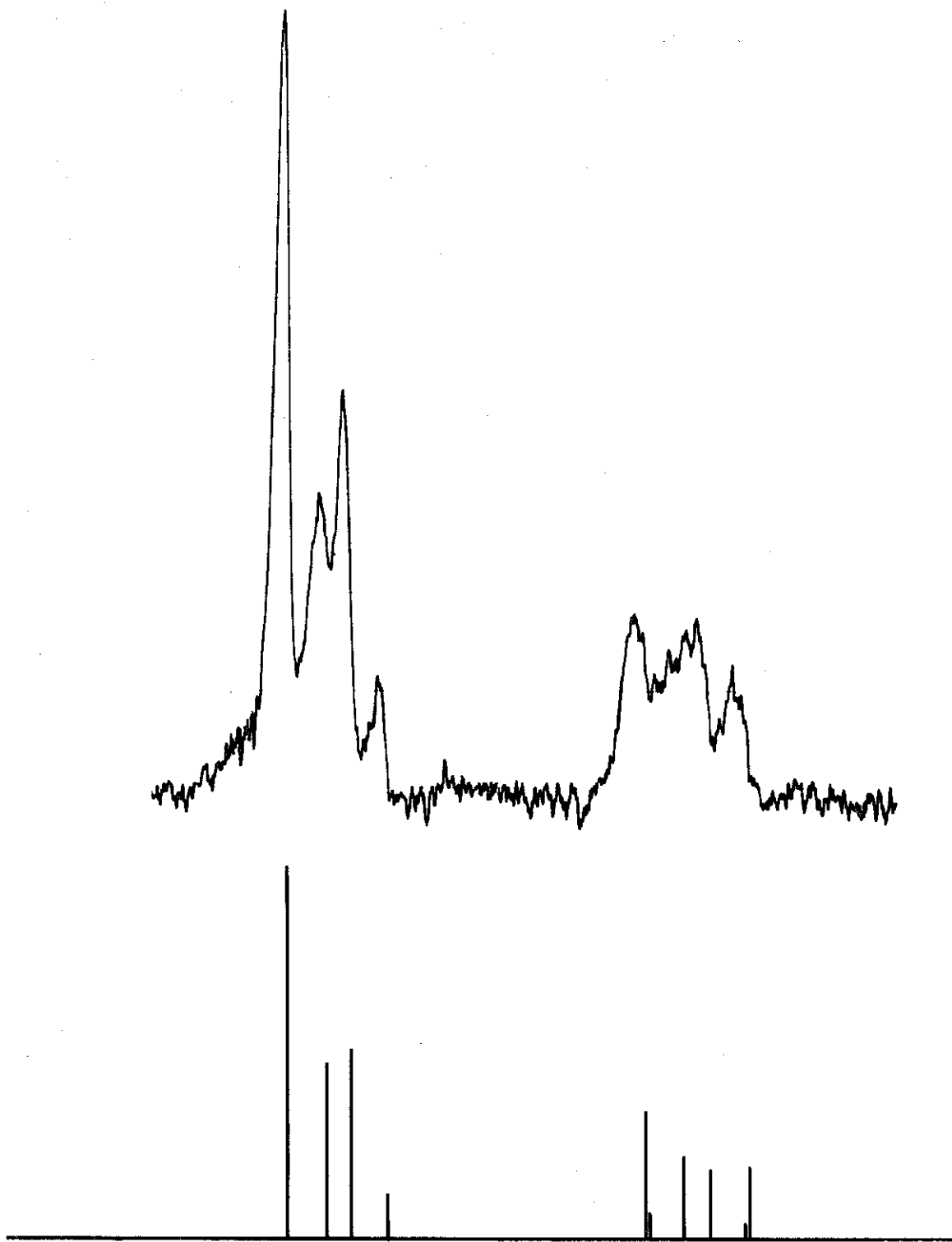


Figure 5: 1-Acetyl-3-methylferrocene in chloroform.

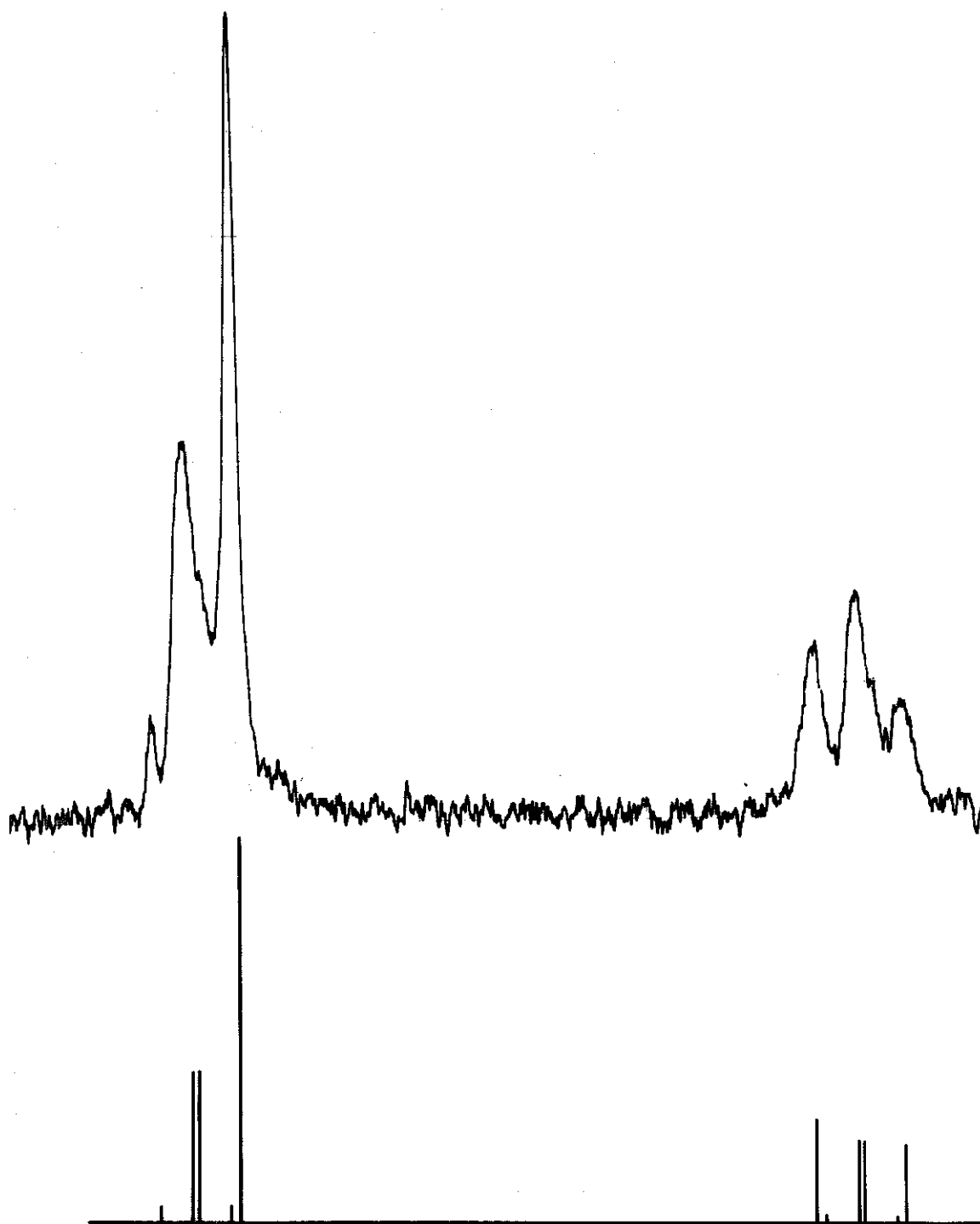


Figure 6: 1-Acetyl-3-methylferrocene in benzene.

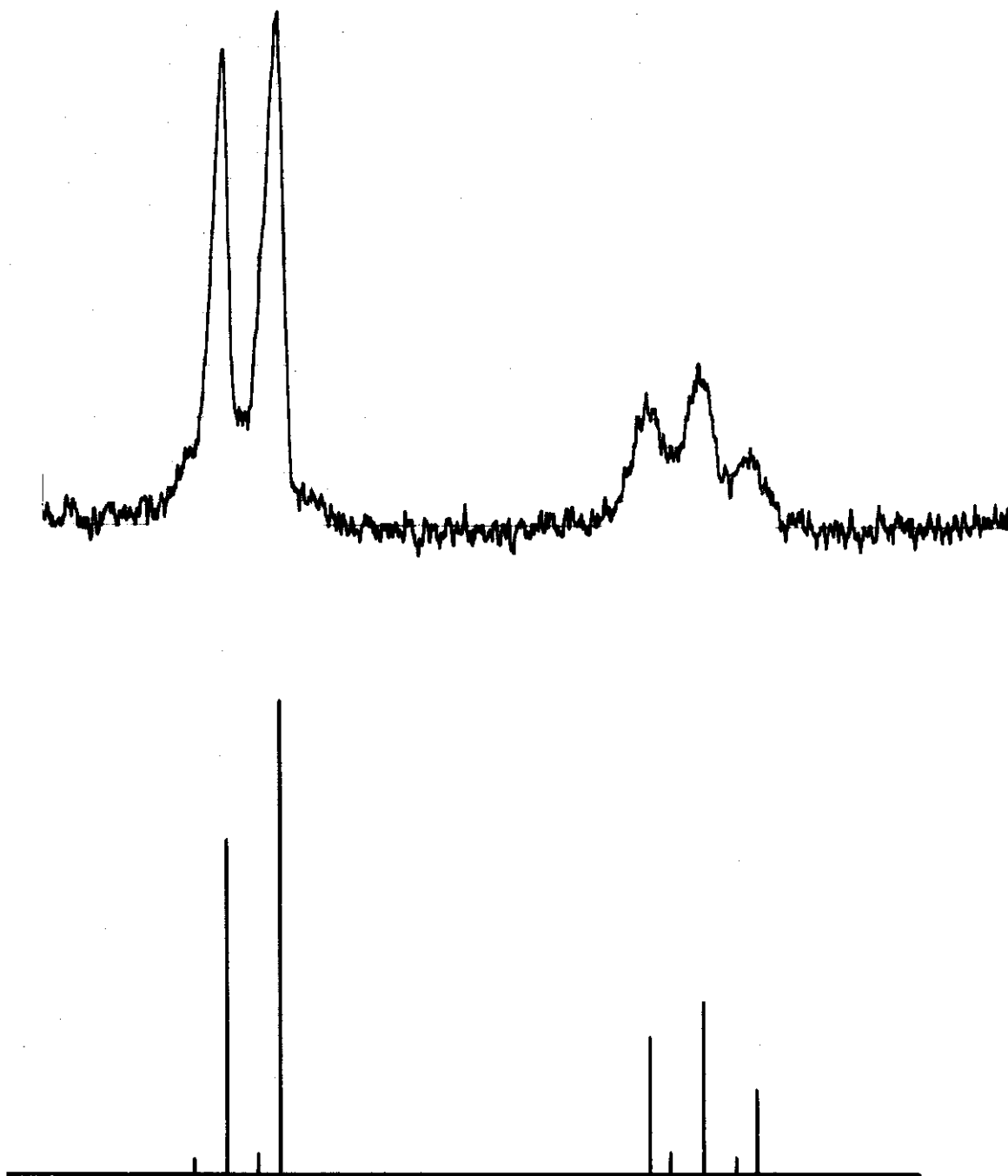


Figure 7: 3-Acetyl-1,1'-dimethylferrocene in carbon tetrachloride.

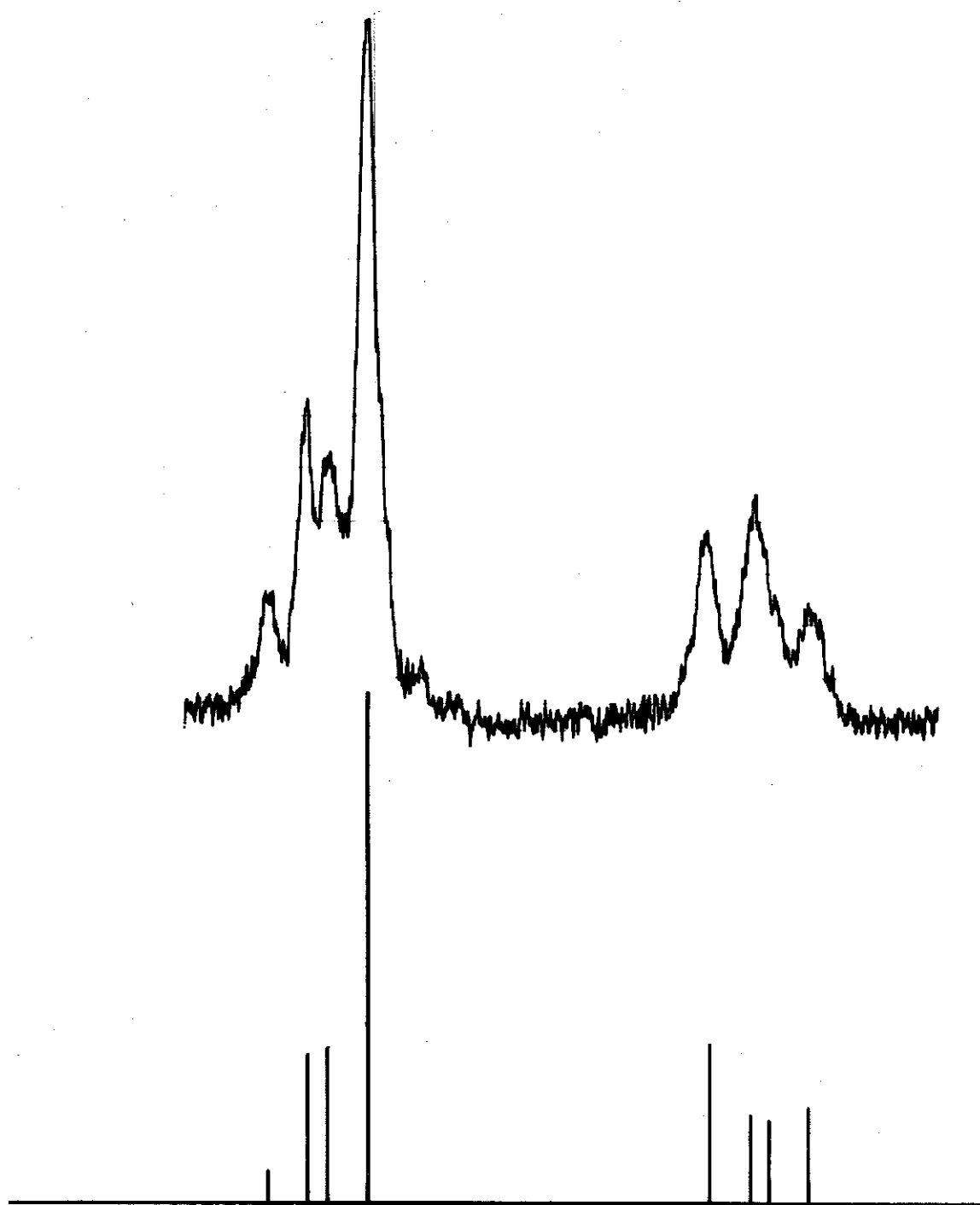


Figure 8: 3-Acetyl-1,1'-dimethylferrocene in chloroform.

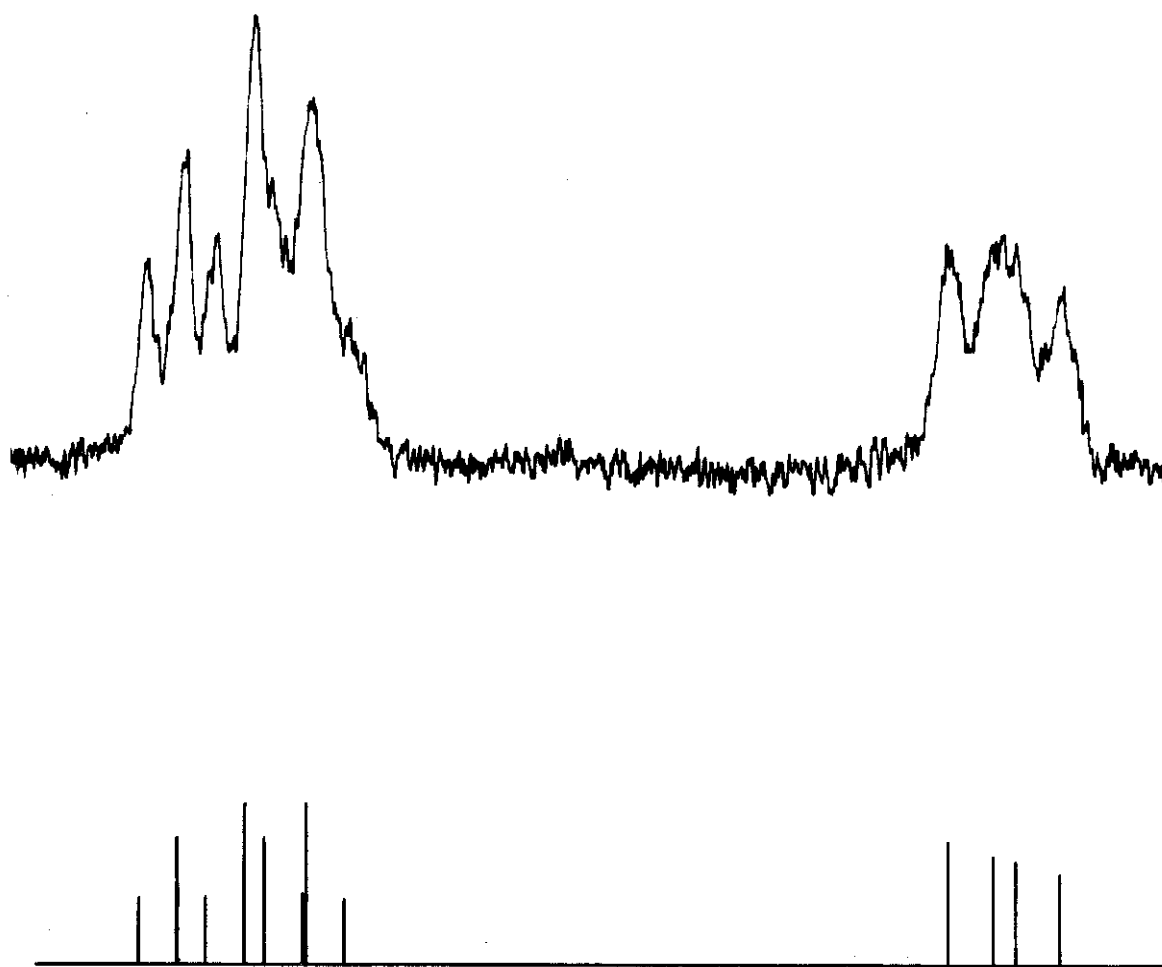


Figure 9: 3-Acetyl-1,1'-dimethylferrocene in benzene.

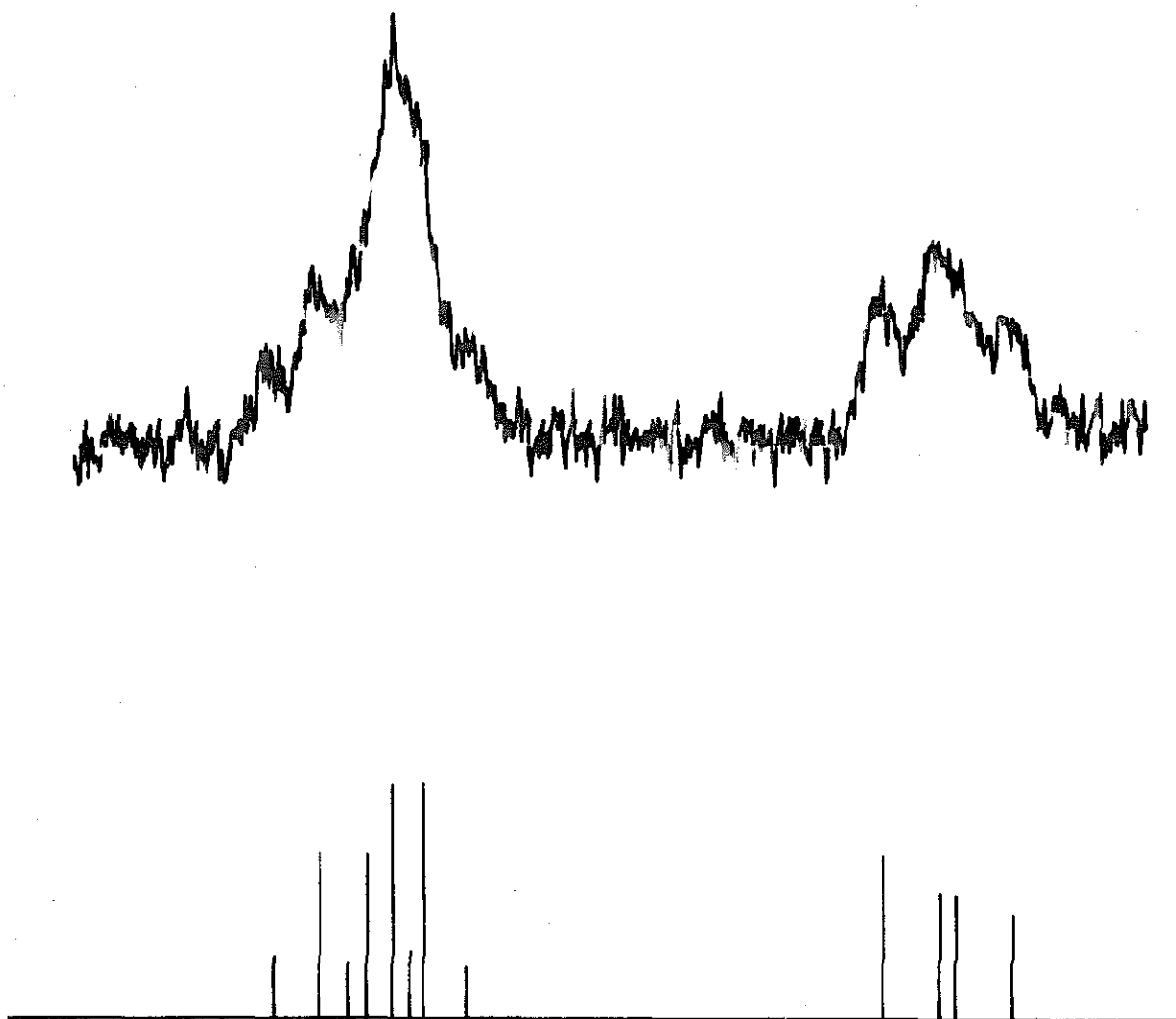


Figure 10: 1,1'-Diacetyl-3,3'-dimethylferrocene in carbon tetrachloride.

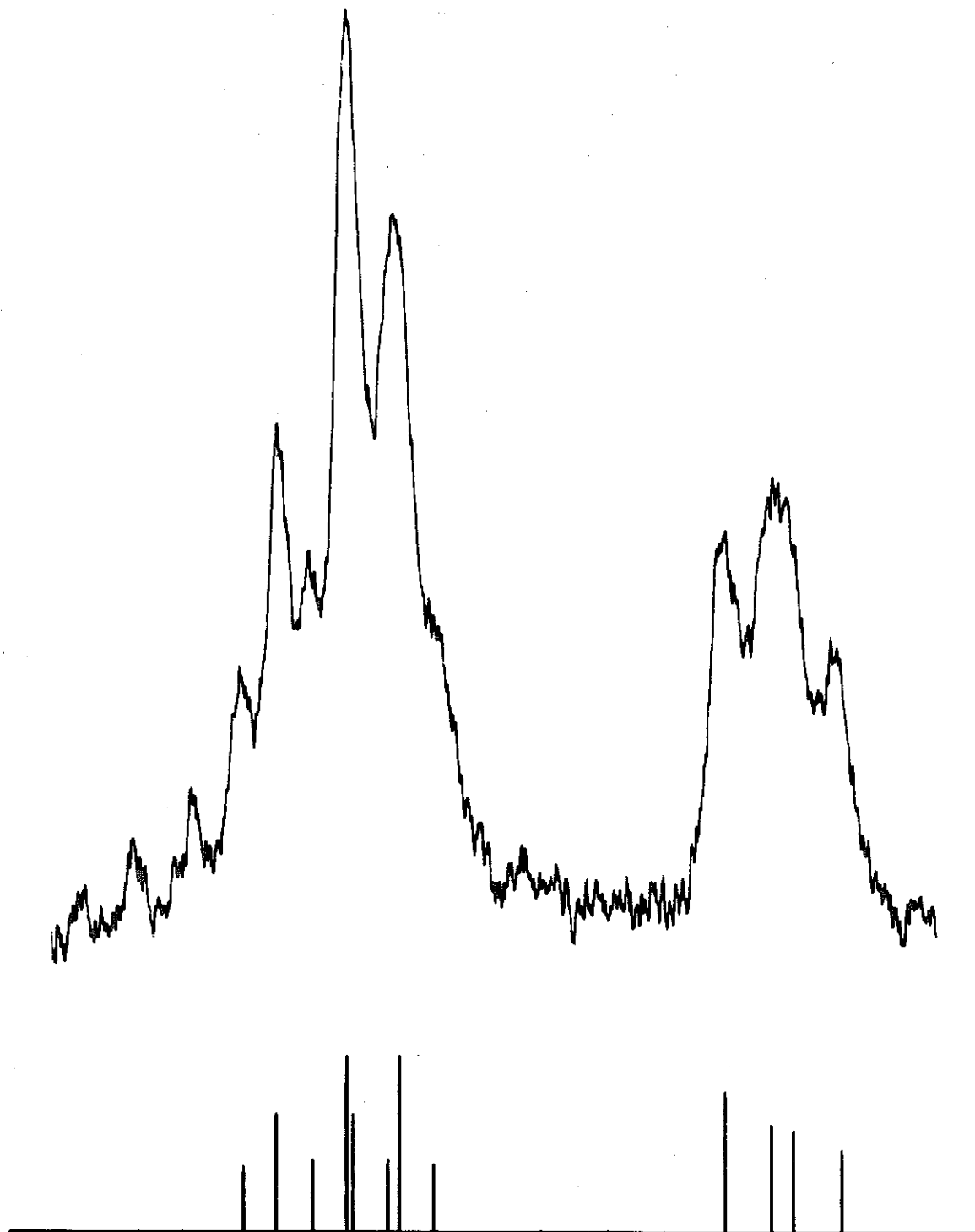


Figure 11: 1,1'-Diacetyl-3,3'-dimethylferrocene in chloroform.

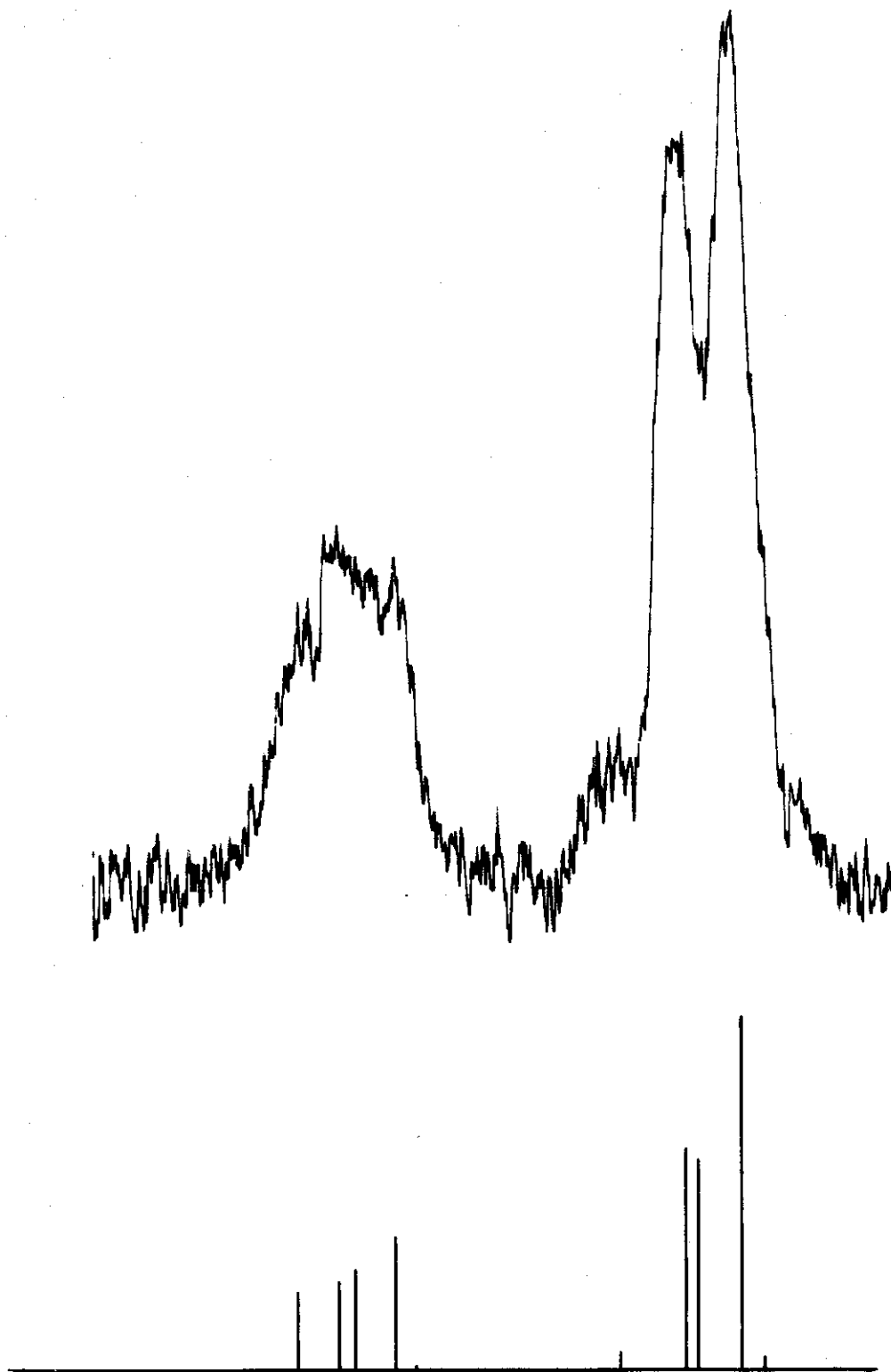


Figure 12: 1,1'-Diacetyl-2,2'-dimethylferrocene in carbon tetrachloride.

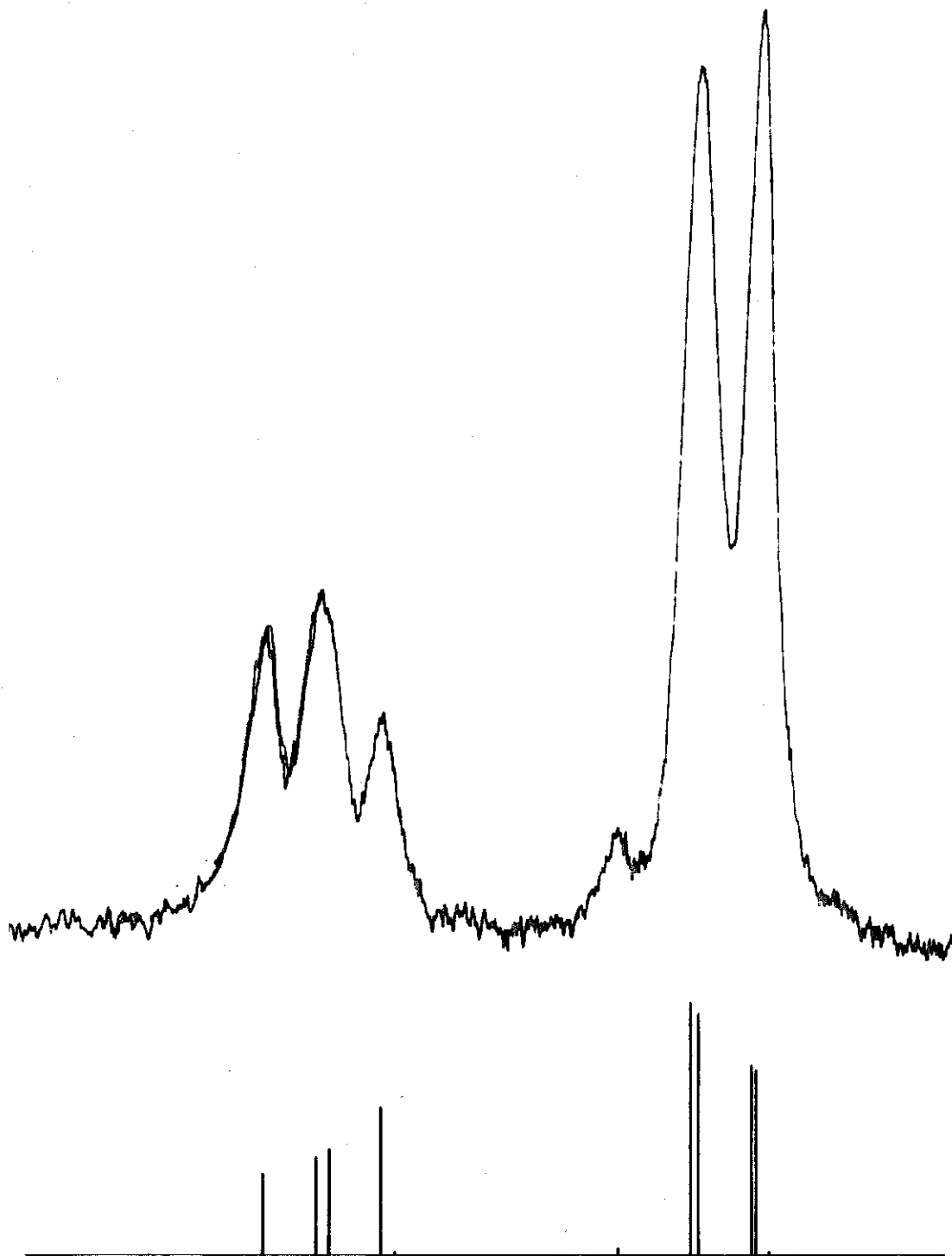


Figure 13: 1,1-Diacetyl-2,2'-dimethylferrocene in chloroform.

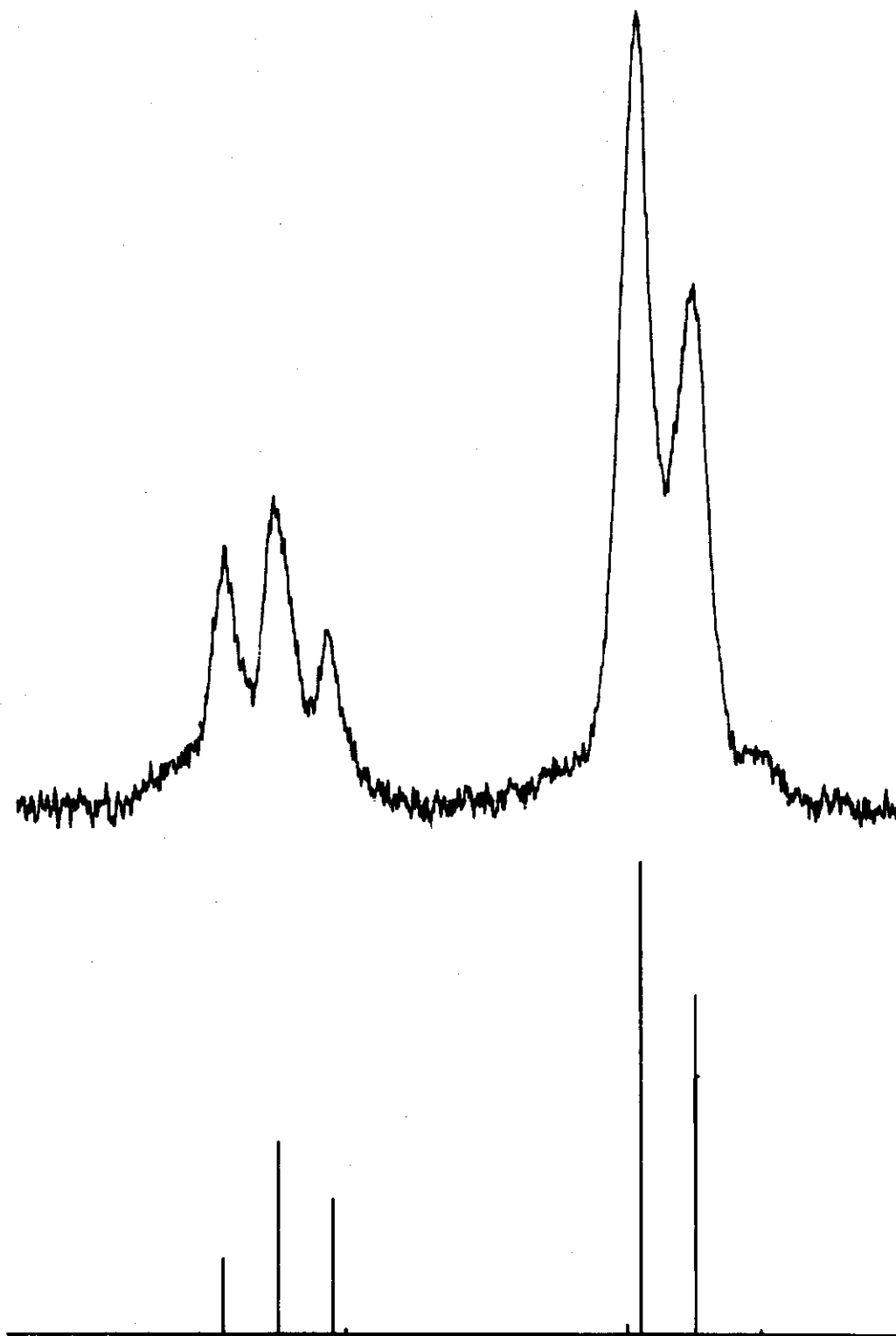


Figure 14: 1,1'-Diacetyl-2,2'-dimethylferrocene in benzene.

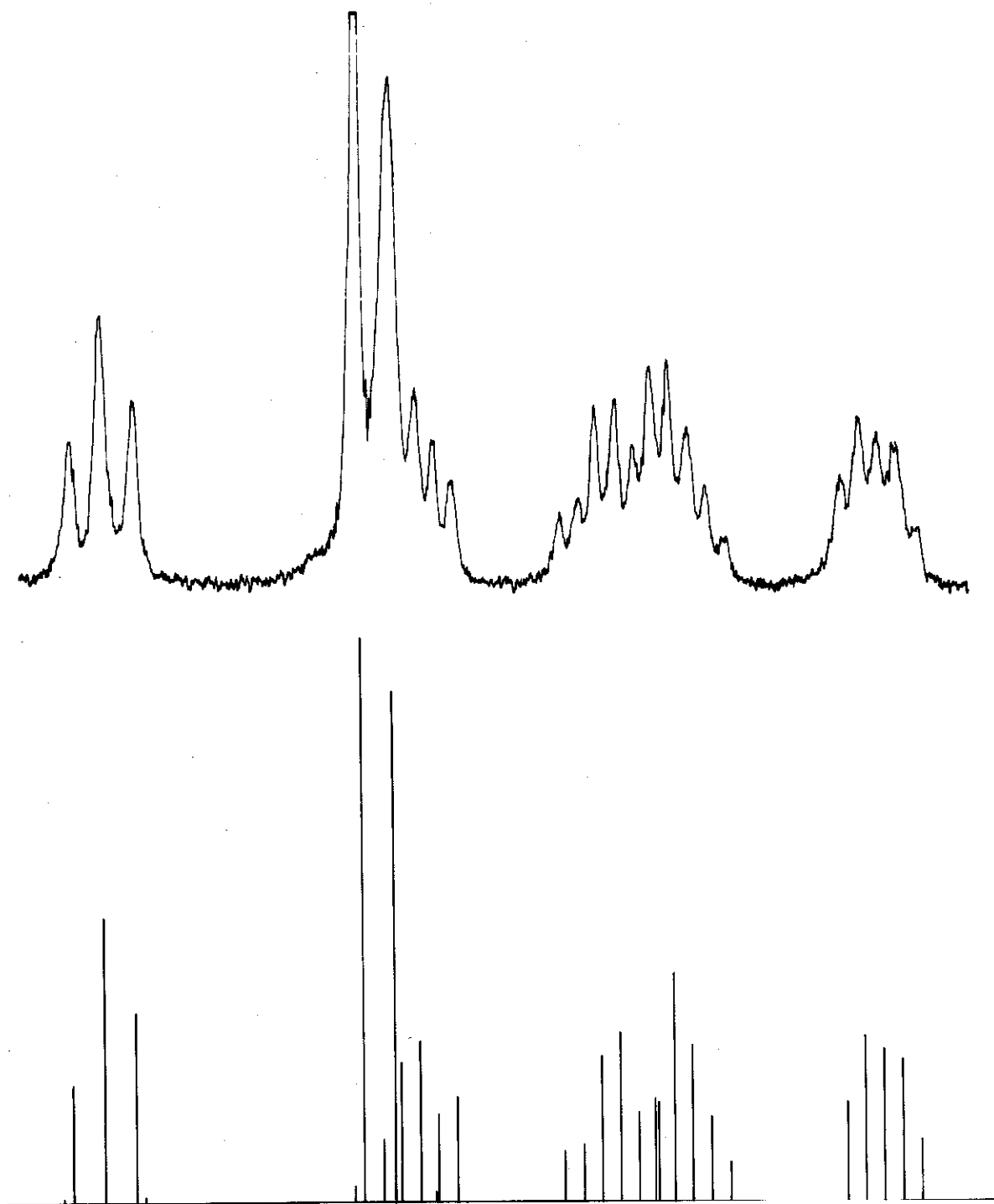


Figure 15: 2-Acetyl-1,1'-trimethyleneferrocene in carbon tetrachloride.

REFERENCES

1. M. Rosenblum, A. K. Banerjee, N. Danieli, R. W. Fish, and V. Schlatter, *J. Am. Chem. Soc.*, 85, 316 (1963).
2. K. L. Rinehart, Jr., D. E. Bublitz, and D. H. Gustafson, *J. Am. Chem. Soc.*, 85, 970 (1963).
3. H. J. Bernstein, J. A. Pople, and W. G. Schneider, *Can. J. Chem.*, 35, 65 (1957).
4. H. S. Gutowsky, C. H. Holm, A. Saika, and G. A. Williams, *J. Am. Chem. Soc.*, 79, 4596 (1957).
5. J. A. Pople, W. G. Schneider, and H. J. Bernstein, *Can. J. Chem.*, 35, 1060 (1957).
6. W. G. Schneider, H. J. Bernstein, and J. A. Pople, *Can. J. Chem.*, 35, 1487 (1957).
7. J. A. Pople, W. G. Schneider, and H. J. Bernstein, "High Resolution Nuclear Magnetic Resonance," McGraw-Hill, New York, N. Y., 1959, p. 98.
8. R. J. Abraham and H. J. Bernstein, *Can. J. Chem.*, 37, 1056 (1959).
9. R. J. Abraham and H. J. Bernstein, *Can. J. Chem.*, 37, 2095 (1959).
10. K. L. Rinehart, Jr., K. L. Motz, and S. Moon, *J. Am. Chem. Soc.*, 79, 2749 (1957).
11. L. M. Jackman, "Application of Nuclear Magnetic Resonance Spectroscopy in Organic Chemistry," Pergamon Press, London, England (1959), pp. 123-125.
12. Reference 7, pp. 132-138.
13. K. B. Wiberg, B. J. Nist, "The Interpretation of N.M.R. Spectra," W. A. Benjamin, Inc., New York, N. Y. (1962).

14. J. D. Swalen and C. A. Reilly, *J. Chem. Phys.*, 37, No. 1, 21 (1962).
15. O. L. Chapman, *J. Am. Chem. Soc.*, 85, 2014 (1963).
16. G. V. Smith and H. Kriloff, *ibid.*, 85, 2016 (1963).
17. P. Laszlo and P. von R. Schleyer, *ibid.*, 85, 2017 (1963).
18. K. L. Williams, *ibid.*, 85, 516 (1963).
19. R. Marsh, N. Jones, and J. H. Richards, unpublished results.
20. H. M. McConnell, *J. Chem. Phys.*, 27, 226 (1957).
21. E. A. Hill and J. H. Richards, *J. Am. Chem. Soc.*, 83, 4216 (1961).
22. E. A. Hill, III, Ph. D. Thesis, California Institute of Technology, Pasadena, 1961, pp. 113-120.
23. M. Rosenblum and R. B. Woodward, *J. Am. Chem. Soc.*, 80, 5443 (1958).
24. K. L. Rinehart, Jr. and K. L. Motz, *Chem. and Ind.*, 1150 (1957).

PART IV
EXPERIMENTAL AND THEORETICAL STUDIES
OF THE CHARGE DISTRIBUTION ON THE
FERROCENYL CARBINYL CARBONIUM ION

A. INTRODUCTION

Investigators have long been aware that the nuclear magnetic resonance chemical shifts of protons on conjugated and aromatic molecules are dependent on the pi-electron density of the carbon atoms to which the protons are bonded (1-8). Several workers (3-5) have assumed that the chemical shift of a proton is linearly related to the charge on the adjacent carbon atom. They have postulated an empirical formula of the form of Equation 1,

$$\delta = k q \quad (1)$$

where a pi-electron charge, q , on a carbon atom results in a chemical shift, δ , on the proton bonded to the carbon atom.

Equation 1 has been found to fit the data for a variety of systems when k is assigned a value of 10. Schaefer and Schneider (7) made a more careful examination of the experimental data available and have suggested that the proportionality constant, k , is 10.7 p.p.m./electron.

Only the cyclopentadienyl negative ion, benzene, and the tropylium cation (5) have sufficiently high symmetry to allow the direct calculation of the pi-electron density at each carbon atom. The pi-electron density of most compounds must be estimated with the aid of one or another form of molecular orbital (MO) calculation.

The azulene molecule is a typical example of a system which requires more extensive calculations to obtain an index of the charge on each of its atoms. For example, some of the MO treatments which have been applied to azulene are: 1) The simple Hückel (HMO) or linear-combination-of-atomic-orbital (LCAO) molecular orbital calculation (9), 2) The self-consistent field calculation (10), 3) HMO with configurational interaction (11), 4) The variable electronegativity method (12), and 5) The omega-technique (13).

Though each molecular orbital technique has its advantages and individual characteristics, no one method stands apart as being decisively better than the rest in the case of azulene. The charge densities on the carbon atoms of azulene can be calculated by applying Equation 1 to the nuclear magnetic resonance chemical shifts of the protons and correcting for the ring currents in the two rings (7). The pi-electron densities calculated in this manner do not agree precisely with the densities derived from any of the molecular orbital calculations, though there is a general agreement in the electron densities from each calculation. It is impossible to determine at this time which of the calculations gives the closest representation of the actual charge densities.

Many molecular orbital calculations have been attempted on ferrocene (14-27), all taking advantage of the high symmetry of the

molecule. In the present work the ferrocenylcarbinyl carbonium ion has been studied. This ion no longer has the symmetry that ferrocene itself has, so less elegant techniques have been used to calculate its molecular orbitals, and the pi-electron charge densities so obtained have been compared with the charge densities predicted from the proton resonance chemical shifts.

B. RESULTS

1. STABILITY OF CARBONIUM ION

Evidence existed before the present work was undertaken that ferrocene and other metallocenes are effective in stabilizing a carbonium ion adjacent to one of the rings (28-30). Empirical observations in this laboratory indicated that ferrocenylmethanol is quite soluble in a variety of strong aqueous acids. As the alcohol is insoluble in neutral polar and aqueous media, one must conclude that it reacts with the acid and exists as a complex or an ionic species in solution.

The ultraviolet and visible spectra (Table I) of ferrocenylmethanol in acid solution are independent of the identity of the acid, and in all cases the original alcohol may be recovered on neutralization of the solution with sodium bicarbonate. The ultraviolet spectrum of the alcohol in acid resembles neither that of the alcohol in organic solvents nor the spectrum of the ferrocinium ion. The most likely identity of the acidified alcohol is either the protonated alcohol (I) or the carbonium ion (II).

TABLE I

Ultraviolet and Visible Absorption Spectral Peaks

Compound	Solvent	Peak (Å)	Absorbance ₁ (mole ⁻¹ cm ⁻¹)
ferrocenylmethanol	ethanol	3240	59.4
		4370	100
ferrocenylmethanol	conc. hydrochloric acid	4580	190
ferrocenylmethanol	conc. sulfuric acid	4580	190
ferrocinium perchlorate	water	2510	11,100
		2800	6,400
		6170	296
ferrocene	conc. sulfuric acid	3540	
		6170	

The carbonium ion is apparently quite stable in concentrated sulfuric acid, as the freezing point of the solution changed by only 0.013° in 24 hours, and this change would be expected merely from the uptake of water by the system. On the other hand, a typical addition of sample might drop the freezing point by 0.2° .

2. NUCLEAR MAGNETIC RESONANCE SPECTRA

The nuclear magnetic resonance spectra of the compounds under consideration are presented in Figures 1-4. The pertinent data are summarized in Table II.

A methyl group does not significantly perturb the n. m. r. spectrum of the ferrocenyl system; however, the spectrum of the corresponding carbonium ion exhibits gross chemical shifts. All of the proton peaks are shifted down-field, as would be expected if the electron density were decreased at each position. The column labeled "experimental" in Table III lists the shifts in parts per million for the proton peaks in ferrocenylcarbonyl carbonium ion from the corresponding peaks in methylferrocene.

All of the resonance peaks were measured against reference peaks of internal standards which had been calibrated against each other. The bulk magnetic susceptibility of the solvent would affect reference and ferrocenyl peaks equally, so the solvent susceptibility cancels out of the measured relative chemical shifts.

Figure 1: The n.m.r. spectrum of methylferrocene in carbon tetrachloride.

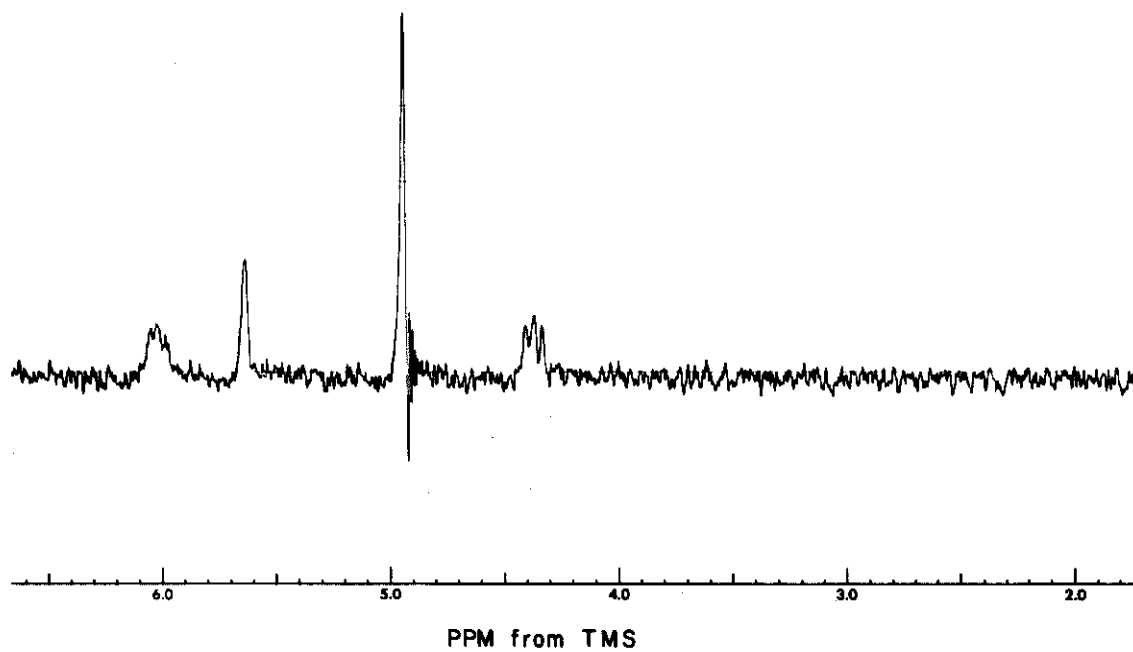
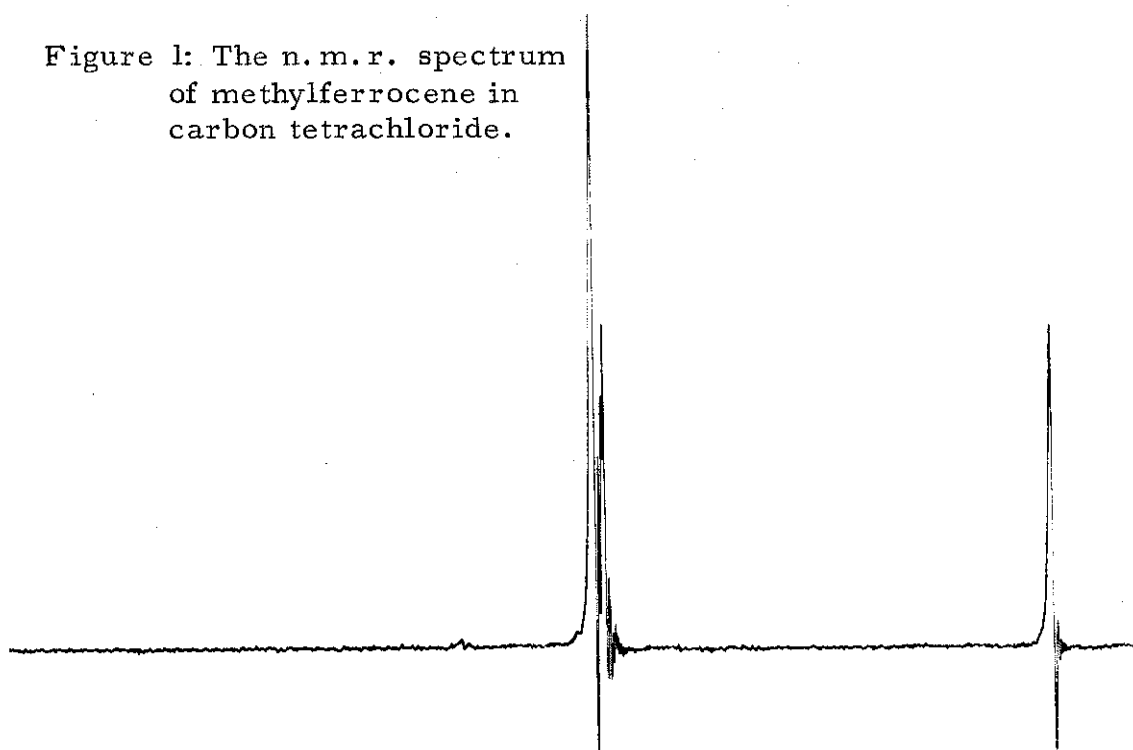


Figure 2: The n.m.r. spectrum of the ferrocenylcarbinylium carbonium ion in trifluoroacetic acid.

Figure 3: The n.m.r. spectrum of the methyl-ferrocenyl-carbinyl carbonium ion in trifluoroacetic acid.

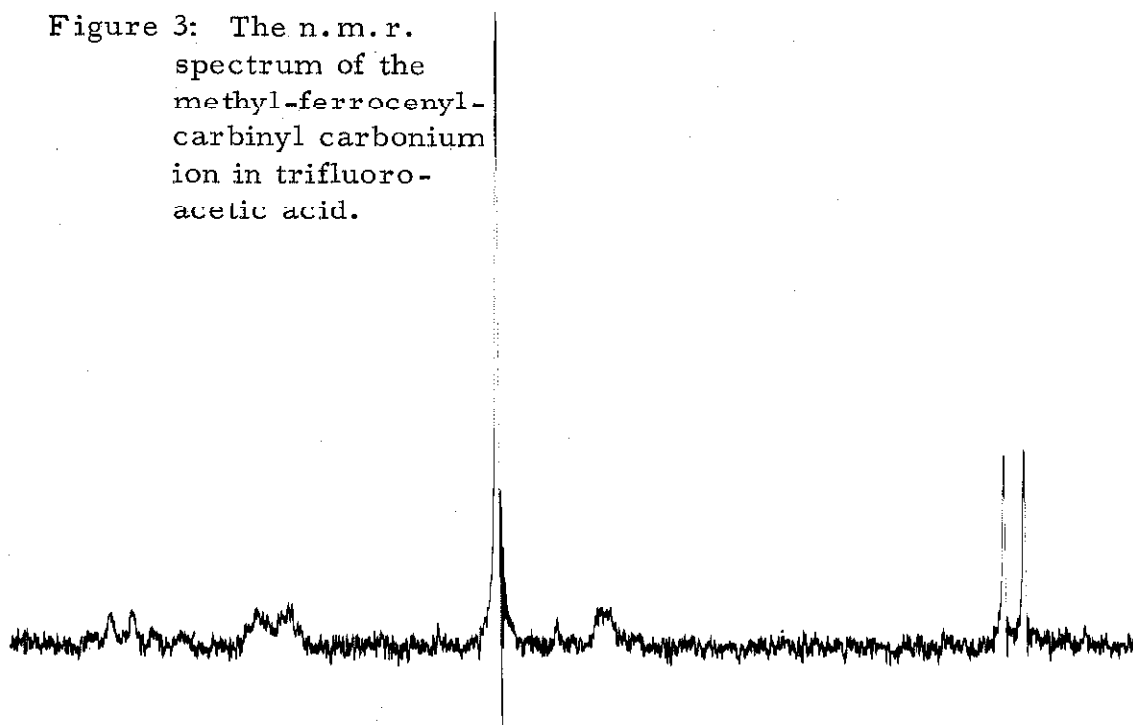


Figure 4: The n.m.r. spectrum of the methyl-(3-methyl-ferrocenyl)-carbinyl carbonium ion in trifluoroacetic acid.

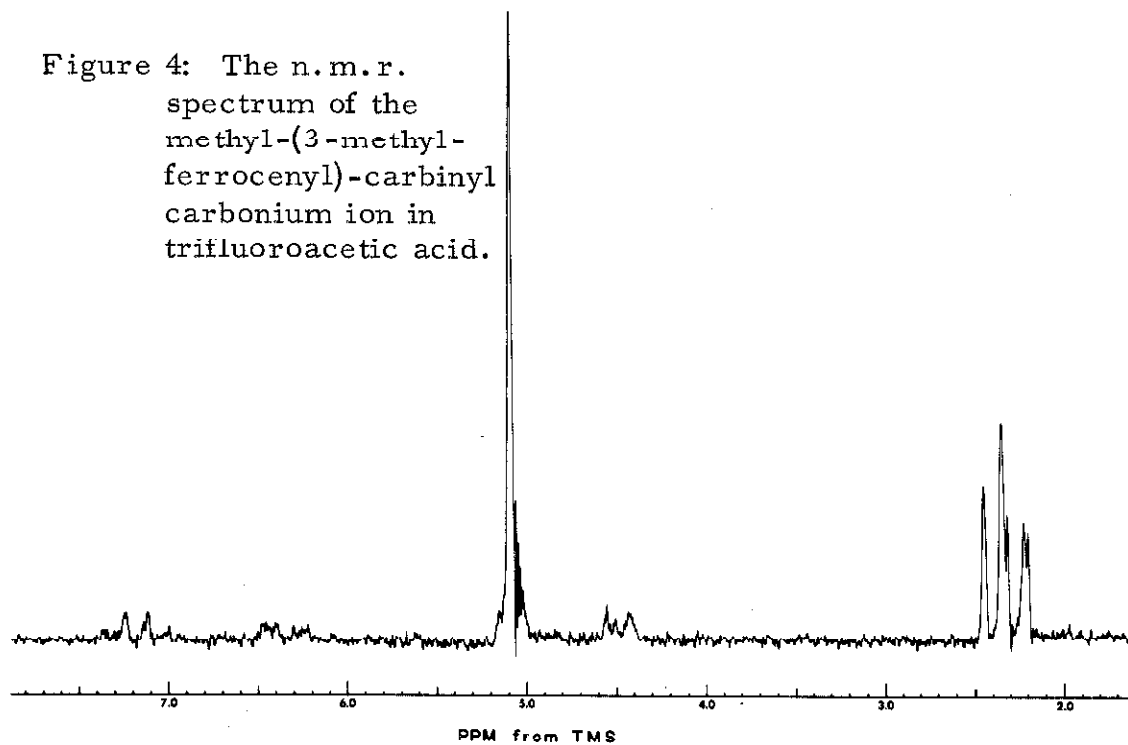
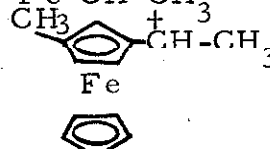
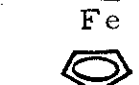


TABLE II

Nuclear Magnetic Resonance Chemical Shifts^a

Compound	Solvent	Unsub-stituted ring	Car-binyl pro-tons	2-pro-tons ^b	3-pro-tons ^c
FcH	CCl ₄	5.93			
Fc-CH ₃	CCl ₄	5.93	7.95	5.98	5.98
Fc-CH ₂ ⁺	BF ₃ ·H ₂ O	4.55	3.87	5.10	3.49
Fc-CH ₂ ⁺	CF ₃ CO ₂ H	4.67	3.97	5.25	3.59
$\begin{array}{c} \text{Fc-CH-CH}_3 \\ \quad \\ \text{CH}_3 \quad \text{CH-CH}_3 \\ \quad \\ \text{Fe} \end{array}$ 	CF ₃ CO ₂ H	4.85	2.73	4.85, 5.43	3.52, 3.68
$\begin{array}{c} \text{Fc} \\ \\ \text{C}_5\text{H}_5^- \end{array}$ 	CF ₃ CO ₂ H	4.91	2.81	4.91, 5.49	3.58, 3.73
C ₅ H ₅ ⁻	tetrahydro-furan	4.46			
C ₆ H ₆	CCl ₄	2.73			

a. Chemical shifts expressed in tau values.

b. Proton on ring carbon adjacent to substituted carbon.

c. Proton on ring carbon beta to substituted carbon.

TABLE III

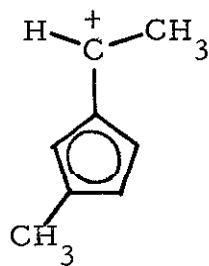
Theoretical Change in the Chemical Shift of Methylferrocene
Protons Upon the Formation of the Alpha Carbonium Ion^a

Type of Calculation	Unsub-stituted ring	Car-binyl proton	2-Proton on ring	3-Proton on ring
1. Experimental	1.26	3.98	.73	2.39
2. Fulvene	0	6.90	3.42	.68
3. Typical single MO calculation	-.59	6.86	1.63	1.33
4. Typical iterated MO calculation	-.64	5.10	2.04	1.38
5. Ring Shifted 1 Å iterated calculation	-.64	5.10	2.07	1.31
6. Ring shifted iterated calculation with 0.8 Å current loop around iron	-.64	2.79	1.37	3.67
7. Ring shifted iterated calculation with 1.2 Å current loop around iron	-.64	3.27	1.60	3.16
8. Ring shifted iterated calculation with octupole approximation for iron	-.64	3.44	1.66	3.08
9. Electric field method applied to calc. 5	-.64	6.18	2.69	1.69
10. Electric field method applied to calc. 8	-.64	4.52	2.28	3.46

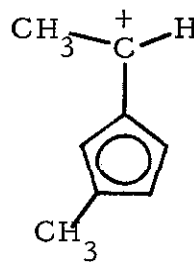
a. Chemical shifts expressed in parts per million with a down-field shift positive.

Nuclear magnetic resonance spectra were observed for both ferrocenylmethyl carbinol and (3-methylferrocenyl)-methyl carbinol in trifluoroacetic acid. Positive assignments were made of the chemical shifts of the α and β ring protons from comparisons of the integrated peak areas of these two compounds. The unexpected result was obtained that the β protons are more strongly deshielded than the protons α to the carbonium ion center. The implications of this phenomenon will be considered in the Discussion section.

The multiple peaks which were observed for the ring protons of these two compounds are almost certainly due to the two possible orientations of the methyl group adjacent to the carbonium center.



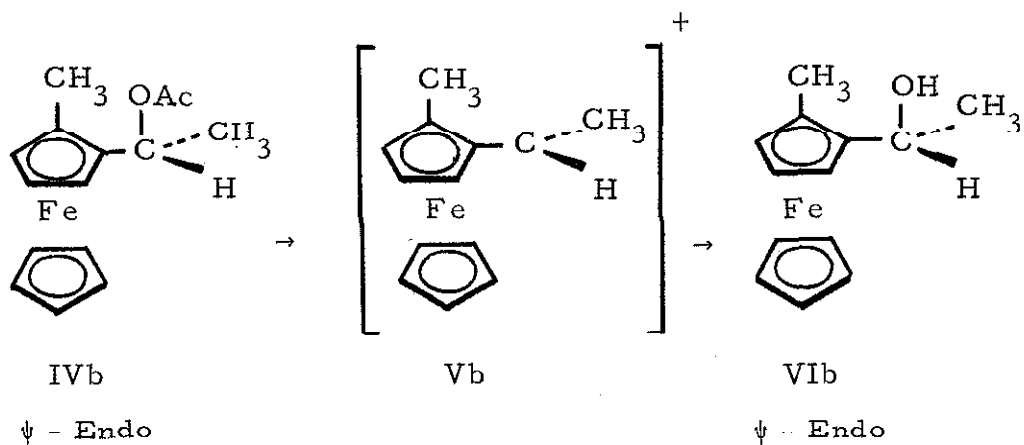
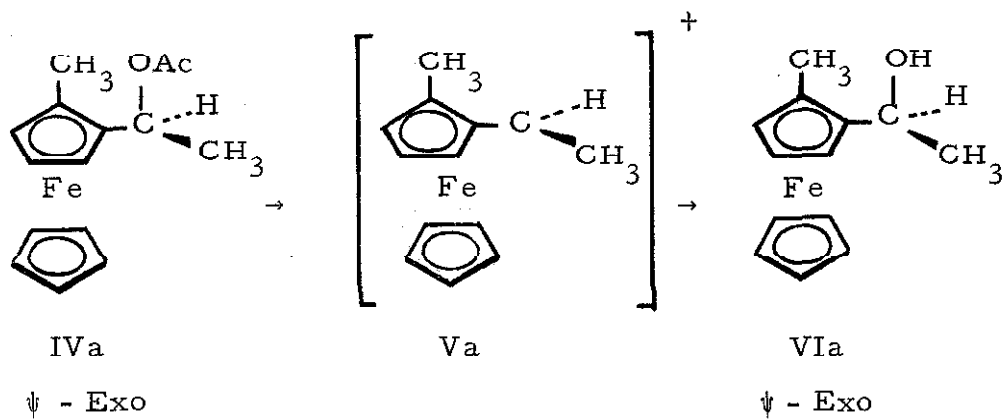
IIIa



IIIb

Hill and Richards (35) have demonstrated in their work on the solvolysis of the stereoisomers of methyl-(2-methylferrocenyl)-carbinyl acetate that these two isomeric carbonium ions do exist as separate entities. They have shown that the ψ -exo and ψ -endo

isomers (their nomenclature) solvolyze with complete stereospecificity, requiring a complete lack of rotation around the carbonyl to ring bond in the carbonium ion intermediates.

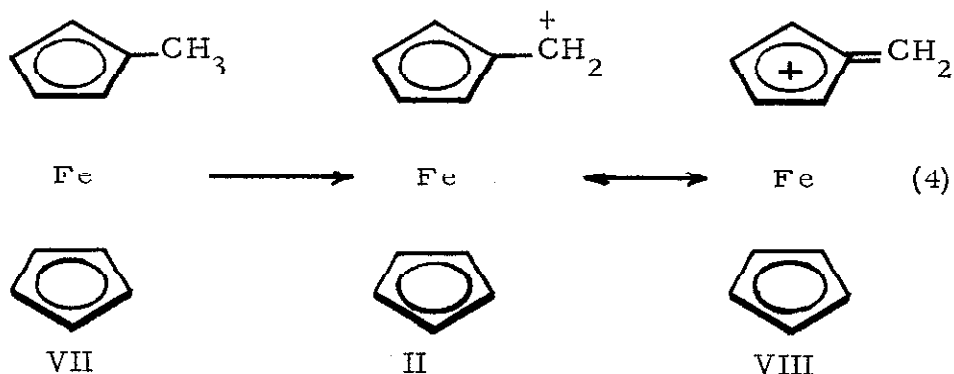


The steric hindrance between the two methyl groups of the methyl-(2-methylferrocenyl)-carbinyl carbonium ion formed from the ψ -endo acetate would make that carbonium ion less stable than the isomer formed from the ψ -exo acetate. This energy difference of the two carbonium ions manifests itself as a difference in the rates of solvolysis of the acetates, the more stable ψ -exo form solvolyzing 12.7 times faster than the ψ -endo isomer. In the present system, the ring methyl group is at the 3-position--far enough away from the carbinyl methyl group so that there is negligible steric interaction and the two isomers have essentially equal energies. In this case an equal population of the two isomers is expected, a prediction which is borne out by the relative intensities of the n.m.r. peaks.

C. DISCUSSION

1. CHEMICAL SHIFTS

The chemical shifts of the ferrocenyl protons are affected by a variety of factors, each of which will be discussed individually. We will be concerned with the changes which occur when a hydride ion is removed from the methylferrocene molecule.

a. Ring Current Effect

A ring current has been observed to exist in cyclic conjugated pi-electron systems in strong magnetic fields (36). The contribution of this ring current to the chemical shift of neighboring protons has been determined both theoretically and empirically (6, 7). The relationship expressed by Equation 5 has been used in the present work to represent this contribution.

$$\delta = 12.0 \left(\frac{a^2}{R} \right) I \quad (5)$$

δ = chemical shift

a = radius of ring containing current

R = distance of proton from center of ring

I = ratio of number of pi-electrons on ring carbons to pi-electrons in benzene

Equation 5, applied to the ring protons in ferrocene, reduces

to:

$$\delta_r = 0.243 n \quad (6)$$

where n is the number of electrons in the pi-system of one cyclopentadienyl ring. The number of electrons is estimated by summing the charge densities on all of the carbon atoms in the ring, using charge density data obtained from a molecular orbital calculation of ferrocene.

On the assumption that the carbonyl protons are planar with the cyclopentadienyl ring, Equation 5 for the chemical shift of the carbonyl protons becomes:

$$\delta_c = 0.083 n \quad (7)$$

In each case, the change in chemical shift with a change in ring current may be found by using the differential form of

Equations 6 and 7.

$$\Delta \delta_r = 0.243 \Delta n \text{ and } \Delta \delta_c = 0.083 \Delta n \quad (8)$$

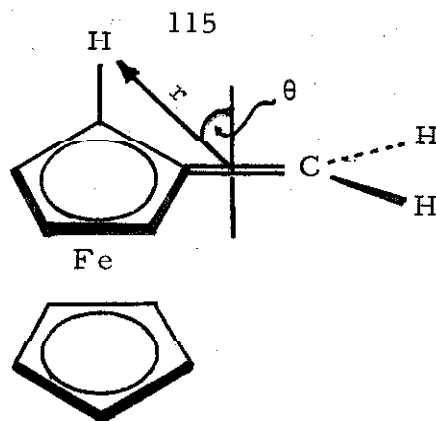
Equations 8 will be used to calculate the contribution of the ring current to the chemical shift.

b. Carbinyl Bond Anisotropy

The ferrocenylcarbinyl carbonium ion (II) is probably stabilized by resonance structures such as VIII, where a pair of electrons are donated to the carbonium center by the adjacent ring. The resulting unsaturated bond would be expected to be anisotropic in a magnetic field (37). The dipole-dipole interaction (Equation 9) derived by McConnell (38) has been used as an approximate representation of the long-range shielding effects of the carbon-carbon double bond.

$$\delta = K \frac{(3 \cos^2 \theta - 1)}{r^3} \quad (9)$$

"r" is the vector between the center of the bond and the proton of interest and "θ" is the angle this vector makes with the normal to the plane of the bond.



The constant "K" was evaluated empirically from the chemical shifts measured for protons of known orientations in 4-carbon to 7-carbon cyclo-olefins (39-41). On the basis of this evaluation, K has been assigned the value 14.1.

The mobile bond order, p , of the carbonyl-to-ring carbon bond has been used as a measure of the pi-electron density between the carbon atoms (42, 43). The assumption has been made that the anisotropic chemical shift will be directly proportional to this pi-electron density. If one takes into account the stereochemistry of the molecule, the chemical shifts in p.p.m. of the carbonyl, alpha, beta, and opposing ring protons become:

$$\delta_c = -3.80 p; \delta_\alpha = -0.915 p; \delta_\beta = -0.22 p; \delta_r = +0.8 p \quad (9a)$$

The effect of the double bond on the unsubstituted ring was calculated by integrating Equation 9 around a complete rotation of the bottom cyclopentadienyl ring.

c. Change in Bond Hybridization

Olah (44) has observed that the C^{13} chemical shift of the trityl carbonium ion is dependent on the bond hybridization as well as the charge density on the carbon. There is probably some change in the hybridization of all the bonds in methylferrocene on the formation of the carbonium ion, though the extent of change cannot be predicted at this time. Certainly the carbonyl carbon in II has a different hybridization (sp^2) than the corresponding carbon in methylferrocene (sp^3).

Even if the precise hybridization of each bond were known, the effect of the hybridization on the chemical shift of bonded protons is not known, and no reasonable estimate can be made at this time. For this reason, the bond hybridization has been ignored in this work, and one can only hope that this omission does not seriously harm the rest of the calculations.

d. Pi-Electron Charge Density on Carbon

As has been indicated in the Introduction, the chemical shift of a proton in a hydrocarbon has been found empirically (7) to be related to the pi-electron density of the adjacent carbon by Equation 1.

$$\delta = 10.7 q \quad (1)$$

At the present time, charge densities for complex systems cannot be calculated with sufficient accuracy to obtain a good estimate of the validity of this equation. The equation has, however, sufficient experimental support to justify its use in this admittedly approximate calculation.

Another, somewhat similar approach has also been used to predict the effect of the pi-electron charge densities on the proton chemical shifts. This approach considers the electric field at the proton due to the combined charge densities of the nearby pi-electron centers (45-49). The effect of an electric field on the proton resonance has been treated theoretically (45-49), and there are indications that a strong electric field reduces the screening at a proton (46, 47). The electric field method has been used successfully by Schweizer et al. (47) to predict the relative positions of the proton resonances in purine, a case where Equation 1 yields incorrect predictions.

The electric field technique predicts that the chemical shift is dependent on the component of the electric field along the C-H bond axis, and also dependent on the square of the total electric field at the proton.

$$\delta = -aE_z - bE^2 \quad (10)$$

The electric fields due to the excess electron densities on the i pi-bonded atoms are added vectorially to obtain the electric field at the proton. Using the values Schweizer has assigned for the constants a and b , Equation 10 becomes:

$$\delta = 12.5 \sum_i \frac{\Delta q_i}{R_i^2} \cos \theta_i - 17.0 \left(\sum_i \frac{\Delta q_i}{R_i^2} \cdot \frac{\bar{R}_i}{R_i} \right)^2 \quad (11)$$

In this equation, \bar{R}_i is the vector from the i -th atom to the proton under study and θ is the angle between this vector and the C-H bond.

Both Equations 1 and 11 will be used to calculate the contribution to the proton chemical shift from the charge densities predicted from molecular orbital calculations.

e. Inductive Effect

A strong positive charge on the $2p$ -pi orbital of a carbon atom induces a polarization into the C-H sigma bond, resulting in a chemical shift effect on the proton resonance frequency. A polarization of a similar nature might be expected in the C-C sigma bond between adjacent carbon atoms. This bond polarization will in effect provide a method for delocalizing a positive charge over the molecule which is independent of the pi-electron system.

Experimentally, this effect manifests itself as a more uniform set

of charge densities calculated from chemical shift data than when the charge densities are calculated from a simple LCAO-MO treatment of the molecule (4,7).

The "omega technique," which is discussed in detail in the section on the molecular orbital calculations, tends to smear the charge distribution predicted from the MO calculations. In the application of this technique, one in effect assigns a higher electronegativity to the atoms with higher positive charges, causing them to attract some of the electron cloud from adjacent atoms. This has the same effect on the total charge distribution as a polarization of the sigma system pulling electrons from the less to the more positive atoms. In fact, MacLean (4) has obtained rather close agreement between charge distributions in benzenium ions calculated using the omega technique and distributions obtained from n.m.r. chemical shifts.

The omega technique has been used in the present work to obtain more realistic molecular orbital calculations, and to compensate for a lack of a specific inductive effect correction in the calculations.

f. Selective Solvation

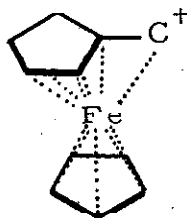
Charged ions in a polar solvent will be solvated with a counterion layer in solution; the more localized the charge, the

more important the effect of the counterions (6,7). These counterions create a strong electric field near the proton (7,45). The effect of an electric field on proton chemical shifts has been discussed in the section on pi-electron charge densities (p. 116).

In spite of the attention that this problem has received, there is not sufficient information about the degree of solvation in most systems to justify predictions of the effect of the solvent on the n.m.r. spectrum. In the present work, the assumption will be made that gross effects of the counterions will already have been included in Equation 1, and any remaining perturbations due to selective solvation will be ignored. As Equation 1 was derived without first removing specific solvation effects, this assumption is probably reasonable.

g. Ring Shift

Hill and Richards (25) have suggested that the stability of the α -ferrocenyl carbonium ion may be enhanced if the ring bearing the carbonium ion is shifted to allow greater overlap of the carbonium center with the metal orbitals.



IX

The present work indicates (see Table III, entries 4 and 5) that very little change occurs in the charge densities and bond orders calculated for the carbonium ion when a structure with a ring shifted 1.0 \AA is assumed rather than a structure where the rings and iron atom are co-axial.

The n. m. r. spectra do, however, present strong evidence that the top ring is shifted in the carbonium ion. The β ring protons are observed to be more strongly deshielded than the α protons, though molecular orbital calculations and the effects considered to this point predict just the reverse order for the ring proton chemical shifts. An attractive explanation for this phenomenon requires the top ring to be shifted away from the axis of symmetry of the magnetic field which has been induced in the iron atom. This shift would move the β protons into a field of intense magnetic deshielding, and at the same time move the α protons into a comparable shielding field. These are just the shifts desired to improve the agreement of the calculated spectrum with experiment, so structure IX will be used as a model for the remaining calculations.

h. Anisotropy of Iron

In ferrocene, the iron atom is in the cylindrically symmetric crystal field of the two cyclopentadienyl rings. This crystal field and bonding situation would be expected to impart a cylindrically

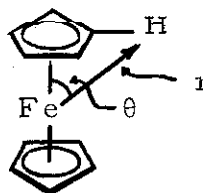
symmetric magnetic anisotropy on the iron atom. The ring protons in ferrocene are in equivalent positions relative to the iron, so the magnetic anisotropy of the iron is not observed in its n.m.r. spectrum. If, however, the top ring is shifted as in IX, its protons are no longer in equivalent positions and the effect of the anisotropy must be examined in detail.

The strong shielding effect of the iron may be deduced from the 1.5 p.p.m. upfield shift of the n.m.r. peak of ferrocene from the n.m.r. peak of the cyclopentadienyl anion. This shielding of the ferrocene protons cannot be entirely attributed to the opposing ring. A current loop approximation of the anisotropy of the ring would predict that each ring shields the other ring by only about 0.25 p.p.m., leaving 1.25 p.p.m. of the high field shift of ferrocene still unaccounted for. Indeed, if one assumes that half the charge on the cyclopentadienyl anion is delocalized by the iron atom, then the combined effects of the factors discussed above would predict a shift of the cyclopentadienyl proton peak to a point 2.16 p.p.m. to lower field than where the peak is actually observed in ferrocene. Thus, the observed upfield shift of ferrocene must be caused in one way or another by the presence of the iron atom.

As a first approximation, the iron was considered to appear like a point dipole to the protons, and Equation 9 was assumed a

valid expression of the magnetic field.

$$\delta = K \frac{(3 \cos^2 \theta - 1)}{r^3}$$



(9)

The geometry of the ferrocene molecule requires the angle theta to be 54.8° . By coincidence, this is almost exactly the angle ($55^\circ 44'$) at which $(3 \cos^2 \theta - 1) = 0$. In other words, the point dipole approximation for the anisotropy of the iron atom predicts that in ferrocene the iron atom will not affect the magnetic field at the ring protons. As the preceding discussion indicates, however, the iron atom is expected to influence the magnetic field. This incongruity probably occurs because the area of high electron density around the iron atom is so large, and the protons are so close to it, that the point dipole approximation is no longer valid. Instead, higher order terms must be included and a more refined treatment used to express the anisotropy of the iron atom.

As a second approximation, the magnetic field induced into the iron atom was considered to resemble the magnetic field caused by a loop of current centered on the iron atom. Equation 12 gives the magnetic field of a current loop as a function of position (50).

$$H_z = \frac{-Ca^2}{(a^2 + r^2 + 2ar \sin\theta)^{5/2}} \left[\begin{array}{c} \cos^2\theta(2a^2 + 2r^2 + ar \sin\theta) \\ + \\ \sin^2\theta(2a^2 - r^2 + ar \sin\theta) \end{array} \right] \quad (12)$$

In Equation 12, "a" is the radius of the current loop, "r" and "θ" are the spherical coordinates of the point of interest from the center of the loop, and "C" is a constant.

As discussed earlier, the anomalous magnetic field at the protons in ferrocene is about 2.16 p.p.m. The ring current on the iron atom was assumed to be completely responsible for this anomalous chemical shift, and this number was used with Equation 12 to empirically evaluate the constant, "C".

Since the $3d_{+2}$ orbitals play the most important part in the bonding, are the greatest in the X-Y plane, and are the highest energy iron orbitals involved in bonding (15), they were chosen as the probably dominant contributors to the magnetic anisotropy. The radial functions for 3d orbitals were used to calculate the expectation value, $\langle r \rangle$, of the distance of the 3d electron from the iron nucleus. The average position of the 3d electron is 0.84 Å from the center of the atom. This value is not too different from the crystal radius of iron (II), which is 0.76 Å (51). Both this value and one which is more in accord with the physical dimensions of

the molecule and the metallic radius (52) of iron (1.2 \AA) were used to represent the radius of the current loop.

The magnetic field at the protons due to this current loop was calculated. Entries 6 and 7 in Table III may be compared with entry 5 to see the chemical shifts predicted by the current loop model. The model using a ring radius of 1.2 \AA comes slightly closer to predicting the observed chemical shifts than the model using a 0.8 \AA radius.

Higher order multipoles were included with the dipole representation of the magnetic field in the final approximation considered. The magnetic quadrupole term was assumed to be zero. This condition is necessary to preserve the symmetry of the molecule to inversion when in a magnetic field (53). The hexadecipole was assumed to be zero for the same reason, and all terms of higher order than it were assumed to have negligible contributions. This assumption is probably quite good, as the higher order terms have more complex symmetries than the molecule and fall off quite rapidly with distance. The only multipole left to be included in the calculation is the magnetic octupole term.

A calculation including both the dipole and octupole contributions to the magnetic field contains two empirical constants which must be evaluated. They may be evaluated in much the same way that

the constant, "C", was evaluated in Equation 12, except that now there are two constants, so the magnetic field due to the iron must be known at two different points on the molecule. Once again, the ring proton in ferrocene will be used for one of the points. The bridge β -protons in 1, 1'-trimethyleneferrocene provide another calibration point of known location in the molecule. A comparison of their chemical shift with the chemical shift of the methyl protons of ethylferrocene reveals that the bridge protons are displaced 0.83 p.p.m. downfield.

The contribution to the magnetic field from a combined dipole and octupole is given by Equation 13 (54).

$$H_z = \frac{C_1}{r} (3 \cos^2 \theta - 1) + \frac{C_2}{r^5} (35 \cos^4 \theta - 30 \cos^2 \theta + 3) \quad (13)$$

"r" and " θ " have the same significance as earlier, and " C_1 " and " C_2 " are the empirical constants for the dipole and octupole terms, respectively. By evaluating Equation 13 at the two above mentioned points, C_1 and C_2 have been found to have the following values:

$$C_1 = -1.39; \quad C_2 = -121.9 :$$

As indicated in Table III, the octupole approximation to the magnetic field of iron results in chemical shift predictions which

are very similar to those predicted by the current loop approximation with a 1.2 \AA current loop.

i. Summary

In this section attempts have been made to explore all of the factors which might reasonably influence the chemical shifts of the protons in the ferrocenylcarbonyl carbonium ion. While some of the effects, such as the cyclopentadienyl ring current, have an unimportant and relatively constant effect on the ring protons, other effects alter the spectrum drastically. For example, the magnetic anisotropy of the iron atom considered in conjunction with the shift of a cyclopentadienyl ring will reverse the anticipated positions of the α and β ring protons.

While these calculations have only succeeded in predicting relative positions of proton resonances and orders of magnitudes of chemical shifts, the calculations are necessary preliminary steps towards the successful understanding of the ferrocenyl system in future studies.

2. MOLECULAR ORBITAL CALCULATIONS

The molecular orbital calculations to be considered here may all be classified as one or another modification of the linear-combination-of-atomic-orbitals method. The only other theory in common usage, the valence-bond theory, is not suited for quantitative or semiquantitative calculations. Valence-bond calculations become exceedingly difficult with large systems, and do not lend themselves to applications where the molecule contains heteroatoms (55).

The first and simplest calculation undertaken was the simple Hückel (56) or LCAO treatment of fulvene, the molecular equivalent to the top ring of the ferrocenyl carbonium ion. As can be seen from entry two of Tables III and IV, this calculation predicts too much positive charge remaining on the carbinyl carbon resulting in an extreme chemical shift.

Entry 3 in Tables III and IV represents a simple LCAO calculation for the full carbonium ion. Once again, too much localization of the positive charge on the carbinyl carbon is predicted.

A variety of values were assumed for the resonance and coulomb integrals, but even variations of α and β by a factor of two or three produced only minor changes in the calculated charge distribution for the carbonium ion. The first appreciable change

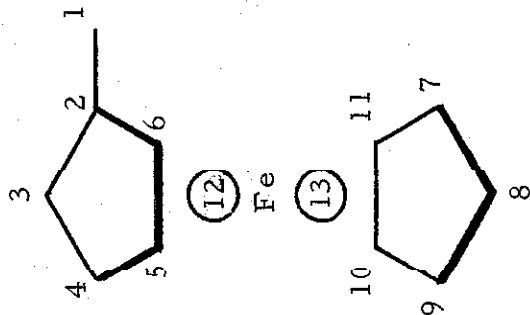
TABLE IV. Parameters Used in Molecular Orbital Calculations

Calc. No. ^b	Input Parameters ^a					E_{C-Fe}
	f_{1-12}	β_{2-12}	β_{3-12}	β_{4-12}	β_{7-13}	
2	-	-	-	-	-	-
3	0.3	0.5	0.5	0.5	0.5	-
4	0.3	0.5	0.5	0.5	1.0	0.5
5	0.48	0.6	0.52	0.35	0.5	0.5
FcH	-	0.5	0.5	0.5	1.0	0.5

Charge Densities and Bond Orders											
	q_1	q_2	q_3	q_4	q_7	q_{Fe}	P ₁₂	P ₂₃	P ₃₄	P ₄₅	P ₇₈
2	+ .384	- .040	+ .270	+ .062	-	-	.751	.447	.555	.662	-
3	+ .382	+ .011	- .046	- .025	- .149	+ 1.492	.742	.397	.730	.472	.596
4	+ .20	+ .17	+ .04	+ .03	- .104	+ 1.03	.797	.23	.76	.38	.551
5	+ .20	+ .17	+ .04	+ .03	- .104	+ 1.03	.798	.230	.763	.380	.551
FcH	-	-	-	-	- .104	+ 1.04	-	-	-	-	.551

a. In all these calculations, $\alpha_C = 0$, $\alpha_{Fe} = -0.5$, and $\beta_{C-C} = 1.0$.

b. Referring back to the entries in Table III.



occurred when α was changed sufficiently to cause the energy levels associated with two of the wave functions to move past one another. When this happened, the resulting charge densities and bond orders took on meaningless values and no longer reflected the physical symmetries of the molecule.

Overlap between adjacent atoms has been neglected in these calculations. While the inclusion of overlap would change the calculated energy levels of the system, we are only concerned with the charge densities and bond orders, both of which are unaffected by a constant overlap between neighboring carbon atoms (57).

The simple LCAO-MO method has previously been recognized to be inadequate to predict the degree of charge delocalization (7). A simple way of looking at this deficiency is to consider that all carbon atoms have been assigned equal electronegativity (equal values of α), although the theory predicts that some of the carbons will have a higher electron density than others. An atom with higher electron density will be less electronegative than one with lower electron density, and must be considered as such.

One straightforward approach to this problem is embodied in the "omega technique" (13, 58, 59). To apply the omega technique, one essentially uses simple LCAO to calculate the charge densities on each carbon atom and then modifies the coulombic integrals by adding (in units of β_0) some fraction, omega, of the charge. The

calculation is then repeated.

$$\alpha_{i+1} = \alpha_0 + q_i \omega \beta_0 \quad \beta_0 = \text{standard reference } \beta \quad (14)$$

The value 1.4 is widely accepted for omega (59); however, in the present work (with many successive iterations), the charge densities from iteration to iteration were found to fluctuate wildly and uncontrollably. Lower values for omega were found to moderate the fluctuations, and $\omega = 1.0$ was accepted as a reasonable compromise between insufficient and uncontrollable corrections.

The simple LCAO approach also suffers from a deficiency in assessing the resonance integrals between adjacent carbon atoms, i. e., pairs of atoms with a high bond order would be expected to be closer together and have larger values of β than pairs with low bond orders.

Good correlations have been observed between bond lengths in molecules and the corresponding calculated bond orders (43, 60, 61). Additionally, Mulliken (62, 63) has suggested a relationship between β and the bond distance, starting with the assumption that the resonance integral is proportional to the overlap integral (64, 65). He has also combined these relationships into an analytical expression for the resonance integral in terms of the bond order (66, 67).

$$\beta = (0.320p + 0.460)\beta_0 \quad (15)$$

The technique of modification of α and β on the basis of previous calculations and then repeated iteration of the calculation to a self-consistent set of parameters has been used successfully by Wheland to calculate the dipole moments of fulvene and azulene (58). Mulliken has also used this technique to study the hyperconjugation energy in aromatic ions and alkyl radicals (66, 67).

In the present work, a program has been written for the IBM 7094 computer which will calculate energy levels, wave functions, charge densities, and bond orders from the secular determinant for a system. One need only specify a set of α 's and β 's to be entered into the secular determinant. On completing these calculations, the computer applies the corrections specified by Equations 14 and 15 to the integrals in the secular determinant input matrix. The computer may be directed to repeat this sequence as many times as desired to achieve a self-consistent set of parameters. In practice, 10 to 15 such iterations have been found to suffice. The program has been given the name "MILMO4" and the Fortran IV version is listed in the Appendix.

Equation 15 will only provide information on the value of the resonance integral between carbon atoms. In the ferrocene molecule, bonding is also observed between carbon atoms and an iron atom, and improved values for β would likewise be helpful here.

Coulson (68,69) has shown that a relationship exists between the resonance integral (β), the bond order (p), and the energy (E) of a bond between two atoms.

$$\partial \beta = \frac{\partial E}{2p} \quad (16)$$

The integral form of Equation 16 was used in the iterative MO program, and was found to yield values for β which would often cause successive iterations to diverge rather than converge. Equation 17 has been used in its place as a means of forcing the series to converge without losing sight of the original relationship.

$$\beta_{i+1} = \frac{1}{2} \left(\frac{E}{2p_i} + \beta_i \right) \quad (17)$$

The total iron-to-carbon bonding energy in ferrocene has been calculated from thermodynamic data to be 53 kcal (70). This figure was derived assuming a standard β_0 for benzene of 18 kcal, so, using this same number, the iron-carbon bonding energy would be $53/18 \times 10 = 0.3\beta_0$ per iron-carbon bond. Dunitz (16), on the other hand, has used molecular orbital theory to obtain a total iron-to-ring bonding energy of 286 kcal/mole. This figure was derived using a standard β_0 of 60 kcal/mole, so these calculations would predict an energy for each iron-carbon bond of $28.6/60 = 0.5\beta_0$.

MILMO4 has incorporated in it the option of applying Equation 17 as a correction on the resonance integrals between iron and

carbon atoms. A series of calculations was undertaken, keeping all of the starting input parameters constant except for the iron-carbon bond energy, which was varied from 0.2β to 0.5β . The primary effect of this increment was to increase the iron-carbon β from 0.3 to 0.65. This change in the input matrix then caused the charge calculated on the iron atom to drop from +1.46 to +1.04, or a gain of 0.4 electron. For reasons discussed in the following section, the latter value was felt to be closer to the actual charge on the iron atom. The data presented in Tables III and IV has therefore been calculated using 0.5β for the energy of the iron-carbon bond.

Different types of interactions between the rings and the iron atom were considered. The iron was assumed to have: 1) two orbitals, each interacting with only one ring and orthogonal to each other; 2) two orbitals, again each interacting with only one ring, but now interacting strongly with each other; and lastly, 3) two orbitals, each interacting equally with every carbon atom.

1) The model which was finally accepted to represent the ferrocene system is one where the iron atom is assigned two orthogonal orbitals, each interacting with the carbon atoms of only one ring. This is the only model which has been found to yield bond orders and charge densities which can always be made to converge, and to yield numbers which are always consistent with the symmetry

requirements of the molecule. A natural consequence of this model is that the molecule is artificially divided into two completely independent parts: the top ring and its iron orbital, and the bottom ring and its iron orbital. Since the bottom half calculation does not depend on whether the top half is ferrocene or carbonium ion, it yields the same results for both cases. In other words, this model predicts that the charge densities on the bottom ring do not change on going to the carbonium ion.

In the actual system, however, an inductive effect is important which is not included in the above model. Evidence of the extent of this inductive transfer of electrons from the iron atom and the bottom ring to the electron-deficient top ring will be discussed shortly.

2) The second model was studied in an attempt to counteract the artificial division of the molecule discussed above. This system was essentially the same as the preceding one, except that the two iron orbitals were no longer considered orthogonal.

Once again, as in the rest of the molecular orbital calculations, the positive charge delocalization is inexplicably confined almost entirely to the top ring, with very little change in charge density on the iron orbitals, and essentially none on the bottom ring. This property was observed to hold true even when a strong interaction between the carbonyl carbon and the iron atom was included,

and also when the two orbitals from the iron atom were allowed to interact strongly with each other, as in the present model. The resistance to change of the charge density calculated for the bottom ring with the formation of the carbonium ion may reflect on the lack of a specific inductive effect incorporated in the model, or it may indicate an underlying fault in the ability of the model to successfully represent the real system.

The computer program had not been written to distinguish types of iron bonds, and it applied the same iterative correction (Equation 17) to the iron-iron interaction as it did to the iron-carbon interaction. Because of this, the iron-iron starting β could be varied from $1\beta_0$ to $100\beta_0$, and sufficient iterations would bring it to the same point (1.098) every time. No attempt was made to apply a different iterative correction to it.

3) If the iron atom is assigned two orthogonal orbitals and each is allowed to interact equally with all the carbon atoms, the first LCAO calculation yields results almost identical with case 1. Further iterations, however, slowly cause the system to lose symmetry, and rather than converging, the sequence of iterations eventually diverges. It is interesting to note that for this model the iron orbitals in the carbonium ion have slightly more positive charge than in neutral ferrocene, but the carbon atoms on the unsubstituted ring are predicted to actually have a higher negative charge than on

neutral ferrocene. There are no particular advantages to a model using this mode of orbital interaction, and there are these several disadvantages, so this model was discarded.

Each of the representations of ferrocene discussed above involves the ten 2p-pi orbitals of the carbon rings interacting with two orbitals on the iron atom. Systems were also examined where the iron atom was assigned one orbital and four orbitals; however, very similar results were obtained in each case. The assignment of two orbitals to the iron atom appears to be general enough so that either of the other models could be represented by appropriate choices for the values of the coulomb and resonance integrals on the iron atom. As models with one iron orbital and with four iron orbitals contributed nothing to the flexibility of the calculations and only complicated the picture, the model with two iron orbitals was used for the final calculations on the ferrocenyl system.

A model with separate orbitals for each ring is also intuitively attractive, because one may take a linear combination of the atomic orbitals of iron which are available for bonding and obtain a strongly bonding hybrid set of orbitals directed uniformly to one ring with a corresponding set of orbitals directed to the other ring (17).

One important point to note is that experimentally the n. m. r. peak of the unsubstituted (bottom) ring of methylferrocene is observed to shift 1.4 p. m. to lower magnetic field on the formation of the

carbonium ion. As mentioned above, none of the molecular orbital calculations in this paper predict any change in the pi-electron charge densities or ring current of that ring. The presence of double bond character in the bond between the carbonyl carbon and top ring is predicted to shift the bottom ring 0.6 p.p.m. in the wrong direction.

It is of interest to examine the experimental evidence for and against interactions which propagate charge variations from one ring to the other. Woodward (71) has measured the acid constants of ferrocene-1,1'-dicarboxylic acid in 2:1 ethanol-water to be 3.1×10^{-7} and 2.7×10^{-8} , and from their similarity he concludes that there is very little interaction between the rings. The acid constants for terephthalic acid, however, show an equally small variation (2.9×10^{-4} and 3.5×10^{-5} in aqueous solution), this variation being entirely attributed to the physical proximity of the negatively charged carboxylate ion to the remaining acid function, resonance and inductive effects through the pi-electron system apparently being negligible (72). Since resonance and inductive effects are important between para positions on a benzene ring, one must conclude that acid dissociation constants do not provide a suitable measure of the magnitude of these effects.

There is considerable evidence that variations in charge are transmitted from one ring to the other in ferrocenyl systems. The presence of an acetyl group on one ring deactivates the other ring towards further acetylation (73), probably due to the formation of a positively charged proton complex with the carbonyl already present in the molecule. Strong correlations have been observed between the electron donor properties of substituents on a ferrocene ring and 1) the strength of a heteroannularly substituted acid function, 2) the stretching frequencies of heteroannular carbonyl groups, and 3) the reversible quarter-wave potentials for the respective substituted ferrocenes (74).

In addition to an inductive coupling of charge between the two rings of ferrocene, the downfield chemical shift of the bottom ring resonance may be caused by the anisotropy of the iron atom. This phenomenon would be related to, and indeed is, an extension of the ring shielding effect discussed on page 122. The change of charge density on the iron atom on going to the carbonium ion could conceivably decrease the anisotropy of the iron, resulting in less shielding of the bottom ring protons. No attempt has been made to put this effect on a quantitative basis, and the effect has been omitted in the above calculations.

3. THE CHARGE ON IRON

A multitude of similar calculations have been performed in this work, each one involving several educated guesses on the values of constants and parameters in the hope of finding some combination of numbers which would successfully predict the n. m. r. spectrum of the system. An easier task, but perhaps still not simple enough, would be to try to predict the charge on the iron atom of ferrocene.

Several other investigators have used molecular orbital techniques to calculate this charge (15, 16, 20, 21), and their results are tabulated in Table V. Each one of them has taken advantage of the high symmetry of ferrocene to simplify the calculation, and yet there are still so many ambiguities that they each arrived at different values.

The present work deals with the carbonium ion, which does not have the high symmetry of ferrocene. For this reason, it was necessary to resort to a more involved calculation, considering each atom-atom interaction individually. The calculation performed in this manner and using the corrections discussed previously results in a prediction of a +1.04 charge on the iron atom of ferrocene. This charge is larger than that predicted by any of the other investigators.

TABLE V

The Charge on the Iron Atom of Ferrocene

Value	Method	Reference
~ 0	MO	15, 16
-0.2 to -1.2	MO	20
+0.682	MO	21
~ 0	pK of carboxylic acid	71
+1.04	MO	present work

The pK of ferrocenoic acid is very near to that of benzoic acid (7.1, 7.5), indicating that the carbon atoms to which the carboxylate group is bonded in the two systems have similar pi-electron charge densities. An alternative explanation may be considered in which the charge densities on the ring carbon atoms of ferrocenoic acid do differ from the densities on the benzoic acid carbon atoms, while at the same time the iron atom in ferrocene interacts with the carboxylate function in an unknown way to compensate for this variation of charge densities, coincidentally resulting in an acid constant similar to the acid constant of benzoic acid.

4. CONCLUSIONS

This study of the ferrocenylcarbinyl carbonium ion has answered very few questions--indeed, it has raised more questions than it has answered: How is the carbonium ion stabilized? Is the substituted ring shifted to allow greater interaction of the carbonium ion with the iron? What does the magnetic field look like in the neighborhood of the iron atom? Do LCAO MO techniques work at all for ferrocenyl systems, and, if so, what are reasonable values for the molecular orbital parameters? What is the charge distribution in ferrocene and in the carbonium ion? What is causing the chemical shift of the unsubstituted ring protons in the carbonium ion relative to the neutral molecule?

Answers have been suggested for some of these questions, but no theory can yet be postulated to encompass all that is known about these systems. Several areas suggest themselves for immediate exploration.

The n. m. r. spectrum of the carbonium ion from ferrocenyl-1, 1'-dicarbinol should be studied to observe the effect of two carbonium ions on the same molecule. If charge delocalization to the other ring is important, the β proton resonance of the di-cation should be shifted even further downfield, while if the major contributor to the proton resonance positions is the ring shift, the chemical shifts of protons α and β to the carbonyl carbon atoms would be expected to appear in comparable places in the mono- and di-cations.

An advanced self-consistent field molecular orbital calculation should be applied to ferrocene to see how close an agreement will exist between its results and the present calculations. Perhaps this more sophisticated calculation will give more accurate pi-electron charge density information, and hence more accurate chemical shift predictions.

In the meantime, the groundwork has been done on these systems, and a frame of reference has been defined from which future studies can build.

D. EXPERIMENTAL

1. COMPOUNDS

a. Ferrocenylmethanol

Phosphorus oxychloride (27.7 g, 0.17 moles), purified by distillation, was mixed with N-methyl formanilide (24.4 g, 0.18 moles) at 0°C. The mixture was allowed to come up to room temperature and react for one hour. Ferrocene (16.5 g, 0.089 moles) was added with vigorous stirring. The mixture was allowed to react in a stoppered flask for four days. The flask was chilled to 0°C and 25 ml of ice water was cautiously added. No reaction occurred for several minutes; then the solution became hot and boiled violently. The material was allowed to cool and was extracted with 200 ml of chloroform. On evaporation of the extract to dryness, a dark brown tar remained. The tar was dissolved in benzene and chromatographed on alumina. A yellow compound was eluted, followed by a deep red compound believed to be the desired ferrocenecarboxaldehyde. The benzene was distilled from this fraction, leaving a deep red-brown tar, which would not crystallize from ethanol. The tar (10 g, 0.04 moles) was dissolved in 250 ml methanol and sodium borohydride (5.0 g, 0.13 moles) was added. A gas was evolved for about a half-hour, after which the methanol was allowed to evaporate. The remaining oil was dissolved in a large quantity of boiling water

and the solution was chilled. A greenish-yellow semi-crystalline solid formed on cooling. The crystals were washed with water and recrystallized from n-hexane, yielding 7.8 g of fine yellow needles. M.p. 77-78°, mixed melting point with ferrocenylmethanol, 77-79°C; reported 76° (30).

b. Methylferrocene

A solution of ferrocenemonocarboxylic acid (2.3 g, 0.01 moles) in 50 ml methanol was refluxed one hour with 2 ml concentrated sulfuric acid. Water was added and the solution was extracted with ether. Evaporation of the ether left 1.25 g of a reddish-brown crystal, m.p. 63-67°; reported for methyl ferrocenylcarboxylate, 70-71°C (75).

The ester (1.25 g, 5.1 mmole) was dissolved in anhydrous ether and lithium aluminum hydride (0.15 g, 4 mmole) in 25 ml ether was added. This was followed by anhydrous aluminum chloride (1.2 g, 9 mmole), and an additional 0.15 g of lithium aluminum hydride, each dissolved in anhydrous ether. The solution was refluxed four hours. Excess hydrides were hydrolyzed with 20 ml water, followed by 20 ml 6N sulfuric acid. The ether layer was washed with water and evaporated, leaving a partially crystalline orange-brown oil of methylferrocene. The product was purified by vacuum sublimation at 50°C onto a dry-ice acetone cold finger,

resulting in a 40% yield. The methylferrocene deposited as a yellow powder, which darkened on contact with air, m.p. 33-35°C.

c. 1,1'-Trimethyleneferrocene

This compound had been previously prepared in these laboratories by E. Alexander Hill (76). It was recrystallized from n-hexane and used directly (m.p. 105-106°C).

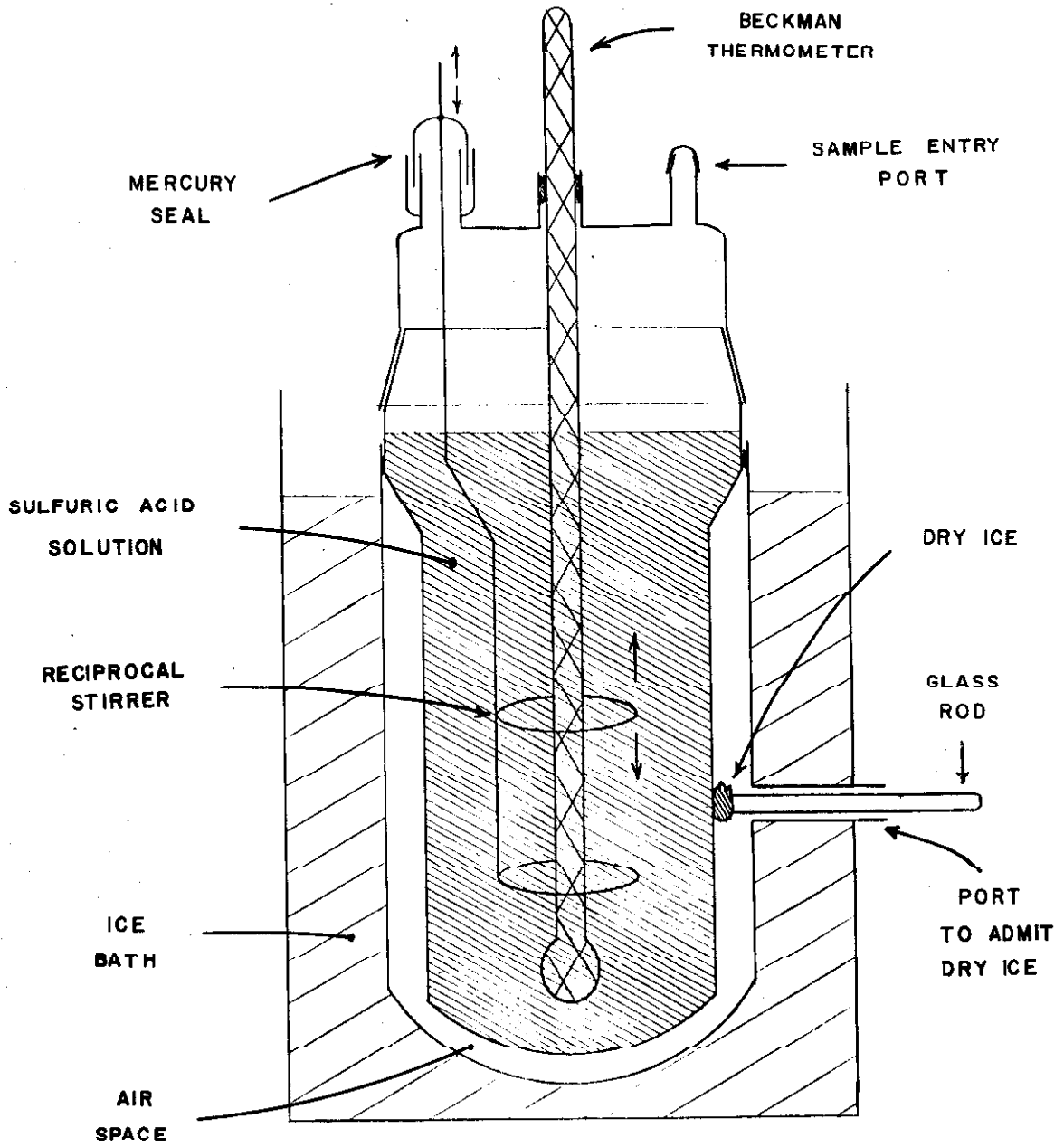
2. FREEZING POINT DEPRESSION

The cryostat used to measure the freezing points is described by Newman (33), and is shown in Figure 5.

A stock solution was made of slightly fuming sulfuric acid by mixing 380 ml concentrated sulfuric acid with 1 lb of 30% fuming sulfuric acid. This mixture was found to be slightly higher than the desired concentration of sulfur trioxide to produce the highest freezing point. The addition of 0.7 ml of water per sample brought the sulfuric acid to the desired concentration just past the freezing point maximum.

A weighed quantity (approximately 90 g) of sulfuric acid was poured into the cryostat. The unit was assembled and all joints greased. The required 0.7 ml of water was added. The cryostat was allowed to equilibrate for several hours, so that the inside surface would lose any water film which may have adhered. The outer

FIGURE 5 FREEZING POINT CRYOSTAT



can was filled with an ice-water slurry. The sulfuric acid solution was stirred and its temperature was recorded every minute. The temperature was estimated to 0.001 degree with a Beckman thermometer. When the temperature fell to the freezing point of the sulfuric acid, a piece of dry ice was placed against the surface of the inner vessel. The dry ice was held there one minute, and upon removal, white crystals of sulfuric acid could be seen. The temperature would continue to drop for several more minutes. It would then suddenly shoot up a degree or two and stay there for from 2 to 15 minutes, depending on the concentration of solute. This maximum point was taken as the freezing point.

Samples were introduced into the solution as compressed pellets and dropped down a glass tube to the surface of the acid. This method of introducing samples required an hour to dissolve each sample. The method was, however, found to be a superior way of insuring that the entire sample reached the acid.

Once the freezing point was obtained for the sample, the inner vessel was removed from the rest of the apparatus and allowed to warm up to room temperature. A sample pellet was introduced into the acid and allowed to dissolve. The freezing cycle was then repeated.

The data obtained in this way were used to calculate the Van't Hoff i Factor, using the formulas in Table VI.

3. NUCLEAR MAGNETIC RESONANCE SPECTRA

The n. m. r. spectra were observed on a Varian Associates A-60 n. m. r. spectrometer at the standard probe temperature ($\sim 35^{\circ}$ C). The carbonium ions were observed in solution in boron trifluoride monohydrate, trifluoroacetic acid, and in sulfuric acid as solvents, with tetramethylammonium bromide present as an internal standard. The chemical shift of the tetramethylammonium bromide proton was taken as $\tau = 6.67$. The remaining compounds were observed as dilute solutions in carbon tetrachloride with an internal standard of tetramethylsilane.

TABLE VI

A. Calculation of Van't Hoff i Factor

$$i = \frac{\Delta T}{\Delta m \times 6.154 (1 - 0.0047t)}$$

Δm = molality of solute in solvent

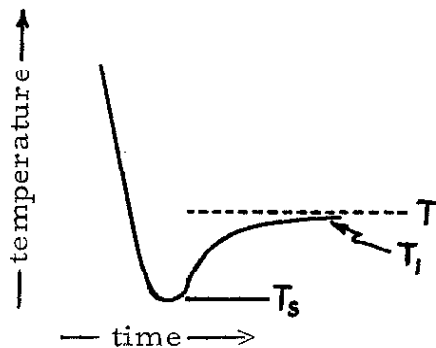
ΔT = change in freezing point when solute is added

t = mean depression = freezing point of sulfuric acid -
mean freezing point of solution

Source: Reference 32

B. Super-Cooling Correction

$$\delta T = T - T_1 = 0.012 (T_1 - T_s) (T_0 - T_1)$$



T = correct freezing point

T_0 = freezing point of pure sulfuric acid

T_1 = measured freezing point

T_s = lowest temperature reached during super-cooling

Source: Reference 31

C. Thermometer Stem Correction

$$T_c = T_o + 0.00016 L (T_o - T_m)$$

T_c = correct temperature

T_o = observed temperature

L = exposed mercury length in degrees

T_m = temperature of exposed stem

Source: Reference 77

E. REFERENCES

1. P. L. Corio and B. P. Dailey, *J. Am. Chem. Soc.*, 78, 3043 (1956).
2. H. Spiesecke and W. G. Schneider, *J. Chem. Phys.*, 35, 731 (1961).
3. H. Spiesecke and W. G. Schneider, *Tet. Let.*, 468 (1961).
4. C. MacLean and E. L. Mackor, *Mol. Phys.*, 4, 241 (1961).
5. G. Fraenkel, R. E. Carter, A. McLachlan, and J. H. Richards, *J. Am. Chem. Soc.*, 82, 5846 (1960).
6. B. P. Dailey, A. Gawer, and W. C. Neikam, *Disc. Faraday Soc.*, 31, 18 (1962).
7. T. Schaefer and W. G. Schneider, *Can. J. Chem.*, 41, 966 (1963).
8. V. R. Sandel and H. H. Freedman, *J. Am. Chem. Soc.*, 85, 2328 (1963).
9. J. D. Roberts, "Notes on Molecular Orbital Calculations," W. A. Benjamin, N. Y., 1961, p. 94.
10. A. Julg, *J. Chim. Phys.*, 52, 377 (1955).
11. R. Pariser, *J. Chem. Phys.*, 25, 1112 (1956).
12. R. D. Brown and M. L. Heffernan, *Australian J. Chem.*, 13, 38 (1960).
13. A. Streitwieser, Jr., "Molecular Orbital Theory," J. Wiley & Sons, N. Y., 1961, pp. 115 and 457.
14. H. H. Jaffé, *J. Chem. Phys.*, 21, 156 (1953).
15. W. Moffitt, *J. Am. Chem. Soc.*, 76, 3386 (1954).

16. J. D. Dunitz and L. E. Orgel, *J. Chem. Phys.*, 23, 954 (1955).
17. J. W. Linnett, *Trans. Faraday Soc.*, 52, 904 (1956).
18. M. Yamazaki, *J. Chem. Phys.*, 24, 1260 (1956).
19. A. D. Liehr and C. J. Ballhausen, *Acta Chem. Scand.*, 11, 207 (1957).
20. D. A. Brown, *J. Chem. Phys.*, 29, 1086 (1958).
21. E. M. Shustorovich and M. E. Dyatkina, *Doklady Akad. Nauk SSSR*, 128, 1234 (1959).
22. E. M. Shustorovich and M. E. Dyatkina, *Doklady Akad. Nauk SSSR*, 133, 141 (1960).
23. R. E. Robertson and H. M. McConnell, *J. Phys. Chem.*, 64, 70 (1960).
24. C. J. Ballhausen and J. P. Dahl, *Acta Chem. Scand.*, 15, 1333 (1961).
25. E. A. Hill and J. H. Richards, *J. Am. Chem. Soc.*, 83, 3840 (1961).
26. M. Rosenblum and W. G. Howells, *J. Am. Chem. Soc.*, 84, 1167 (1962).
27. G. Wilkinson and F. A. Cotton, *Progress in Inorg. Chem.*, I, 1 (1959).
28. J. H. Richards and E. A. Hill, *J. Am. Chem. Soc.*, 81, 3484 (1959).
29. G. R. Buell, G. McEwen, and J. Kleinberg, *Tet. Letters*, #5, 16 (1959).
30. G. D. Broadhead, J. M. Osgerby, and P. L. Pauson, *J. Chem. Soc.*, 650 (1958).
31. R. J. Gillespie, E. D. Hughes, and C. K. Ingold, *J. Chem. Soc. (London)*, 2473 (1950).

32. J. L. O'Brien and C. Niemann, *J. Am. Chem. Soc.*, 73, 4264 (1951).
33. M. S. Newman, H. G. Kuivila, and A. B. Garrett, *J. Am. Chem. Soc.*, 67, 704 (1945).
34. L. P. Hammett and A. J. Deyrup, *J. Am. Chem. Soc.*, 55, 1900 (1933).
35. E. A. Hill and J. H. Richards, *J. Am. Chem. Soc.*, 83, 4216 (1961).
36. J. A. Pople, W. G. Schneider, and H. J. Bernstein, "High-Resolution Nuclear Magnetic Resonance," McGraw-Hill Book Co., 1959, pp. 180, 250.
37. L. M. Jackman, "Nuclear Magnetic Resonance Spectroscopy," Pergamon Press, N. Y., 1959, p. 129.
38. H. M. McConnell, *J. Chem. Phys.*, 27, 226 (1957).
39. J. A. Pople, *Disc. Faraday Soc.*, 34, 7 (1962).
40. J. A. Pople, *Mol. Phys.*, 1, 175 (1958).
41. K. B. Wiberg and B. J. Nist, *J. Am. Chem. Soc.*, 83, 1226 (1961).
42. Reference 9, p. 53.
43. Reference 13, pp. 55, 165.
44. G. A. Olah, E. B. Baker, and M. B. Comisarow, *J. Am. Chem. Soc.*, 86, 1265 (1964).
45. M. J. Stephen, *Mol. Phys.*, 1, 223 (1958).
46. T. W. Marshall and J. A. Pople, *Mol. Phys.*, 1, 199 (1958).
47. M. P. Schweizer, S. I. Chann, G. K. Helmkamp, and P.O.P. Ts'o, *J. Am. Chem. Soc.*, 86, 696 (1964).
48. A. D. Buckingham, *Can. J. Chem.*, 38, 300 (1960).

49. J. I. Musher, *J. Chem. Phys.*, 37, 34 (1962).
50. J. D. Jackson, "Classical Electrodynamics," Wiley and Sons, N. Y., 1962, p. 142.
51. L. C. Pauling, "The Nature of the Chemical Bond," Cornell University Press, N. Y., 1960, p. 518.
52. Ibid., pp. 256, 403.
53. N. F. Ramsey, "Nuclear Moments," John Wiley & Sons, N. Y., 1953, p. 9.
54. J. C. Slater and N. H. Frank, "Electromagnetism," McGraw-Hill Book Co., N. Y., 1947, pp. 224, 230.
55. Reference 13, pp. 24-26.
56. Reference 13, pp. 33-62.
57. Reference 13, pp. 101-102.
58. G. W. Wheland and D. E. Mann, *J. Chem. Phys.*, 17, 264 (1949).
59. A. Streitwieser, Jr., *J. Am. Chem. Soc.*, 82, 4123 (1960).
60. Reference 9, p. 55.
61. C. A. Coulson, "Valence," Clarendon Press, Oxford, 1952, p. 253.
62. R. S. Mulliken, C. Rieke, and W. G. Brown, *J. Am. Chem. Soc.*, 63, 41 (1941).
63. Reference 13, pp. 103-105.
64. R. S. Mulliken, *J. Chim. Phys.*, 46, 675 (1949).
65. R. S. Mulliken, *J. Phys. Chem.*, 56, 295 (1952).
66. N. Muller, L. W. Pickett, and R. S. Mulliken, *J. Am. Chem. Soc.*, 76, 4770 (1954).

67. N. Muller and R. S. Mulliken, *J. Am. Chem. Soc.*, 80, 3489 (1958).
68. C. A. Coulson, *Proc. Roy. Soc. (London)*, A169, 413 (1939).
69. C. A. Coulson and H. C. Longuet-Higgins, *ibid.*, A191, 39 (1947).
70. F. A. Cotton and G. Wilkinson, *J. Am. Chem. Soc.*, 74, 5764 (1952).
71. R. B. Woodward, M. Rosenblum, and M. C. Whiting, *J. Am. Chem. Soc.*, 74, 3458 (1952).
72. B. J. Thamer and A. F. Voigt, *J. Phys. Chem.*, 56, 225 (1952).
73. M. Rosenblum and R. B. Woodward, *J. Am. Chem. Soc.*, 80, 5443 (1958).
74. D. W. Hall, Ph. D. Thesis, California Institute of Technology, 1963, Part II.
75. R. A. Benkeser, D. Groggin, and G. Schroll, *J. Am. Chem. Soc.*, 76, 4025 (1954).
76. E. A. Hill, III, Ph. D. Thesis, California Institute of Technology, 1961, p. 164.
77. "Handbook of Chemistry and Physics," 39, 2144 (1957).

F. APPENDIX

· FORTRAN IV LIST OF COMPUTER PROGRAM MILMO4

```

$IBJOB
$IBFTC M04
C   PROGRAM FOR DIAGONALIZING A 20X20 MATRIX USING FIGVV
C   NEEDS ONLY UPPER MATRIX ELEMENT INPUT
C   CALCULATES ENERGY LEVELS, WAVE FUNCTIONS, CHARGE DENSITIES,
C   AND BOND ORDERS
C   USES THE OUTPUT TO GENERATE A NEW INPUT MATRIX AND REITERATES
C   MMAX=NUMBER OF CARDS ENTERED, N=SIZE OF MATRIX,
C   L=NUMBER OF ELECTRONS IN WAVE FUNCTION.
C   ITR=NUMBER OF ITERATIONS, IRON=FIRST IRON ORBITAL, INPRT=0 MEANS
C   FULL OUTPUT FORMAT, INCLB / 0=NO BETA CORRECTION, 1=ONLY C-C CORR.
C   2=ONLY IRON-C CORRECTION, 3=BOTH. W=VALUE OF OMEGA,
C   ENGY=C-IRON BOND ENERGY IN UNITS OF BETA.
C   MODIF / 0=NEW SET OF DATA, 1=SAME INPUT MATRIX AS BEFORE,
C   2=USE PREVIOUS OUTPUT FOR INPUT TO NEXT SET.
C   WRITTEN BY MILTON LEVENBERG
C
C   CLEAR AND SET ARRAYS
C
ODIMENSION A(400), V(400), VALU(20), QTOT(20), PTOT(150),
IIND(150), JIND(150), TITLE(12), STOR(20), A1(400), B(800), A2(20),
2A3(150)
5 READ (5,9000) (TITLE(I), I=1,12)
  READ (5,9002) MMAX,N,L,ITR,IRON,INPRT,INCLB,W,ENGY,MODIF
  ITNO=0
  KONTR=0
  B(1)=0.0
  IF (MODIF-1) 10,6,8
6 DO 7 I=1,400
7 A(I)=A1(I)
  GO TO 31
8 IF (BOND.LT.0.0) GO TO 5
  DO 9 I=1,400
9 A1(I)=A(I)
  GO TO 31
10 DO 20 I=1,20
  VALU(I)=0.0
  STOR(I)=0.0
  A2(I)=0.0
20 QTOT(I)=0.0
  DO 26 I=1,400
  A(I)=0.0
  A1(I)=0.0
26 V(I)=0.0
C
C   DISPLAY OF INPUT MATRIX
C
DO 30 M=1,MMAX
  READ (5,9003) I,J,C
  INDX=N*(I-1)+J
  A(INDX)=C
  A1(INDX)=C
  INDX=N*(J-1)+I
  A(INDX)=C
  A1(INDX)=C
  IND(M)=I
  JIND(M)=J
  IF (I-J) 30,29,30
29 A2(I)=C
30 CONTINUE

```

```

31 WRITE (6,9001) (TITLE(I),I=1,12)
   WRITE (6,9004) ITNO
   FLN=N
   IF (FLN-8.0) 35,35,40
35 DO 37 I=1,N
   DO 36 J=1,N
   INDX=N*(I-1)+J
36 STOR(J)=A(INDX)
37 WRITE (6,9005) (STOR(J), J=1,N)
   GO TO 50
40 DO 42 I=1,N
   DO 41 J=1,8
   INDX=N*(I-1)+J
41 STOR(J)=A(INDX)
42 WRITE (6,9005) (STOR(J), J=1,8)
   IF (N.LE.14) GO TO 43
   WRITE (6,9001) (TITLE(I),I=1,12)
43 WRITE (6,9006)
   DO 45 I=1,N
   DO 44 J=9,N
   INDX=N*(I-1)+J
44 STOR(J)=A(INDX)
45 WRITE (6,9005) (STOR(J), J=9,N)
50 CONTINUE

C
C   DIAGONALIZATION OF MATRIX
C
   CALL EIGVV (A,V,VALU,N,B)
67 CONTINUE

C
C   DISPLAY OF EIGENVALUES AND EIGENVECTORS
C
   WRITE (6,9001) (TITLE(I),I=1,12)
   IF (ENGY) 168,167,168
167 WRITE (6,9014) L,W
   GO TO 169
168 WRITE (6,9015) L,W,FNGY
169 WRITE (6,9007) ITNO
   WRITE (6,9005) (VALU(I),I=1,8)
   IF (KONTR) 73,68,73
68 WRITE (6,9008)
   DO 70 I=1,N
   DO 69 J=1,8
   INDX=N*(J-1)+I
69 STOR(J)=V(INDX)
70 WRITE (6,9005) (STOR(J), J=1,8)
   IF (FLN-8.0) 77,77,77
72 WRITE (6,9001) (TITLE(I),I=1,12)
   WRITE (6,9009)
73 WRITE (6,9005) (VALU(I),I=9,N)
   IF (KONTR) 77,173,77
173 WRITE (6,9008)
   DO 75 I=1,N
   DO 74 J=9,N
   INDX=N*(J-1)+I
74 STOR(J)=V(INDX)
75 WRITE (6,9005) (STOR(J), J=9,N)
77 CONTINUE

C
C   CALCULATION OF CHARGE DENSITY FOR L ELECTRONS

```

```

C
DO 90 I=1,N
QTOT(I)=0.0
FLL=L
K=1
79 INDX=N*(K-1)+I
Q=V(INDX)*V(INDX)
IF (FLL-2.0) 87,85,80
80 K=K+1
FLL=FLL-2.0
QTOT(I)=QTOT(I)+2.0*Q
GO TO 79
85 QTOT(I)=QTOT(I)+2.0*Q
GO TO 88
87 QTOT(I)=QTOT(I)+Q
88 QTOT(I)=1.0-QTOT(I)
90 CONTINUE
C
C CALCULATION OF BOND ORDERS
C
DO 101 M=1,MMAX
PTOT(M)=0.0
FLL=L
K=1
94 INDM=N*(K-1)+IND(M)
JINDM=N*(K-1)+JIND(M)
P=V(INDM)*V(JINDM)
IF (FLL-2.0) 100,98,95
95 K=K+1
FLL=FLL-2.0
PTOT(M)=PTOT(M)+2.0*P
GO TO 94
98 PTOT(M)=PTOT(M)+2.0*P
GO TO 101
100 PTOT(M)=PTOT(M)+P
101 CONTINUE
IF (KONTR) 120,110,120
110 WRITE (6,9001) (TITLE(I), I=1,12)
120 WRITE (6,9010) ITNO
WRITE (6,9011) (IND(M),JIND(M),PTOT(M),M,QTOT(M), M-1,N)
N2=N+1
WRITE (6,9013) (IND(M),JIND(M),PTOT(M), M=N2,MMAX)
C
C TEST DIVERGENCE OF BOND ORDERS
C
DO 140 M=1,MMAX
BOND=PTOT(M)
IF (BOND) 130,140,140
130 WRITE (6,9012)
GO TO 5
140 CONTINUE
C
205 DO 206 I=1,400
206 A(I)=A1(I)
C
C OMEGA-TECHNIQUE CORRECTION TO ALPHA
C
DO 210 M=1,N
INDX=N*(M-1)+M
210 A(INDX)=A2(M)+W*QTOT(M)

```

```

C
C CORRECTION TO RESONANCE INTEGRAL (BETA)
C
      IF (INCLB) 220,215,220
215 IF (ITR-ITNO) 5,5,218
218 ITNO=ITNO+1
      KONTR=IMPRT*(ITR-ITNO)
      IF (KONTR) 50,31,50
C
220 DO 230 M=1,MMAX
      I=IND(M)
      J=JIND(M)
      IF (I-J) 224,230,224
224 IF (IRON-I) 236,236,225
225 IF (IRON-J) 236,236,235
235 IF (INCLB-?) 240,230,240
236 IF (INCLB-1) 230,230,260
C
240 BETA=0.92*(1.0+PTOT(M))+0.46
C
243 INDX=N*(I-1)+J
      A(INDX)=BETA
      INDX=N*(J-1)+I
      A(INDX)=BETA
      GO TO 230
C
260 IF (ITNO.GT.0) GO TO 265
      INDX=N*(I-1)+J
      A3(M)=A(INDX)
265 BETA=(FNGY/(2.0*PTOT(M))+A3(M))/2.0
      A3(M)=BETA
      GO TO 243
230 CONTINUE
      GO TO 215
C
C FORMAT STATEMENTS
C
9000 FORMAT (12A6)
9001 FORMAT (1H1,12A6)
9002 FORMAT (7I5,2F5.1,I5)
9003 FORMAT (2I5,F10.0)
9004 FORMAT (49H0INPUT MATRIX                                ITERATION NUMBER ,I3//)
9005 FORMAT (1H0,8F13.7)
9006 FORMAT (23H0INPUT MATRIX -- PART 2//)
9007 FORMAT (49H0EIGENVALUES                                ITERATION NUMBER ,I3//)
9008 FORMAT (1H0,/22HEIGENVECTORS (COLUMNS)//)
9009 FORMAT (22H0EIGENVALUES -- PART 2//)
90100FORMAT (12HOROND ORDERS,36X,16HCHARGE DENSITIES,16X,17HITERATION N
NUMBER ,I3,//25H ATOM ATOM      BOND ORDER,20X,20HATOM      CHAR
2GE)
9011 FORMAT (1H ,I3,I5,F16.7,20X,I3,7X,F11.7)
9012 FORMAT (85HOROND ORDERS HAVE TAKEN NEGATIVE VALUES. THE ITERATION
1 SEQUENCE HAS BEEN TERMINATED.)
9013 FORMAT (1H ,I3,I5,F16.7)
9014 FORMAT (21H0NUMBER OF ELECTRONS=,I2,10X,6HOMEGA=,F4.2)
9015 FORMAT (21H0NUMBER OF ELECTRONS=,I2,10X,6HOMEGA=,F4.2,10X,
124HCARRON-IRON BOND ENERGY=,F5.2,5H BETA)
      FND
$DATA

```

0239 CARDS

PROPOSITIONS

PROPOSITION I.

I. INTRODUCTION

Spectrometers in current use for the infrared and visible regions measure the decrease of intensity of a light beam as the sample under investigation absorbs in a particular spectral region. A sample present in trace quantities, or one which interacts only weakly with the light beam, causes only a small change in the intensity of a beam of light--often a change of the same order of magnitude as the noise in the light source and the instrument. Dual beam instruments have been built which lessen this problem by comparing the resultant light beam with a reference beam which has gone through similar optics but not through the sample. The light beams are compared by a chopping apparatus which allows the detector to alternately examine one and then the other beam at a suitable switching rate. Noise in the light source near the switching frequency or one of its harmonics remains and is detected as a spurious absorption signal. A new technique is proposed for comparing the light beams continuously, bringing only the instantaneous difference of intensity of the two beams to the detector.

II. PRINCIPLES OF OPERATION

The Michelson interferometer has been used for years for extremely accurate measurements of length and of the degree of

flatness of optical surfaces (1). The Twyman interferometer (Figure 1) is a modification of the Michelson interferometer which uses a lens system to produce a light beam with a plane wave front (2). Half the light from the source is reflected from the half-silvered mirror to mirror 1 and back, while the rest of the light passes through to mirror 2 and back. Half the light returning from each path is directed to the exit lens and out the instrument. The compensating plate is included to insure equal optical paths even though the beam to mirror 1 must travel through the glass backing of the half-silvered mirror three times while the other beam only travels through the mirror backing once.

The two beams of light to mirror 1 and mirror 2 retain phase coherence. If the mirrors are adjusted properly and the optical path lengths are precisely equal, the returning beams will interfere destructively, leaving a uniformly dark field at all frequencies (3). The two beams interfere destructively rather than constructively because their reflections off of the half-silvered mirror occur on opposite sides of the surface. A beam of light reflected from an interface from the side with the higher index of refraction will be 180° out of phase with an identical beam reflected from the side of the interface with the lower index of refraction (4).

If a sample cell is inserted in one leg of the interferometer and a carefully matched cell containing only solvent is put in the

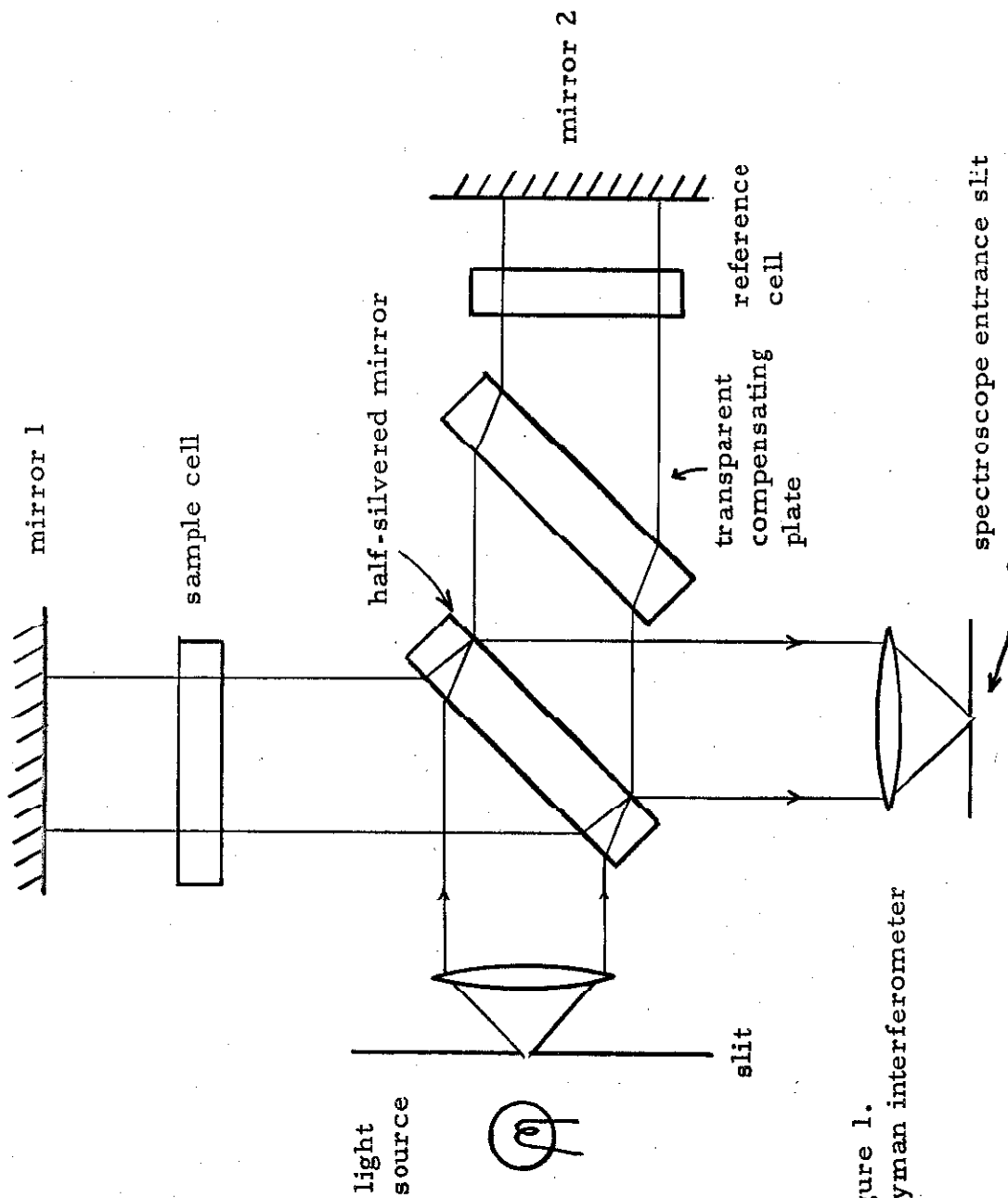


Figure 1.
Twyman interferometer

other leg, the destructive interference will not be complete at frequencies where the sample selectively absorbs energy. If the output of the interferometer is then led into a spectrometer and the beam intensity is scanned as a function of frequency, energy will appear in the beam only at wavelengths where the sample does absorb. With a suitably intense source of input light, a large output may be obtained for a very small relative absorption of the sample.

A noise fluctuation of the input source intensity at any frequency will cause the same relative fluctuation of the final output intensity, resulting in only a small perturbation of the output signal. On existing dual-beam spectrometers, however, noise pulses occurring near a harmonic of the switching frequency will add linearly to the signal, often completely obliterating weak signals.

Beam chopping techniques may still be applied to the output of the interferometer if desired to facilitate electronic amplification of the detected signal.

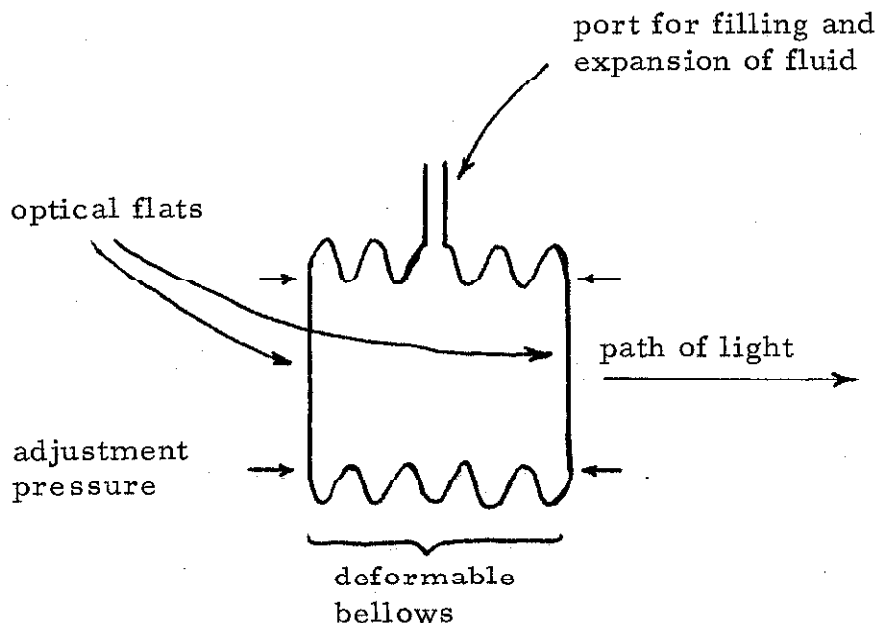
III. PROBLEMS IN DESIGN AND CONSTRUCTION

A certain amount of care must be taken in the construction of the interferometer, and the specific problems which may be encountered will now be discussed.

The lenses (or focusing mirrors) in the interferometer should be of very high optical quality and must be capable of passing the spectral range to be studied.

The half-silvered mirror and compensating plate should be made from the same piece of high quality optical glass or fused quartz, carefully ground optically flat, and to constant thickness to within 750 \AA . (All of the tolerances to be specified at this point have been calculated on the assumption that the optical paths of the two legs are 20 cm long and must be equal to within 500 \AA .) The precision of agreement of the two path lengths will double if the specified tolerance is halved.

The windows of the sample cells should be cut from a single optically flat blank. The remaining walls of the cells may be constructed with a rigid but deformable bellows. This will allow a fine adjustment of the path length through the application of pressure from the external mounting system.



As before, both the thickness of the optical walls and the internal path lengths should be equal in the two cells to within 750 Å. This tolerance is easily attainable with present techniques.

The mirrors are silvered by means of standard evaporation techniques (5). The reflectivity of silver drops to too low a value to be useful in the near ultraviolet, and in this range an aluminum film should be used instead (6). The half-silvered mirror should ideally reflect about half the light and transmit the rest; however, the exact ratio is not critical because of the symmetry of the system. The light from each optical path is reflected once from the half-silvered mirror and transmitted through it once, so the final relative intensities of the two paths are not affected by the degree of silvering.

The totally reflecting mirrors (mirrors 1 and 2) are prepared by the same techniques, but with a heavier layer of metal deposited on them. They are mounted securely on the interferometer frame in holders which allow fine adjustment of their relative alignments and positions. With present mounting systems, it is not difficult to achieve alignment of the mirrors to 0.05 wavelength of light or better (1).

The density of the air in the optical path will be a function of the temperature and pressure, and if the temperature or air pressure of one of the legs of the interferometer changes during an experiment, then the optical path length of that leg will change and

erroneous signals will result. In keeping with the aforementioned criteria, the air pressure of the two paths should be kept equal to within 1.2 mm Hg and the temperature should be regulated to within 0.5° C. These limits should not be difficult to attain in an enclosed and insulated system.

The change of length due to thermal expansion of the mechanical framework holding the optical components must also be considered. If the frame is constructed out of a material with a suitably low coefficient of thermal expansion, such as Invar, the change of optical path length with temperature will be of the same magnitude as that found for the change of the index of refraction of the air path. In fact, these two effects oppose each other, and to first order will cancel and make the system insensitive to slow changes in temperature.

One must remember that any change in temperature or pressure affecting the two balanced legs of the interferometer will not have any effect on the resultant signal. For this reason, fairly wide fluctuations in external conditions may be tolerated if they act uniformly on the entire system.

None of these tolerances are impossible to attain; in fact, present instrumentation will allow a considerable improvement in most tolerances over the specified values. The values stated are the upper limits which will still provide usable performance from the

system. The final proof that such tolerances are attainable is perhaps the fact that such interferometers do exist and are in common usage in optical laboratories throughout the world.

IV. CONCLUSION

Due to the expense of the precision components and the need for constant and expert attention to the instrument, this spectrometer would not be a practical instrument for most laboratories to consider. On the other hand, the improvement in instrument sensitivity made available by this technique will allow the study of trace quantities of materials and low concentration reaction intermediates not accessible through present instrumentation. This consideration will merit the construction of such an instrument in a few laboratories intimately concerned with such problems.

References

1. C. Candler, "Modern Interferometers," Hilger Publications, Great Britain, 1951, pp. 108-190.
2. Reference 1, p. 136.
3. Reference 1, pp. 112, 137.
4. S. Tolansky, "An Introduction to Interferometry," Longmans, London, 1955, p. 37.
5. S. Tolansky, "Multiple-Beam Interferometry of Surfaces and Films," Clarendon Press, Oxford, England, 1948, pp. 24-33.
6. Reference 1, p. 310.

PROPOSITION II.

I. INTRODUCTION

In recent years the limits of frequencies of infrared and electron paramagnetic resonance measurements have been rapidly approaching each other. Infrared measurements have been performed successfully at 0.7 mm (1, 2), while currently available e. p. r. spectrometers are capable of making measurements at 8.5 mm and 12 kilogauss (3).

It is proposed that technology has advanced to the point where an e. p. r. experiment may be performed using infrared sources and optics rather than microwave klystrons and waveguides to provide the irradiating field. Superconducting magnets are already available which will provide fields of over 100 kilogauss (4-7), and it is predicted that magnets which will be capable of attaining fields of 150 to 300 kilogauss will be built in the near future (7, 8).

At 300 kilogauss, an organic radical with a spectroscopic splitting factor, g , equal to 2.0, will have a Zeeman splitting equivalent to radiation with a wavelength of 0.3 mm, while the currently available 100 kilogauss magnets would require a 1.0 mm infrared beam. Other paramagnetic materials with g values greater than two, such as rare earth ions, could be studied with radiation of even shorter wavelength. At these intense magnetic fields, however, many such systems will

have the spin and orbital angular momenta decoupled (Paschen-Back effect), resulting in lower g values (9, 10).

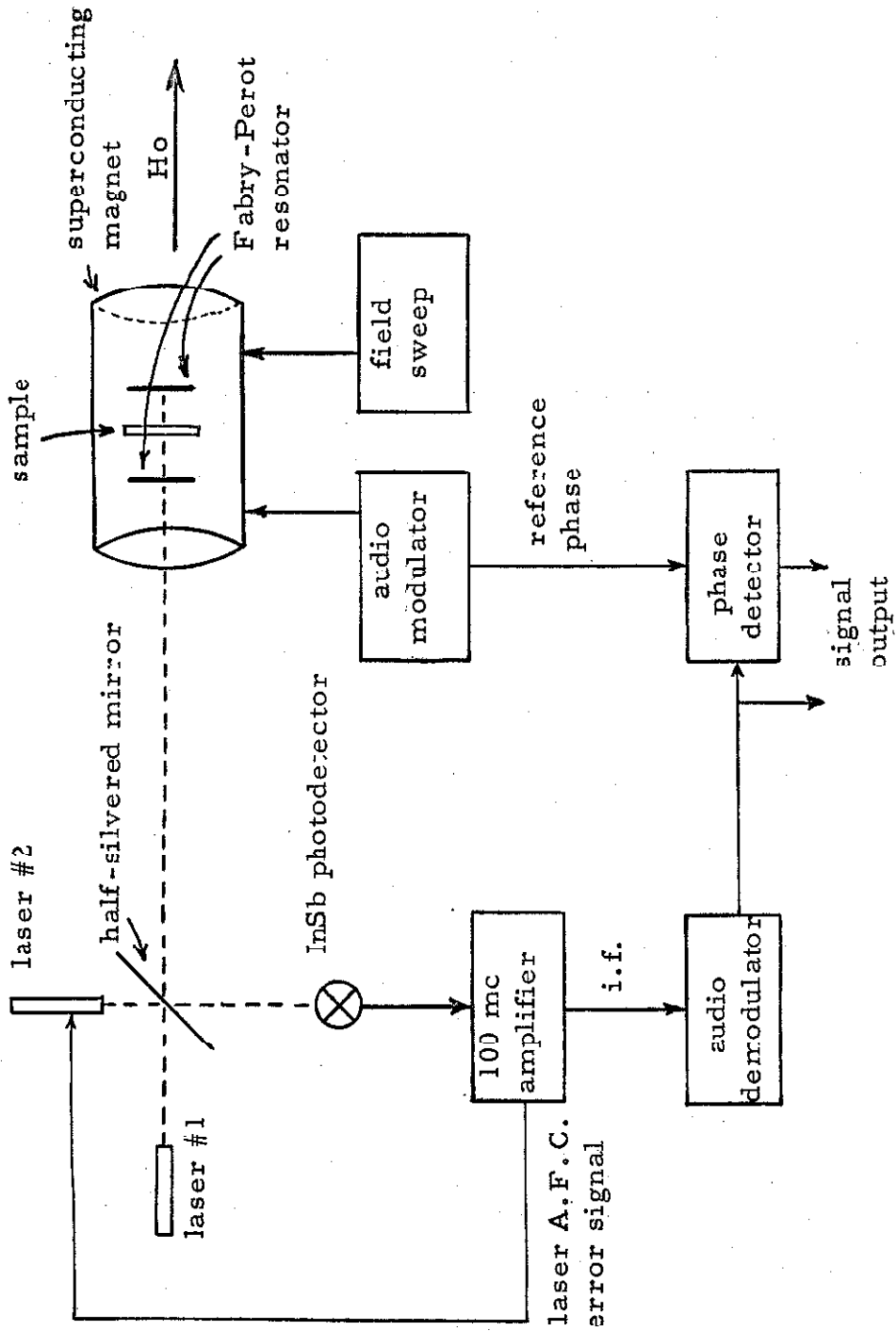
II. THE INSTRUMENT

The optics in these experiments can be considerably simpler than in an infrared spectrometer, because it will not be necessary to scan the frequency of the infrared radiation. With suitable interference filters to insure monochromatic radiation, the infrared beam may be left at one wavelength and the magnetic field swept until the resonance condition occurs in the system. In fact, a very sharply monochromatic source of light such as a laser beam may be used. Continuously emitting lasers operating at 0.133 mm and 0.118 mm have already been reported (11, 12).

An improvement in sensitivity of the system over conventional infrared detection techniques may be realized if a hybrid optical-electronic system is used to examine the e.p.r. transition. A typical system is illustrated in Figure 1.

In this system two almost identical lasers are operated at, for example, 100 mc apart. The output of one of the lasers (laser no. 1) is directed at the sample. The sample is in the field of a superconducting magnet, and the magnetic field is oriented parallel to the laser beam. The sample may be contained in a Fabry-Perot resonator if it becomes necessary to increase the extent of interaction of the sample with the beam. The Fabry-Perot resonator is

Figure 1. Block diagram of proposed e.p.r. spectrometer.



essentially a pair of parallel mirrors precisely spaced to allow constructive interference for light of the laser frequency. The light is thus reflected back and forth through the sample many times. The mirror closest to the laser is not completely silvered, so light from the laser may enter and then return via the same path.

A sample at least 0.2 mm on a side will always be in at least one magnetic field maximum, since these maxima will occur every 0.15 mm for light with a wavelength of 0.3 mm. The sample would ideally be suspended in an inert matrix in the form of a sheet normal to the light beam and covering most of the cross-section of the resonator. A suitable inert matrix, for example, might be a thin sheet of paraffin. Paraffin has been found to be relatively transparent at these frequencies (13).

Part of the light beam returning from the Fabry-Perot resonator is intercepted by a half-silvered mirror oriented at 45° to it, and is reflected to a suitable photodetector. Light from a second laser is directed through the same mirror so that the two beams impinge on the photodetector at the same point and in precise alignment with each other. The axes of the two beams should be aligned to within one second of an arc.

The technique of observing two laser beams simultaneously and obtaining a difference frequency (photomixing) is quite common (14-19). In fact, difference frequencies only 2 cps wide have been

observed when two helium-neon lasers were beat together under optimum conditions (20).

To observe photomixing, one must use a square law detector (one which produces a current output proportional to the light power incident on it), and the detector must both work at the frequency of the incident light and be able to respond sufficiently rapidly to follow the resultant beat frequency. Most photodetectors are square law devices and no other type will be considered at this time. None of the photodetectors in common use, however, are sensitive to light in the 0.1 to 1.0 mm range. These photodetectors require the incident photon to eject an electron from a treated surface or to generate a charge carrier pair in a semiconductor. The photons in the present system, however, are not sufficiently energetic for most detectors to react, and also the detectors may be opaque to these wavelengths. The most common methods of detecting radiation in the sub-millimeter range are by use of a thermocouple, a bolometer, a Golay cell, or some other device which depends on the local heating caused by the impinging radiation. Unfortunately, all of these devices have large thermal inertias, and none of them will respond to beat frequencies over a few hundred cycles per second.

One photoconductor has been reported which shows promise of high speed operation and sensitivity in the spectral region of

interest. Putley (21) has studied n-type indium-antimony semiconductors and found them to be sensitive to radiation from 0.2 mm to 8.6 mm. The time constant of these photoconductors is predicted to be small enough to allow the detection of a 100 kmc beat frequency (22). For optimum performance, these photodiodes should be operated at low temperatures.

No information is available at this time on the feasibility of using a video detector crystal to demodulate the laser beam though such crystals are used universally for this purpose at X-band and K-band microwave frequencies.

The 100 mc difference frequency of the two lasers is amplified with conventional electronic techniques. When the frequency drifts from the nominal i. f. frequency, an error signal is generated. The error signal is fed back to laser no. 2 and is used to correct its frequency of oscillation such that the beat frequency always remains at its nominal value.

The original frequency offset and the automatic frequency control function both require that the laser frequency be variable in some predictable and facile manner. Several methods have been explored for shifting the frequency of a c.w. laser. Probably the most useful technique for the present purpose is to change the laser mirror spacing slightly and shift the cavity resonance modes. An ingenious method has been developed to accomplish this, taking

advantage of the magnetostrictive properties of the laser supporting framework (16, 23). The physical dimensions of the laser and its frequency of oscillation will vary by a slight but reproducible amount when an electric current is passed through electromagnet coils wound around the support frame.

Several other less convenient ways of shifting the laser frequency have been developed. When a laser is operated in a magnetic field, its frequency is split into several components by Zeeman splitting of the energy levels (16, 24). In another study, the laser frequency of the ruby laser has been found to be temperature dependent in a predictable way (25). A change of wavelength of 0.006 μ per degree centigrade has been observed.

If the magnetic field containing the original paramagnetic sample is modulated at an audio frequency, the 100 mc intermediate frequency will be amplitude modulated by this audio frequency when (and only when) the sample is in resonance. This audio modulation can be extracted from the intermediate frequency to obtain the resonance signal for the sample. A comparison of this signal with the original modulation frequency will provide the first derivative of the resonance signal.

III. CONCLUSIONS

This spectrometer will serve two major purposes which justify its construction. First, its successful operation will

demonstrate a merger of two heretofore relatively dissimilar fields: radio frequency spectroscopy and optical spectroscopy. Secondly, and more important from a practical standpoint, this spectrometer is ultimately capable of much greater sensitivity for the detection of paramagnetic species than any presently existing e.p.r. spectrometer. This comes about because the signal power absorbed by a sample goes as the square of the applied magnetic field (26). At 300 kilogauss, this spectrometer will be operating at a magnetic field 25 times larger than that used by existing equipment. If a substantial fraction of this 600-fold improvement in sensitivity can be realized in practice, many systems may be studied which are out of reach of present instrumentation.

The system which has just been described uses one of many possible combinations of instrumentation which are available at the present time. The particular design was chosen as one which has a high likelihood of succeeding. It is impossible to predict at this time what problems may arise which have not been foreseen, but the difficulties which do arise should not be insurmountable.

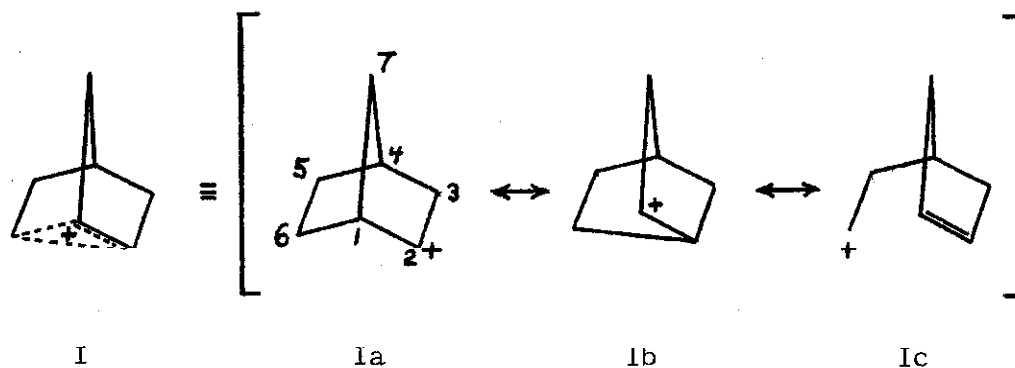
References

1. T. K. McCubbin, Jr. and W. M. Sinton, *J. Opt. Soc. Am.*, 40, 537 (1950).
2. T. K. McCubbin, Jr. and W. M. Sinton, *ibid.*, 42, 113 (1952).
3. Varian Data Sheet on V-4503, 35 G.C., e.p.r. spectrometer.
4. *Chem. and Eng. News*, p. 30, Nov. 30, 1964.
5. *Chem. and Eng. News*, p. 35, Feb. 22, 1965.
6. *Systems Design*, p. 62, Dec. 1964.
7. *EEE - Circuit Design Engineering*, p. 29, Oct. 1964.
8. Private communication, Varian Associates Instrumentation Staff, Varian Advanced NMR Workshop, Oct. 1964.
9. G. Herzberg, "Spectra of Diatomic Molecules," N.Y., 1950, p. 28.
10. H. A. Bethe and E. E. Salpeter, "Quantum Mechanics of One- and Two-Electron Atoms," N. Y., 1957, pp. 210-211.
11. *Electronic Industries*, p. 8, Aug. 1964.
12. *Chem. and Eng. News*, p. 38, Feb. 8, 1965.
13. T. K. McCubbin, Jr. and W. M. Sinton, *J. Opt. Soc. Am.*, 40, 537 (1950); *ibid.*, 42, 113 (1952).
14. O. S. Heavens, "Optical Masers," Wiley & Sons, N. Y., 1964, p. 89.

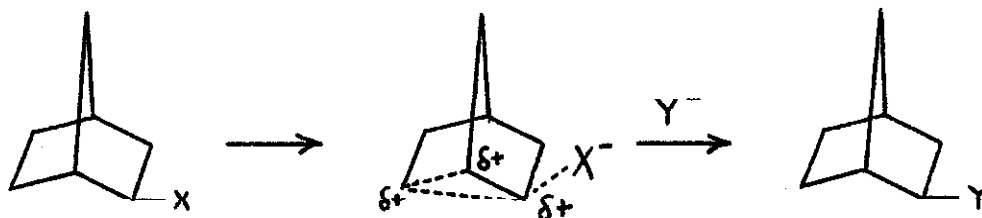
15. B. A. Lengyel, "Lasers," Wiley & Sons, N. Y., 1962, p. 97.
16. R. Paananen, C. L. Tang and H. Statz, Proc. IEEE, 51, 63 (1963).
17. W. M. Macek, D. T. M. Davis, Jr., R. W. Olthuis, J. R. Schneider and G. R. White, in "Proceedings of the Symposium on Optical Masers," Polytechnic Press, N. Y., 1963, p. 199.
18. E. A. Ballik, ibid., p. 231.
19. A. E. Siegman, S. E. Harris and B. J. McMurty, ibid., p. 511.
20. Ref. 15, p. 51.
21. E. H. Putley, J. Phys. Chem. Solids, 22, 241 (1961).
22. G. Lucovsky, M. E. Lasser and R. B. Emmons, Proc. IEEE, 51, 166 (1963).
23. R. A. Paananen, Proc. IRE, 50, 2115 (1962).
24. R. L. Fork and C. K. N. Patel, Proc. IEEE, 52, 208 (1964).
25. Ref. 14, p. 50, p. 88.
26. a. J. D. Roberts, "Nuclear Magnetic Resonance," McGraw-Hill Book Co., N. Y., 1959, p. 97; b. J. A. Pople, W. G. Schneider and H. J. Bernstein, "High-Resolution Nuclear Magnetic Resonance," McGraw-Hill Book Co., N. Y., 1959, p. 39.

PROPOSITION III.

The solvolysis of norbornyl derivatives has attracted the attention of chemists for many years (1-3). A nonclassical carbonium ion intermediate (I) has been postulated in the solvolysis of



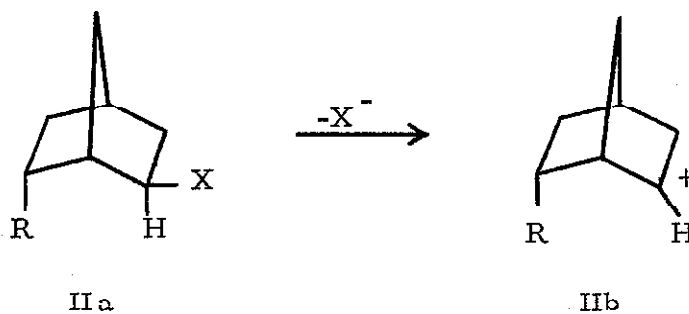
2-norbornyl derivatives in which the 6-carbon assists the transition state from the backside.



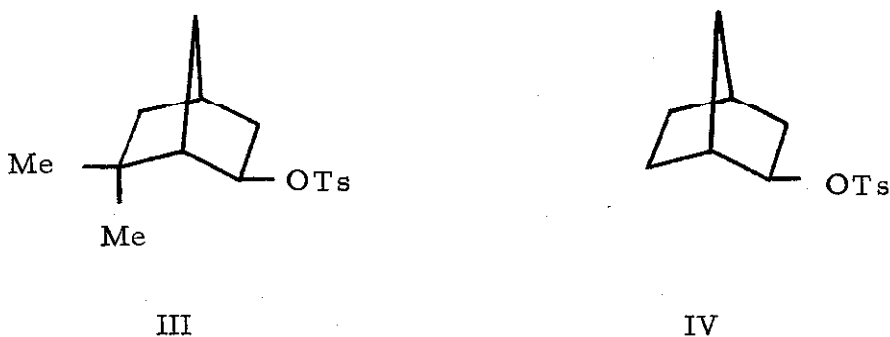
The nonclassical carbonium ion has been proposed as an intermediate to explain: 1) the fast rate of solvolysis of the exo isomer, 2) the high ratio of the rate of solvolysis of the exo isomer relative to the endo isomer, and 3) the great predominance of the exo isomer in the resulting product. Brown (4) argues that these observations

do not necessarily imply a nonclassical intermediate, while most current opinion seems to hold that the nonclassical norbornyl cation does exist (5).

In addition to anchimeric assistance to the stability of the intermediate, the rate of solvolysis of these norbornyl derivatives is affected in a predictable way by steric and conformational considerations (6). A large substituent in the 6-endo position would crowd the 2-endo proton in the reactant (IIa) and thus make the ionization to the intermediate carbonium ion IIb more favorable.



From this point of view, the solvolysis of 6,6-dimethyl-2-exo-norbornyl tosylate (III) should be faster than the solvolysis of 2-exo-norbornyl tosylate (IV) itself.

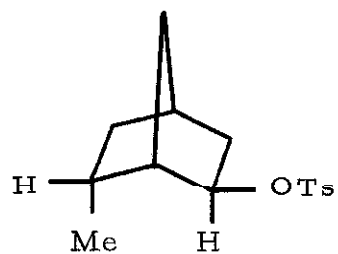


The electron-donating properties of the methyl substituents in III should stabilize resonance structure Ic, where the positive charge on the intermediate is delocalized to the 6 position. The transition state of a reaction leading to a carbonium ion is thought to resemble the structure of the carbonium ion itself (7), so the ionization of III to its carbonium ion should be faster than the ionization of IV to its less stable carbonium ion.

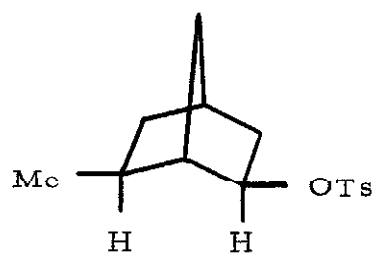
Although both steric and electronic factors predict that the solvolysis of 6,6-dimethyl-2-norbornyl tosylate should be faster than the solvolysis of 2-norbornyl tosylate, Schleyer et al. (7) have observed a rate decrease by a factor of 20 in the solvolysis of the gem-dimethyl derivatives of both the exo and the endo tosylates. Schleyer suggests that the steric interactions might increase on going to the transition state in the gem-dimethyl compound; however, he is by no means certain that this is the actual cause of the rate retardation.

In view of the controversy over the existence of the non-classical norbornyl cation, one would like to have as much information as possible on the factors governing the acceleration or deceleration of the rate of solvolysis of these derivatives. It is therefore proposed that the rates of solvolysis of the norbornyl tosylates in Table I be studied to determine if the depression of rate is governed by steric or electronic effects or perhaps by another factor unrecognized as yet.

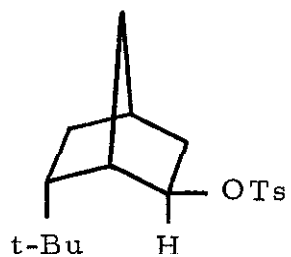
Table 1. Norbornyl derivatives for which solvolysis studies are proposed.



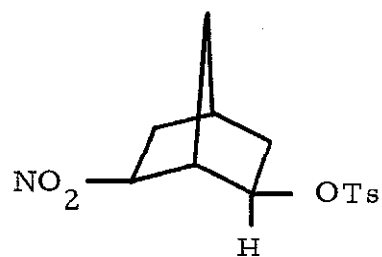
V



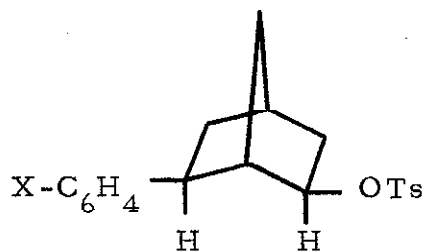
VI



VII



VIII



IX

X = NH₂, CH₃, H, NO₂
as para substituents on
the benzene ring

Compounds V and VI should have identical electronic properties yet have different steric effects on the system. The t-butyl group in compound VII should have an intense steric influence on the system which should dominate any other factors. The nitro group in VIII should polarize the molecule to decrease any anchimeric assistance from the C-6 position. The 6-exo phenyl derivatives (IX) should provide a series with relatively constant steric requirements but varying inductive effects.

A correlation of the rates of solvolysis of the norbornyl tosylates in Table 1 with the specific properties of each of them should provide an insight into the factors influencing the solvolysis and the identity of the transition state and intermediate carbonium ion.

References

1. F. Brown, E. D. Hughes, C. K. Ingold and J. F. Smith, *Nature*, 168, 65 (1961).
2. S. Winstein and D. Trifan, *J. Am. Chem. Soc.*, 74, 1147, 1154 (1952).
3. A. Streitwieser, Jr., "Solvolytic Displacement Reactions," McGraw-Hill Book Co., N. Y., 1962.
4. H. C. Brown, F. J. Chloupek and Min-Hon Rei, *J. Am. Chem. Soc.*, 86, 1246-1248 (1964).
5. S. Winstein, E. Clippinger, R. Howe, and E. Vogelfanger, *J. Am. Chem. Soc.*, 87, 376 (1965).
6. P. von R. Schleyer, *J. Am. Chem. Soc.*, 86, 1854, 1856 (1964).
7. P. von R. Schleyer, M. M. Donaldson and W. E. Watts, *J. Am. Chem. Soc.*, 87, 375 (1965).

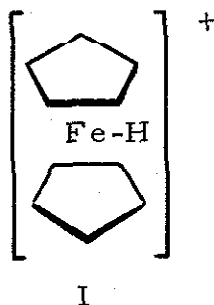
PROPOSITION IV.

In recent years many investigators have studied families of ferrocene derivatives to obtain an insight into the nature of the transmission of electronic effects through the ferrocenyl system (1-5). Correlations have been found between such a variety of properties as the ionization constants of the carboxylic acids, the rates of the reactions of the carboxylic acids with diphenyldiazomethane to form the esters, the Hammett sigma constants for the substituents, Taft's polar σ^* , the carbonyl stretching frequencies of the carboxylic acids and esters, the solvolysis rates for the carbinyl acetates, and the chronopotentiometric quarter-wave potentials (1, 4, 5). The only one of these measurements which directly reflects the magnitude of the electron density on the iron atom is the chronopotentiometric study (1, 4, 5).

The quarter-wave potential appears to be a convenient number by which the electronic properties of various substituents may be compared, and an independent study of the electron density on the iron atom would provide a useful supplementary correlation. A measurement of the relative basicity of the iron atom in different derivatives would provide just such a study.

When ferrocene is dissolved in boron trifluoride monohydrate, the only detectable cationic species in solution is I, in which a proton

is bonded directly to the metal atom (6, 7).

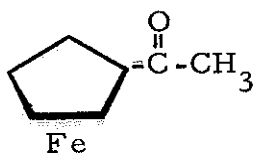


The rate of exchange of this proton between ferrocene and the solvent may be adjusted to fall within the range observable by n.m.r. spectroscopy (7). By the shapes of the n.m.r. peaks, and their change of shape with variations in the system, it is possible to calculate this rate of exchange (8).

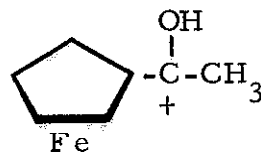
It is proposed that the relative rates of exchange be measured for the protons bonded to the iron atoms in a series of substituted ferrocenes, and that these proton exchange rates be compared to the quarter-wave oxidation potentials for the same compounds. A particularly good correlation would lend support to the postulate that the quarter-wave potential of these derivatives accurately represents a measure of the electron density on the metal atom.

In choosing compounds for this study, one must remember that the measurements are to be made in a strong acid solution and that many of the substituents will be affected by the solvent. For example, one would not be observing the proton exchange from the

metal atom of acetylferrocene (II), but from the metal atom of the conjugate acid (III).



II



III

References

1. For a good survey of the earlier work in this area, see David W. Hall, Ph. D. Thesis, California Institute of Technology, Pasadena, California, 1963, Part II.
2. M. Rosenblum, J. O. Santer, and W. G. Howells, *J. Am. Chem. Soc.*, 85, 1450 (1963).
3. R. A. Benkeser, Y. Nagai, and J. Hooz, *J. Am. Chem. Soc.*, 86, 3742 (1964).
4. G. L. K. Hoh, W. E. McEwen, and J. Kleinberg, *J. Am. Chem. Soc.*, 83, 3949 (1961).
5. W. F. Little, C. N. Reilley, J. D. Johnson, K. N. Lynn, and A. P. Sanders, *J. Am. Chem. Soc.*, 86, 1376 (1964).
6. T. J. Curphey, J. O. Santer, M. Rosenblum, and J. H. Richards, *J. Am. Chem. Soc.*, 82, 5249 (1960).
7. This thesis, Part II.
8. J. A. Pople, W. G. Schneider, and H. J. Bernstein, "High-Resolution Nuclear Magnetic Resonance," McGraw-Hill Book Co., N. Y. (1959), Chapter 10.

PROPOSITION V.

The ferrocenylmethyl radical has been shown to possess a degree of stability comparable to the methybenzyl radical in polymerizing styrene systems (1). Resonance structures with extensive delocalization of the unpaired electron spin have been proposed to explain the stability of the benzyl radical (2); however, no comparable explanation has yet been offered for the observed stability of the ferrocenylmethyl radical.

It is proposed that the electron paramagnetic resonance spectrum of the ferrocenylmethyl radical be examined for the purpose of determining the degree of delocalization of the unpaired electron and gaining an insight into the cause of the observed stability of the radical.

One previous attempt has been made to observe these radicals (1). Methylferrocene powder was irradiated with X-rays and then examined in an e.p.r. spectrometer. No resonance was observed; however, it is possible that radicals might have been formed initially but then recombined prior to the c.p.r. investigation (3), since the compound was examined close to its melting point (m.p. 35°C).

Many investigators have been successful in observing active free radicals by freezing them in an inert matrix. For example, Jen et al. (4) has observed the e.p.r. spectrum of the methyl

radical frozen in an inert argon matrix at 4° K. The radical was generated by radio frequency excitation of methane in the vapor phase and was then trapped in an argon matrix on a cold-finger. The radical was also generated by u. v. irradiation of a sample of methyl iodide frozen in argon. Porter (5, 6) has observed the absorption spectrum of the benzyl radical generated in an organic glass by separate irradiation of toluene, benzyl chloride, benzyl alcohol, and benzylamine with ultraviolet light. He successfully used several different matrices, such as a mixture of ether, isopentane, and ethanol frozen at liquid nitrogen temperature (EPA glass). Ingram et al. has observed the e. p. r. spectrum of the benzyl radical using the same system (7).

Either of the systems described above might prove suitable in an examination of the ferrocenylmethyl radical. One should be able to generate this radical by the ultraviolet light irradiation of an inert matrix of a ferrocenylcarbonyl halide.

In examining the cause of failure of the preliminary e. p. r. experiment on methylferrocene, one must not exclude the possibility that polycrystalline methylferrocene may have an unusually high anisotropic contribution to the hyperfine interaction energy. If this is the case, then the entire hyperfine pattern in the methylferrocene sample may have been smeared into one line, so broad that it was

not observable (8). If no spectrum was observed for this reason, then an e.p.r. spectrum will be readily observable from a single oriented crystal of irradiated methylferrocene.

In whichever way the e.p.r. spectrum of the ferrocenyl-methyl radical is finally obtained, it will yield valuable information about the electron delocalization and subsequent stability of the molecule.

References

1. This thesis, Part I.
2. L. Pauling, "The Nature of the Chemical Bond," Cornell University Press, N. Y. (1960), p. 623.
3. G. C. Pimentel, "Radical Formation and Trapping in the Solid Phase," in Formation and Trapping of Free Radicals, A. M. Bass and H. P. Broida, eds., Academic Press, N. Y. (1960), p. 72.
4. C. K. Jen, S. N. Foner, E. L. Cochran, and V. A. Bowers, *Phys. Rev.*, 112, 1169 (1958).
5. I. Norman and G. Porter, *Proc. Royal Soc.*, A230, 399 (1955).
6. G. Porter and E. Strachan, *Trans. Faraday Soc.*, 54, 1595 (1958).
7. D. J. E. Ingram, W. G. Hodgson, C. A. Parker, and W. T. Rees, *Nature*, 176, 1227 (1955).
8. C. K. Jen, "Electron Spin Resonance Studies of Trapped Radicals," reference 3, p. 220.